Ümmü Gülsüm BAKLACI

M.S. Thesis In Chemistry

January 2009

# SYNTHESIS AND CHARACTERIZATION OF NOVEL PORPHYRAZINE COMPOUNDS BEARING OCTA SUBSTITUTED AROMATIC GROUPS

by

Ümmü Gülsüm BAKLACI

January 2009

# SYNTHESIS AND CHARACTERIZATION OF NOVEL PORPHYRAZINE COMPOUNDS BEARING OCTA SUBSTITUTED AROMATIC GROUPS

by

Ümmü Gülsüm BAKLACI

January 2009

# SYNTHESIS AND CHARACTERIZATION OF NOVEL PORPHYRAZINE COMPOUNDS BEARING OCTA SUBSTITUTED AROMATIC GROUPS

by

Ümmü Gülsüm BAKLACI

A thesis submitted to

the Graduate Institute of Sciences and Engineering

of

Fatih University

in partial fulfillment of the requirements for the degree of

Master of Science

in

Chemistry

January 2009
Istanbul, Turkey

## APPROVAL PAGE

I certify that this thesis satisfies all the requirements as a thesis for the degree of Master of Science.

_____
Assist. Prof. Metin TÜLÜ
Head of Department

This is to certify that I have read this thesis and that in my opinion it is fully adequate, in scope and quality, as a thesis for the degree of Master of Science.

_____
Assist. Prof. Ergün GONCA
Supervisor

Examining Committee Members

Prof. Dr. Naz Mohammed AGH-ATABAY _____

Assist. Prof. Ergün GONCA _____

Assist. Prof. Sadık GÜNER _____

It is approved that this thesis has been written in compliance with the formatting rules laid down by the Graduate Institute of Sciences and Engineering.

_____
Assist. Prof. Nurullah ARSLAN
Director

# SYNTHESIS AND CHARACTERIZATION OF NOVEL PORPHYRAZINE COMPOUNDS BEARING OCTA SUBSTITUTED AROMATIC GROUPS

By Ümmü Gülsüm BAKLACI

M. Sc. Thesis in Chemistry
January 2009

Supervisor: Assist. Prof. Dr. Ergün GONCA

## ABSTRACT

An important group of coordination compounds is that of tetrapyrrol derivatives which receive interest due to both practical and theoretical point of view. Porphyrins, porphyrazines, phthalocyanines and tetrabenzoporphyrins, modified by the attachment of peripheral substituents, have found wide applications in diverse areas such as electrophotography, optic data collection, chemical sensors, catalysis, electron transfer, liquid crystal, laser technology and the photodynamic therapy of tumors as well as in their classical fields as pigments and dyes.

In this study, we report novel porphyrazines with eight 4-biphenyl substituents appending to the periphery positions. Magnesium porphyrazinate substituted with eight 4-biphenyl groups on the periphery positions has been synthesized for the first time from the cyclotetramerization of 1,2-bis(4-biphenyl)maleonitrile in the presence of magnesium butanolate. Its demetalation by treatment with trifluoroacetic acid, resulted in a partially oxidized product, namely, octakis(4-biphenyl)-2-*seco*-porphyrazine-2,3-dione. Further reaction of this product with copper(II) acetate, zinc(II) acetate and cobalt(II) acetate has led to the metallo derivatives, [octakis(4-biphenyl)-2-*seco*-2,3-dioxoporphyrazinato] M(II) (M= Cu, Zn, Co).

Moreover, we report new soluble porphyrazines with eight (*p*-tolyl) and (*o*-tolyl) substituents appending to the peripheral positions. Magnesium porphyrazinates have been synthesized for the first time by cyclotetramerization of 1,2-bis(*p*-tolyl)maleonitrile and 1,2-bis(*o*-tolyl)maleonitrile in the presence of magnesium butanolate. Their demetalation by treatment with trifluoroacetic acid resulted in a partially oxidized products, namely, octakis(*p*-tolyl)-2-*seco*-porphyrazine-2,3-dione and octakis(*o*-tolyl)-2-*seco*-porphyrazine-2,3-dione. Further reaction of these products with copper (II) acetate, zinc (II) acetate and cobalt (II) acetate has led to the metallo derivatives, [octakis(*p*-tolyl)-2-*seco*-2,3-dioxoporphyrazinato] M(II) and [octakis(*o*-tolyl)-2-*seco*-2,3-dioxoporphyrazinato] M(II) (M= Cu, Zn, Co). These novel

compounds have been characterized by elemental analysis, together with FT-IR, $^{1}H$ NMR, UV-Vis and mass spectral data.

**Keywords:** 4-biphenyl, *o*-tolyl, *p*-tolyl, porphyrazines, *seco*-porphyrazines, cyclotetramerization.

# OKTA SÜBSTİTÜE AROMATİK GRUPLAR İÇEREN YENİ PORFİRAZİN BİLEŞİKLERİNİN SENTEZİ VE KARAKTERİZASYONU

Ümmü Gülsüm BAKLACI

Yüksek Lisans Tezi-Kimya Bölümü
Ocak 2009

Tez Yöneticisi: Yrd. Doç. Dr. Ergün GONCA

## ÖZ

Değişik periferal sübstitüentlerin bağlanmasıyla oluşturulan porfirinler, porfirazinler ftalosiyaninler ve tetrabenzoporfirinlerin çeşitli alanlarda geniş uygulamaları bulunmuştur. Bu alanlar elektrofotografik, optik veri toplama, kimyasal sensörler, katalizler, elektron transferi, sıvı kristal, lazer teknoloji ve tümörlerin fotodinamik terapisidir.

Bu çalışmada biz yeni periferal pozisyondaki 8 tane 4-bifenil sübstitüentleri içeren porfirazinleri sentezledik. Öncelikle magnezyum butanolat içerisindeki 1,2-bis(4-bifenil)maleonitrilin siklotetramerizasyonundan periferal pozisyondaki 8 tane 4-bifenil grupları ihtiva eden magnezyum porfirazin sentezlendi. Trifluoroasetik asit ile muamele edilerek oktakis(4-bifenil)-2-*seko*-porfirazin-2,3-dion isimli metalsiz türevine dönüştürüldü. Bu ürünün bakır (II) asetat, çinko (II) asetat ve kobalt (II) asetat tuzları ile reaksiyona sokulmasıyla metallo-porfirazinler, [oktakis(4-bifenil)-2-*seko*-2,3-dioksoporfirazinato] M(II) (M= Cu, Zn, Co) elde edilmiştir. Bu ürünlerin karakterizasyonu $^{1}$H NMR, FT-IR, UV-Vis, kütle ve elementel analiz gibi çeşitli spektral verilerle gerçekleştirilmiştir

Ayrıca bu çalışmada biz yeni çözülebilen periferik pozisyondaki 8 tane (*p*-tolil) ve (*o*-tolil) sübstitüentleri içeren porfirazinleri sentezledik İlk önce magnezyum butanolat içerisinde 1,2-bis(*p*-tolil)maleonitril ve 1,2-bis(*o*-tolil)maleonitrilin siklotetramerizasyon yöntemiyle magnezyum porfirazinleri sentezlendi. Trifluoroasetik asit ile muamele edilerek oktakis(*p*-tolil)-2-*seko*-2,3-porfirazinato ve oktakis(*o*-tolil)-2-*seko*-2,3--porfirazinato isimli metalsiz türevlerine dönüştürdü. Bu ürünün bakır (II) asetat, çinko (II) asetat ve kobalt (II) asetat tuzları ile reaksiyona sokulmasıyla metallo-porfirazinler [oktakis(*p*-tolil)-2-*seko*-2,3-dioksoporfirazinato] M(II) and [octakis(*o*-tolil)-2-*seko*-2,3-dioksoporfirazinato] M(II) (M= Cu, Zn, Co) elde

edilmiştir. Bu ürünlerin karakterizasyonu $^{1}$H NMR, FT-IR, UV-Vis, kütle ve elementel analiz gibi çeşitli spektral verilerle gerçekleştirilmiştir

**Anahtar Kelimeler:** 4-bifenil, *o*-tolil, *p*-tolil, porfirazinler, *seko*-porfirazinler, siklotetramerizasyon.

# ACKNOWLEDGEMENTS

Firstly, I would like to thank my supervisor, Assist. Prof. Ergün GONCA, who assisted me with his useful advises and discussions during my study.

I also would like to appreciate Assist. Prof. Hatice A.DİNÇER for her help and encouragement.

Lastly, but in no sense the least, I am especially grateful to Nürüfe KEMİKLİ, Neslihan CENAN, all my colleagues and also my special thanks to my family.

It has been a real joy to work with all of them.

# TABLE OF CONTENTS

# LIST OF TABLES

# LIST OF FIGURES

# LIST OF ABBREVIATIONS

| | |
|---|---|
| M | Metal |
| $H_2AP$ | Azaporphyrine |
| $H_2DAP$ | Trans-diazaporphyrine |
| $H_2MATBP$ | Monoazatetrabenzoporphyrine |
| $H_2NTBP$ | Tribenzo (1-phenyl-2-3-naphthalo) porphyrine |
| $H_2OED$ | Octaethylporphyrine |
| $H_2MAP$ | Monoazaporphyrine |
| $H_2TATBP$ | Triazatetrabenzoporphyrine |
| $H_2TBP$ | Tetrabenzoporphyrine |
| $H_2TPP$ | Meso-tetraphenylporphyrine |
| $H_2TPrP$ | Meso-tetra (n-propyl) porphyrine |
| MAP | Metalloazaporphyrine |
| MP | Metalloporphyrine |
| MTAP | Metallotetraazaporphyrine |
| FAB | Fast Atom Bombardment |
| EAS | Electron Absorption Spectrum |
| MO | Molecular Orbital |
| DCM | Dichloromethane |
| DMF | N,N-dimethylformamide |
| DCE | Dichloroethane |
| NMR | Nuclear Magnetic Resonance |
| IR | Infrared |
| UV / VIS | Ultraviolet / Visible Spectrum |
| Å | Angstrom |
| Pyr | Pyrrole |
| LCAO | Linear Combination of Atomic Orbital |
| LUMO | Lowest Unoccupied Molecular Orbital |
| HOMO | Highest Occupied Molecular Orbital |
| L | Ligand |

| | |
|---|---|
| $M(P)L_4$ | Metal monotetrapyrroles |
| $M(P)_2$ | Bistetrapyrroles |
| $M_2(P)_3$ | Tristetrapyrroles |

# CHAPTER 1

# INTRODUCTION

An important group of coordination compounds is that of tetrapyrrol derivatives which receive interest due to both practical and theoretical point of view [1-4]. A 16 - membered electron rich conjugated planar macrocyclic core is common in all these structures. When this main core is composed of four pyrrol units bound to one another through methine (-CH=) bridges, it is called porphyrin (Fig.1.1.a). Four-benzo condensation on each of the pyrrol groups result with tetrabenzoporphyrin (Fig.1.1.b). Changing methine bridges with aza functions (=N-) in porphyrins result with porphyrazines (or tetraazaporphyrins) (Fig.1.1.c). The benzo-condensed porphyrazines are the well-known phthalocyanines (Fig.1.1.d).

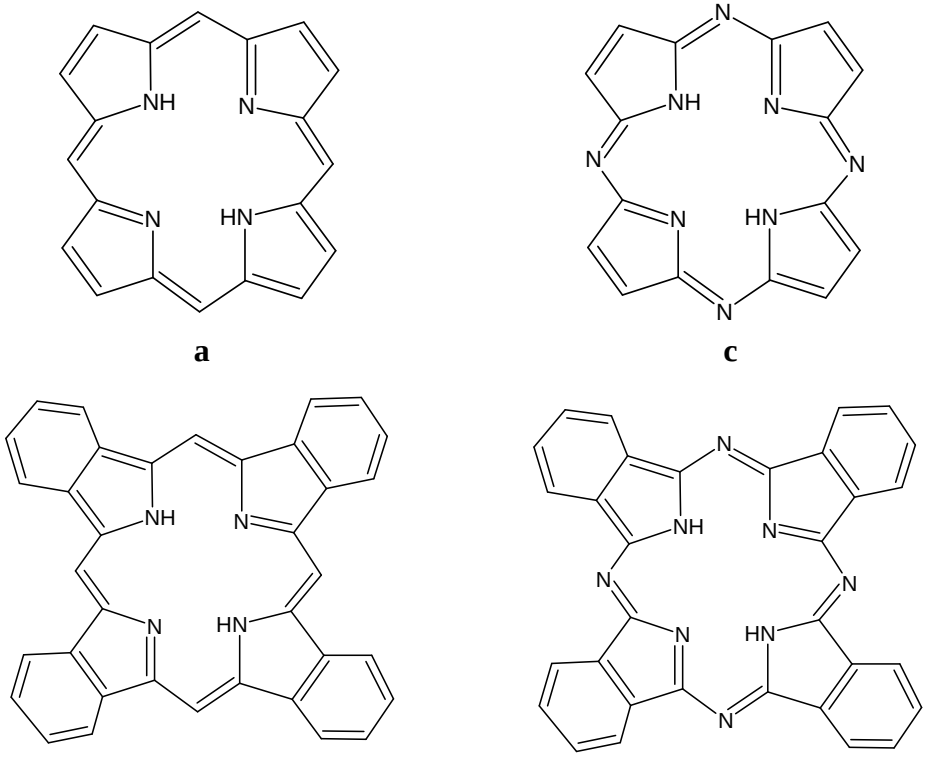


**Figure 1.1** (**a**) Porphyrin, (**b**) Tetrabenzoporphyrin, (**c**) Porphyrazine, (**d**) Phthalocyanine

Porphyrazines and related molecules have also been a theme of considerable theoretical interest due to their high symmetry, planar molecular arrangements, and electronic delocalization. A large number of theoretical works have been devoted to the understanding of the atomic scale structure of these molecules, their building blocks and the mechanisms of charge transport and optical properties. Molecular design of porphyrazines for various Q-band splitting modes has attracted considerable experimental interest, where the ring symmetry modification has been introduced as a new methodology.

One of the most important properties of tetrapyrrol ligands is their ability to coordinate to metal ions, yielding stable inter complex salts. Stable complexes of porphyrins, porphyrazines and phthalocyanines result from formation of four equivalent σ bonds (N → M) that is filling of vacant s, $p_x$, $p_y$ and (n - 1) $d_{x2-y2}$ or n $d_{x2-y2}$ orbitals of the cation with σ electrons of the central nitrogen atoms which are called as coordinating N atoms. The resulting σ bonds are strong that in the case of metals $Cu^{2+}$, $Ni^{2+}$, $Co^{2+}$ and $Zn^{2+}$ that in solid complexes practically no replacement of the metal ions takes place at $H_2SO_4$ concentrations ranging from 2 to 7 M. In the case of coordination of triply or quadruply charged ions the formation of a complex involves, in addition to d, s, and $p^2$ orbitals, $p_z$ and $d_{z2}$ orbitals that participate in the attachment of the extra ligand along the z-axis perpendicular to the plane of the molecule.

The formation of σ bonds (N →M) in porphyrin and porphyrazine complexes leads to four electron pairs of the coordinating nitrogen atoms being excluded from the conjugation. The antibonding π orbitals (π*) of the macroring are filled with the heteroatomic n orbitals. The attendant decrease in the energy of these antibonding π orbitals favors conjugation of the heteroatomic n electrons which have not taken any part in the coordination to the metal. As a result the remaining n electrons acquire a π rather than a σ character and are not easily protonated with acids. In many cases where the metal ion has filled d orbitals of π symmetry ($d_{xy}$, $d_{xz}$, $d_{yz}$) it forms backward dative π bonds with the macrocyclic tetrapyrrol ligand. The metal serves as a donor of π electrons and the ligand as their acceptor. These bonds are opposite in direction to σ bonds, that is M → N, and are called backbonding. The d-π electrons of the metal fill the antibonding π orbitals of porphyrazine. The filling of antibonding π orbitals increases their energy, which prevents the n electrons of the meso-N atoms from

entering into a π conjugation as well as enhancing their σ character and capacity for acid protonation.

In addition to electronic and charge effects of coordination complexes with cyclic π ligands such as porphyrins, phthalocyanines, porphyrazines and other macroheterocyclic compounds, may in some cases display steric effects of coordination. If coordination distorts the planar structure of a conjugated cyclic system, the conjugation of n electrons of the nitrogen atoms with the macroring π system weakens. As a result the basicity of the molecules increases. If coordination to a metal creates a more coplanar π system than the ligand, the opposite is true.

The porphyrazine is isoelectronic with the porphyrin, but because of its nitrogen atoms at the meso positions chemically much closer to the technologically important phthalocyanines. To investigate the electronic properties of the phthalocyanines it is, therefore, necessary to address the influence of those nitrogens on the electronic structure.

In the visible absorption spectra of porphyrins, the highly conjugated aromatic macrocycle shows an intense absorption in the region of about 400 nm which is referred to as the Soret Band (Fig.1.2). Visible spectra of porphyrins also show four weaker bands, the Q bands, at longer wavelengths from about 450-700 nm giving rise to reddish purple color of porphyrins [5].

The effects of meso-tetraaza substitution on the UV-Visible absorption bands of porphyrins are to date well documented. Porphyrazine complexes exhibit for instance a significant red shift and an intensification of the lowest energy $\pi \rightarrow \pi^*$ Q band, and a more complicated Soret band region due to additional $\pi \rightarrow \pi^*$ transitions introduced by azamethine groups [6,7].

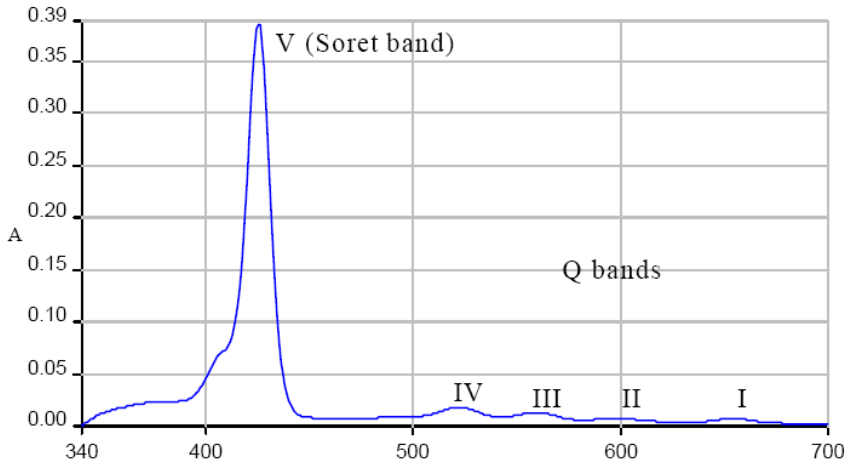


**Figure 1.2** UV-Visible spectrum of a porphyrin.

The UV-visible spectra in porphyrazines are influenced by substituents and the presence or absence of a metal at the centre. Peripheral substitution influences the UV-visible spectra with *cis*- and *trans*- isomers showing different split in LUMOs. *Trans*-isomers show large splitting compared to *cis*-peripherally substituted porphyrazines. In non-metalated porphyrazines with reduced symmetry, reduction in symmetry removes degeneracy of $e_g$ LUMO and gives a split Q-band (Fig.1.3) [8]. In cases where a lone pair of electrons in peripheral ligating atoms (N) becomes bonded to metal ions, the Q-band is split into two sharp bands (Fig.1.4) because their interaction with the porphyrazine ring is suppressed [8].

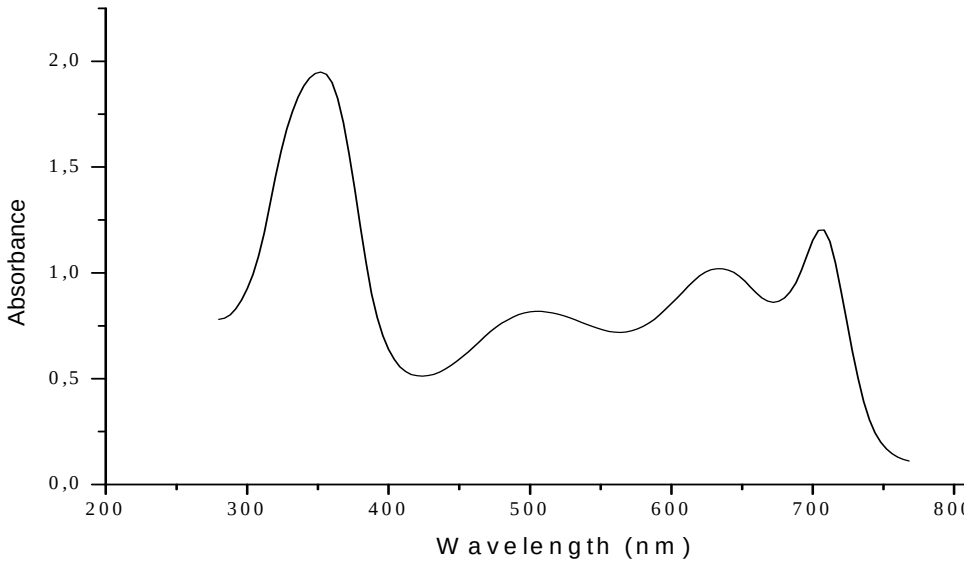


**Figure 1.3** Electronic absorption spectrum of $H_2Pz$.

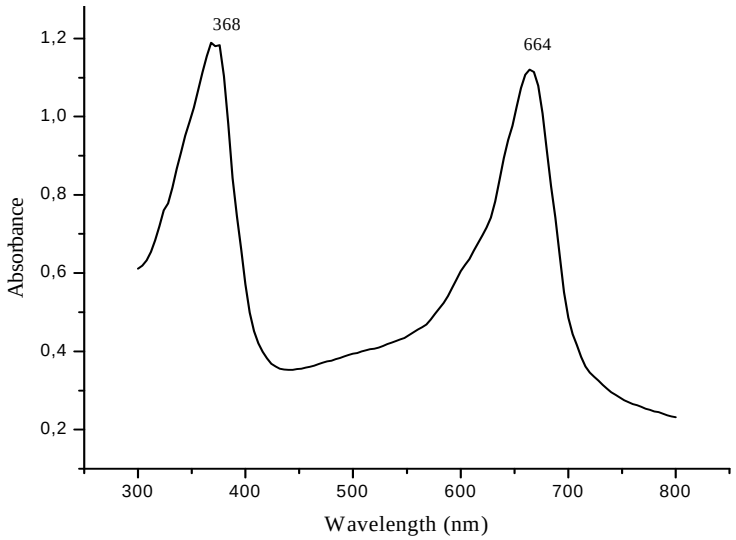


**Figure 1.4** Electronic absorption spectrum of MgPz.

For nonmetalated (metal-free) porphyrazines ($D_{2h}$ symmetry), the UV-visible spectra show two lower energy split Q-bands at 550-700 nm and a higher energy Soret (B) band at 300-400 nm, which are assigned to $a_u \rightarrow b_{2g}$ (Qx), $a_u \rightarrow b_{3g}$ (Qy) and $b_{1u} \rightarrow b_{2g}$ (Qx), $b_{1u} \rightarrow b_{3g}$ ($B_y$) transitions (Fig.1.5). These transition bands are assigned to excitations from the two highest-occupied molecular orbitals (HOMO) ($a_{1u}$ and $a_{2u}$) into lowest unoccupied molecular orbitals (LUMO, $e_g$) [8,9]. The lower energy peak which could be found at 400-500 nm is assigned to n-π* transitions from the lone-pair electrons in external meso-nitrogen atoms into a π* ring system.

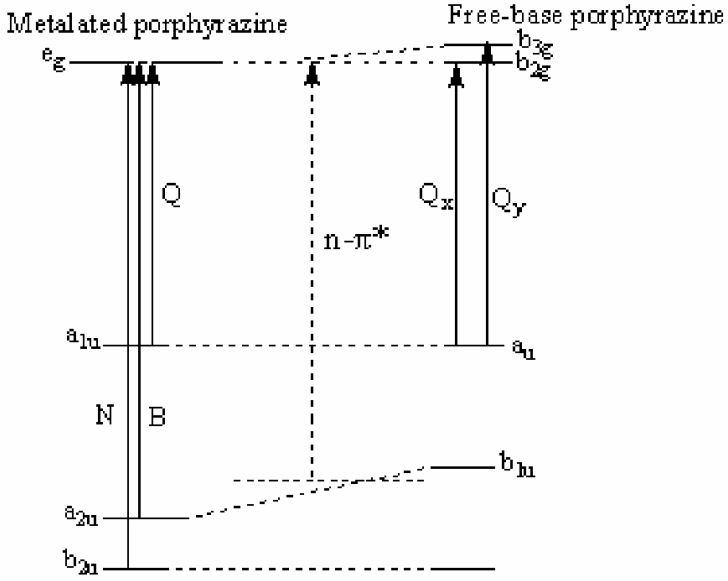


**Figure 1.5** Electronic transitions in the visible and close UV regions of metalated and non-metalated porphyrazines.

Metalated porphyrazines exhibit two intense $\pi \rightarrow \pi^*$ absorbances, a low energy Q band that is accompanied by a slight higher energy shoulder and a higher energy B band. For metalated porphyrazines, the symmetry of the chromophore is $D_{4h}$ with the two LUMOs $b_{2g}$ and $b_{3g}$ giving rise to a two-fold degenerate $e_g$ level resulting to an unsplit Q and B absorptions associated with transitions $a_{1u} \rightarrow e_g$ and $a_{2u} \rightarrow e_g$ [10,11].

The molecules from the porphyrazine class have gained interest from the scientific community due to both their potential in technological applications and their relationship to biological important porphyrins, such as chlorophyll and hemoglobin molecules, that play a vital role in life processes. The remarkable construction of porphyrazines, characterized by high symmetry, planarity, and electron delocalization, made these molecules attractive for theoretical studies as well.

X-ray crystallography is the most reliable method for the evaluation of the molecular geometry in the solid state. X-ray data have been reported for the free-base porphyrin ($H_2P$) and some of its derivatives: meso-substituted tetraphenylporphyrin ($H_2TPP$), tetrapropylporphyrin ($H_2TPrP$) as well as β-substituted octaethylporphyrin ($H_2OEP$). Among azaporphyrins, only the structures of two tetrabenzoderivatives, namely monoazatetrabenzoporphyrin ($H_2MATBP$) and tetrabenzotetraazaporphyrin commonly named phthalocyanine ($H_2Pc$) have been studied by this method. The average structural data are represented in Table 1.1.

The skeleton of common porphyrin ligands can be considered as almost planar since the deviations of the C and N atoms from the mean plane do not exceed 0.006 nm. The symmetry of the skeleton is in most cases $D_{2h}$. A $D_{4h}$ skeletal symmetry was found for monoclinic $H_2P$ and tetragonal $H_2TPP$. $D_{2h}$ distortion of the porphyrin ligands is connected above all with the inequivalent of the five-membered rings composing the macrocycle. In two trans-located pyrrole type-rings (A) the bonds $C_\alpha$-$C_\beta$ are about 0.002-0.003 nm shorter, $C_\beta$-$C_\beta$ bonds are about 0.002 nm longer and the inner angle formed by the nitrogen atom is 2.5-4$^o$ larger compared with a pair of the neighboring pyrrolenine-type rings. At the same time the bond lengths between $C_\alpha$ atoms and the inner nitrogen atoms vary only slightly in these two ring types and are 0.002-0.003 nm shorter than the bonds of $C_\alpha$ atom with $C_{meso}$ atom (Fig.1.6). The symmetric alkyl or aryl substitution in the meso or β positions has little influence the changes in the bond

lengths and values of the angles do not exceed 0.002 nm and $2^{o}$. The dimensions of the central coordination cavity (measured as a distance between the intracyclic N atoms $N_{pyr}$ and macrocycle center $C_t$) vary slightly in the range 0.204-0.206 nm (Table 1.1). One can expect that the direct substitution of the carbon atom in the conjugated π system of the porphyrin with a heteroatom, namely aza-substitution in the meso positions, should produce significantly greater changes in the geometry of the reaction center and that is the case in fact.

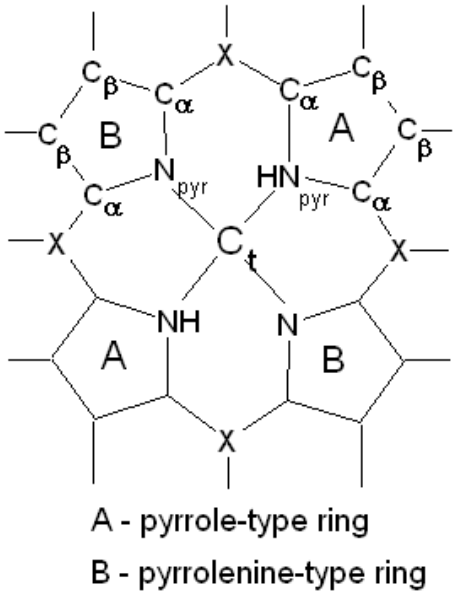


**Figure 1.6** Pyrrole-type and Pyrrolenine-type Rings.

**Table 1.1** Average geometrical parameters for the CN skeleton of porphyrin and azaporphyrin ligands.

| Geometric parameter | $H_2P$[a] | $H_2OEP$[a] | $H_2TPP$[a] | $H_2MATBP$ | $H_2Pc$ | $H_2Pc$ | $H_2TAP$ |
|---|---|---|---|---|---|---|---|
| $C_\alpha$-X (nm) | 0.1376<br>0.1387 | 0.1390 | 0.1400 | 0.125 (N)<br>0.139 (C) | 0.1335 | 0.132 | 0.133 |
| $C_\alpha$-$N_{pyr}$ (nm) | 0.1377<br>0.1380 | 0.1364<br>0.1367 | 0.1364<br>0.1374 | 0.145 | 0.1340 | 0.137 | 0.136 |
| $C_\alpha$-$C_\beta$ (nm) | 0.1452<br>0.1431 | 0.1462<br>0.1438 | 0.1455<br>0.1428 | 0.147 | 0.1490 | 0.147 | 0.144 |
| $C_\beta$-$C_\beta$ (nm) | 0.1345<br>0.1365 | 0.1353<br>0.1373 | 0.1347<br>0.1355 | 0.152 | 0.1390 | 0.140 | 0.134 |
| $N_{pyr}$- $C_t$ (nm) | 0.2051 | 0.2062 | 0.2060 | | 0.1913 | | 0.194 |
| $C_\alpha$-X-$C_\alpha$ ($^0$) | 126.9 | 127.7 | 125.6 | 111 (N)<br>143 (C) | 115<br>119 | 122<br>125 | 122 |
| $C_\alpha$-$N_{pyr}$-$C_\alpha$ ($^0$) | 106.1<br>108.5 | 105.7<br>109.6 | 106.2<br>109.2 | 109 | 109 | 109 | 108 |
| X-$C_\alpha$-$N_{pyr}$ ($^0$) | 125.1 | 125.0 | 126.2 | 132 (N)<br>123 (C) | 131 | 127<br>130 | 128 |

[a] Data are given for pyrrolenine and pyrrole-type rings.

The only X-ray study of metal-free phthalocyanine made by Robertson in 1936 showed that the $H_2Pc$ molecule is planar and has $D_{2h}$ symmetry. Unlike porphyrins this $D_{2h}$ distortion of the tetragonal symmetry of the skeleton owes its origin not to the inequivalence of pyrrole rings but to the difference in the angles formed by neighboring meso-nitrogen atoms. The bonds composing the inner 16-membered macroring in $H_2Pc$ are shorter than in the porphyrins. The bonds formed by the bridge atoms (in this case meso-nitrogen atom) are considerably shortened. Thus the alternation of the bonds of the inner macrocycle which is noticeable in porphyrins (about 0.137 nm for $C_\alpha$-$N_{pyr}$ and 0.139-0.140 nm for $C_\alpha$-$C_{meso}$ bonds) is barely perceptible in phthalocyanine ($C_\alpha$-$N_{pyr}$, 0.134 nm; $C_\alpha$-$N_{meso,}$ 0.133-0.134 nm). The values of the angles formed with participation of the bridge atoms also change. In comparison with porphyrins the angle $C_\alpha$-$X_{meso}$-$C_\alpha$ is decreased by $10^o$ and the angle $N_{pyr}$-$C_\alpha$-$X_{meso}$ increased by $6^o$. These changes in bond lengths and angles lead to a significant shrinkage of the central

coordination cavity, by 0.026 nm compared with porphyrins. The geometry data for $H_2Pc$ obtained by Hoskins et al. by a neutron diffraction method differ somewhat from the data of Robertson. However the observed change in the dimensions of the reaction center as one goes from porphyrins to phthalocyanine is the same.

Recently the results of the first X-ray investigations of complexes of tetraazaporphyrins were published. Comparison of these structural data with the data on corresponding complexes of porphyrins, tetrabenzoporphyrin and phthalocyanine reveal the separate influence of aza and benzo substitution. In order to reveal what structural changes are produced in the CN skeleton of the porphyrin ligand by tetrabenzo and tetraaza substitution we consider the available structural data on the metal free compounds ($H_2P$, $H_2OEP$, $H_2TPP$ and $H_2Pc$) and complexes of Fe (ClFePc, ClFeOETAP, ClFeTPP, and $C1O_4FeOEP$) and Ni (NiPc, NiTBP and NiTMP). Aza substitution reduces the angles formed by a bridge atom and shortens the bonds composing the inner 16-membered ring. In the case of porphyrins the bond between $C_\alpha$ atom and meso-atom is especially shortened. Only the $N_{pyr}$-$C_\alpha$ bonds change significantly in the isoindole fragments whereas in the pyrrole fragments the isolation of ethylene double bonds is distinct and their geometry changes drastically. Benzo substitution has little impact on the geometry of the inner macroring in tetraazaporphyrins, while in the porphyrins the bonds and angles formed by the bridge carbon atom are significantly reduced.

Thus the comparison of metallocomplex structures reveals that aza substitution affects the geometry more strongly than benzo substitution and that its effect is more pronounced in porphyrins (and their alkyl and aryl derivatives) than in tetra-benzoporphyrins. One can expect that in the free ligands, in the absence of a central metal ion rigidly bonding the inner nitrogen atoms, the effect of aza substitution will be greater.

# CHAPTER 2
# GENERAL INFORMATION ABOUT PORPHYRIN AND PHTHALOCYANINE COMPLEXES

## 2.1 General Concepts of Porphyrin and Phthalocyanine Complexes

Metalloporphyrins, which include, such important natural complexes as chlorophyll (Fig.2.1), haem of the blood (Fig.2.2), and others, represent a vast and unique group of intercomplex compounds [12].

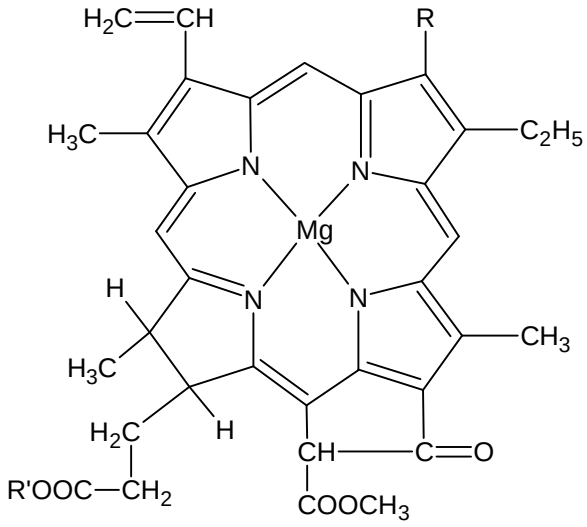


1a: R' $C_{20}H_{39}$; R = $CH_3$, 1b: R' = $C_{20}H_{39}$; R = CHO

**Figure 2.1** Chlorophyll.

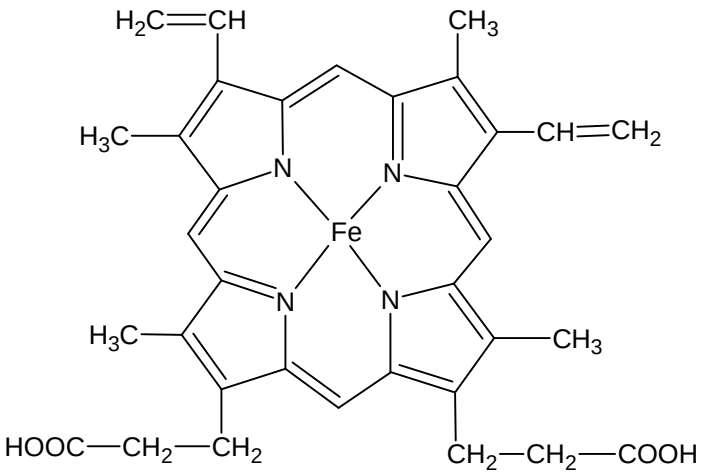


**Figure 2.2** Haem of the blood.

The central metal atom displaces two hydrogen ions from the porphyrin ligand and practically finds itself in a symmetrical electrostatic field of four nitrogen atoms with which it may form four equivalent, or almost equivalent, coordinate, donor-acceptor bonds. If the interaction between the metal and the porphyrin anion is primarily electrostatic, labile ion complexes are formed. These include complexes of $Na^{+}$, $K^{+}$, $Rb^{+}$, $Cs^{+}$, $Be^{2+}$, $Sr^{2+}$, $Ba^{2+}$, $Ca^{2+}$, and some other ions. But if the electrostatic interaction involves filling of the vacant orbitals of the central atom by the electrons of the donor N atoms of the ligand, stable porphyrin complexes of the covalent or predominantly covalent type are formed. In this case we have complexes of $Fe^{2+}$, $Fe^{3+}$, $Co^{2+}$, $Ni^{2+}$, $Cu^{2+}$, $Zn^{2+}$, $Mn^{3+}$, $Cr^{3+}$, $Al^{3+}$, $Ga^{3+}$, $Si^{4+}$, $Ge^{4+}$, $Sc^{3+}$, $Ti^{4+}$, $VO^{2+}$, $Pt^{4+}$, $Os^{4+}$, and other cations. Most of the above complexes are formed by biometals. As will be seen from what follows, complexes of porphyrins with $Mg^{2+}$, that is chlorophyll and its structural analogues, do not belong either to purely ionic complexes or to the stable group of predominantly covalent complexes. This peculiarity of chlorophyll, stemming from its intermediate position in the complex stability series, is to some extent responsible for its unique role in nature.

In contrast to chlorophyll, the complex of protoporphyrin with $Fe^{2+}$ ($Fe^{3+}$) is one of the most stable metalloporphyrins of the covalent type. This property is fully consistent with both the biological composition of the medium in which haem acts in a complex with protein and with its biological functions.

The specific features of metalloporphyrins as intercomplex compounds are due not only to the polydentate (tetradentate) nature of the ligand but also to its rigidity. The latter is determined by the planar structure of the large ring of the porphyrin molecule, by the unique conjugation in it which is due to the strong π-electron interaction over the entire large ring (so-called macroring), and by the particularly favorable structure of the coordination center, consisting of four nitrogen atoms, on account of which most metal ions easily enter this space, coming into close contact with the nitrogen atoms. Because of its high rigidity the porphyrin ligand imposes specific requirements on the geometric parameters of the metal ion, whereby they form two clearly defined groups of stable or labile complexes.

Characteristically, the metal ion that has entered into coordination with a porphyrin is in fact a partner of the conjugated porphyrin system and may either stabilize or destabilize it. Owing to this direct contact with the atoms of the conjugated system, it influences all, even the most remote parts, of the large molecule and alters the oxidation-reduction, acid-base, electron-optical, and all other properties of the porphyrin. In this connection it is of particular interest for a coordination chemist to use metalloporphyrins in examining the effect of the nature of the metal involved, the type of chemical bonding, and its strength on the major properties of porphyrins.

A specific feature of metalloporphyrins is their insolubility in water and solubility in organic solvents in cases where no significant solvation centers are present among the functional substituents of the ligand. This is the reason why most studies of porphyrins and metalloporphyrins have been conducted in non-aqueous media.

Another salient feature of porphyrins is their structural diversity, which can be seen in Figure 1.1.a.

Porphyrins differ in the nature of the bridging groups occupying meso positions in the porphyrin molecule. The bridging groups may only be -CH=, -(X)C=, -N=, or their combinations. The structural diversity of porphyrins is further enhanced by the presence of various pyrrole substituents ($R_1$-$R_8$) which may be H, $CH_3$, $C_2H_5$, $CH=CH_2$, $CH(OH)CH_3$, C(O)H, COOH, $CH_2COOH$, and $CH_2CH_2COOH$. If it is also taken into consideration that one or more pyrrole double bonds may be hydrogenated and that adjacent substituents $R_1$-$R_8$ and $R_\alpha$-$R_\delta$ may form closed cycles, then the diversity of

molecular structures of porphyrins azaporphyrins, phthalocyanines, and so on becomes more evident. It should be emphasized that a porphyrin molecule ceases to exist as soon as at least one double bond in the macroring is hydrogenated.

The specific features and great diversity of porphyrins particularly metalloporphyrins, are the factors responsible for their importance and wide distribution in nature, their extensive use in various physical, physicochemical, quantum-chemical and biological studies as well as in the production of dyes, semiconductors, and catalysts. The structural diversity of porphyrins and metalloporphyrins opens up enormous possibilities for studying the effect of functional substituents and central atoms on the properties of porphyrins. Such studies will make it possible in the future to provide an answer to the question why Nature has chosen, as the basic component of the photosynthetic and respiratory molecular system, porphyrins with a particular combination of functional such as can be found in chlorophyllic acids and protoporphyrin.

An important characteristic of porphyrin complexes is their extremely high stability to dissociation. This is one of the reasons why nobody has been able so far to measure quantitatively the equilibria of their formation in a direct manner and to characterize this stability in terms of a definite constant. The kinetic method has been widely used in investigating the stability of porphyrin and phthalocyanine complexes.

The capacity of complexes for additional coordination is to some or other degree their common property. However one can hardly find another instance where, the coordination of additional ligands is as manifest as in the case of planarly coordinated metalloporphyrins. It is referred to as extra coordination for the ligands are attached along the z axis passing through the metal atom at a right angle to the plane of the porphyrin molecule. Extra coordination is an important property of such metalloporphyrins as chlorophyll, haem of the blood, catalyses, and others for it results in attachment of the active metal complex to the molecule of the carrier protein and is essentially a transport reaction as far as oxygen, hydrogen peroxide, and the electron are concerned.

Finally, an important and unique feature of porphyrins and their metal derivatives is their electronic absorption and emission spectra. The diversity of the

latter, corresponding to the great variety of porphyrins, the typical arrangement of spectral bands, the sensitivity to certain effects on the molecule, and their complexity, make them not only a most reliable means for identifying porphyrins but also a rich source of information on the structure of porphyrins, the type of their coordinations, the interaction between substituents and ionizing media, and the intramolecular energies.

Porphyrin molecules perform their biological and catalytic functions only within metalloporphyrins. These functions are determined by the coordination (donor acceptor, complexing) properties of the porphyrin molecule and metal. Since they are bound in the metalloporphyrin molecule by a very strong chemical interaction which ensures the integrity of the entire molecule, we may speak of coordination properties of metalloporphyrins, meaning their capacity for further coordination to extra ligands and for staying together that is coexisting in proton-donor media.

Thus the coordination properties of porphyrins determine the conditions for and rates of formation of metalloporphyrins and their ability to survive in various media (including proton-donor, oxidation-reduction, and photoexciting ones) without undergoing protolytic dissociation and oxidative or photo-oxidative degradation. They also determine the capacity of porphyrins for acting as photosynthetic, respiratory pigments and enzyme (catalytic) systems.

Investigations of coordination phenomena involving porphyrin molecules are, thus, of paramount importance in the chemistry of porphyrins. Work in this field has been under way over the past two or three decades and is rapidly progressing with studies being conducted in many countries [13]. However, the total volume of research into coordination phenomena involving metalloporphyrins is still far from being adequate to the scientific magnitude of the problem. This lag of the coordination chemistry of porphyrins is primarily due to the complexity and unavailability of most porphyrin ligands and to the long established concept of poor stability and ephemeral nature of porphyrin molecules isolated from natural sources under conditions normally prevalent in complex formation studies. This is probably why in many physicochemical studies use is made of stable synthetic porphyrins such as tetramethyltetraethylporphyrin (etioporphyrin), α, β, γ, δ-tetraphenylporphyrin and α, β, γ, δ-tetrapyridylporphyrin.

Naturally, of greatest practical interest are the coordination properties of two most important natural porphyrins-chlorophyllic acid (phaeophytine) and protoporphyrin as well as their complexes. In this work they are given primary attention. At the same time, it should be borne in mind that no solution to problems concerning the effect of functional substituents and the structure of a porphyrin molecule as a whole on its activity in biological and other processes can be found without investigating as many porphyrins of different structure as possible, including synthetic ones. This aspect of the problem is also treated at length in the present monograph.

The question as to the role of the central metal atom in molecules of biologically active metalloporphyrins is yet to be answered. Magnesium is present in chlorophyll, while the haem of haemoglobine, cytochromes, and catalase contains an iron atom. To answer the question why these two and no other metals are involved in biological evolution one must examine the effect of the species of the metal atom on all physicochemical phenomena occurring with the participation of porphyrins in photosynthesis, oxygen transport, intracellular oxidation, and other processes. The most interesting in this respect are the electron-optical, oxidation-reduction, and coordination properties. Systematic studies into the kinetic stability of metal analogues of chlorophyll and haemin have given insight into the specific role the magnesium atom plays in the chlorophyll molecule from the standpoint of coordination properties of metalloporphyrins.

As far as the iron atom is concerned, the picture is much clearer. Its particular role stems from the abundance of iron in the Earth’s crust rather than from the specific features of its electronic structure since the function of reversible addition and oxygen transport can be performed by other metals as well, for example, cobalt, which may form complexes with porphyrins, possessing a sufficiently high thermodynamic stability and capable of withstanding oxidative degradation in the presence of active haemoglobine [14].

## 2.2 Synthesis, Isolation and Purification of Porphyrin and Phthalocyanine Complexes

Complex compounds of chlorophyllic acid, protoporphyrin and most of their structural analogues are synthesized from available ligand molecules of porphyrins and metal salts. Therefore the problem of synthesis of complexes is determined entirely by the availability of respective porphyrins. Only in the case of phthalocyanine or its polymers are complexes easier to synthesize in sizable amounts from semi-products that is from structural units making up a phthalocyanine ligand, in the presence of a metal.

The majority of TAP structures prepared from 1937 to 1990 have been collected by Luk'yanets and Kobayashi [15]. Since porphyrazines are analogs of phthalocyanines with the only differences of the absence of the fused benzene ring on the pyrole units, the synthetic methods applied to phthalocyanines can be used to synthesize porphyrazines.

Porphyrazine can be synthesized from functionalized nitriles such as maleonitriles, fumaronitriles and phthalonitriles. Like benzoporphyrazines (phthalocyanines), the synthesis of porphyrazines is limited to Linstead macrocyclisation in which the dinitrile **1** or **2** undergoes a macrocyclisation reaction under reflux in the presence of a magnesium alkoxide in the corresponding alcohol (typically 1-butanol or 1-pentanol) or dimethylaminoethanol to yield **3** (Fig.2.3). Magnesium porphyrazines such as **3** are easily demetalated under acidic conditions to form the free-base porphyrazine such as **4** [16,17].

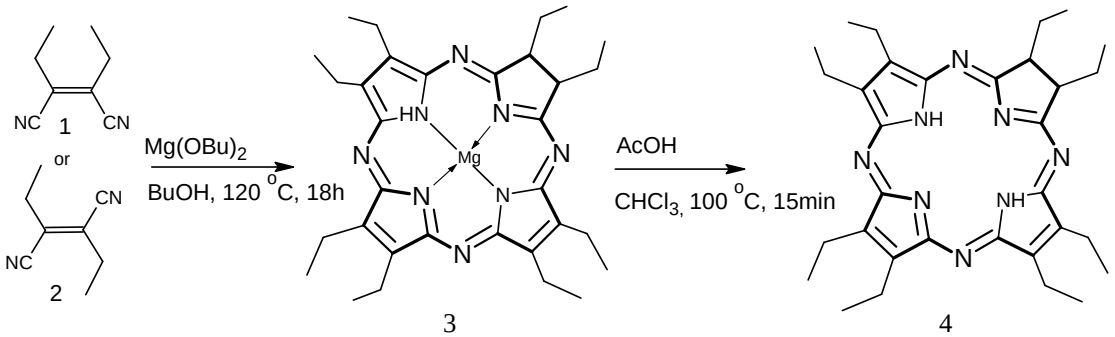


**Figure 2.3** An example of porphyrazine synthesis.

Removal of magnesium can be achieved by treating a solution of magnesium octaethyltetraazaporphyrin **3** in chloroform and acetic acid for 15 minutes, to give free-base porphyrazine **4**. The above synthetic method is known as Linstead magnesium template macrocyclisation. The same synthetic method is also applicable if two different precursors are macrocyclised to form different porphyrazine hybrids (Fig.2.4) [18].

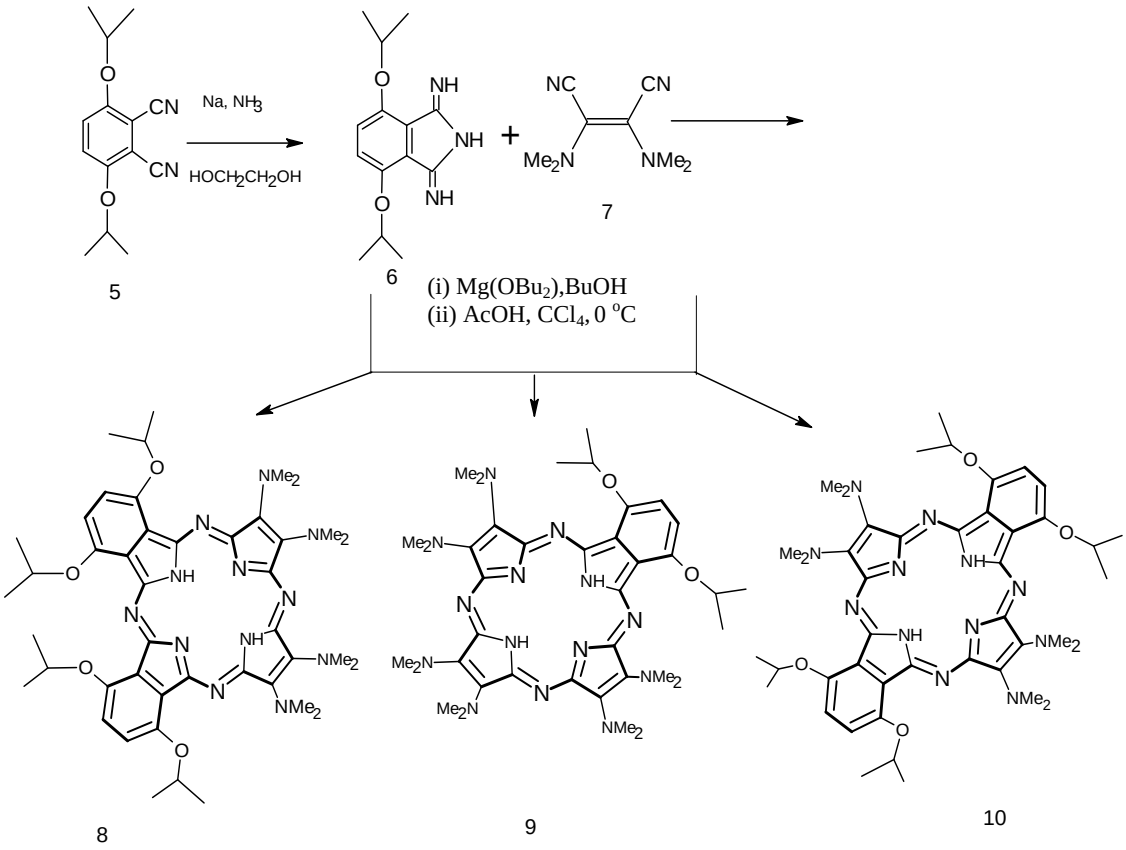


**Figure 2.4** Synthesis of porphyrazine molecules from two different precursors.

Since phthalonitrile **5** is unreactive in the synthesis of either the phthalocyanine or porphyrazine, it is first converted into its corresponding 1,3-diiminoisoindoline **6** to increase its reactivity. A suspension of phthalonitrile **5** in 1,2-ethanediol is bubbled with ammonia gas in the presence of sodium metal. The 1,3-diiminoisoindoline **6** derived from hydroquinone isopropyl ether **5** is then reacted with dimethyl aminomaleonitrile **7** to give porphyrazine hybrids **8**, **9**, **10** (Fig.2.4) [18].

Some metal free porphyrazines can be prepared directly from succinoimidines by heating in high boiling solvents such as chlorobenzene and nitrobenzene (Fig.2.5) [15].

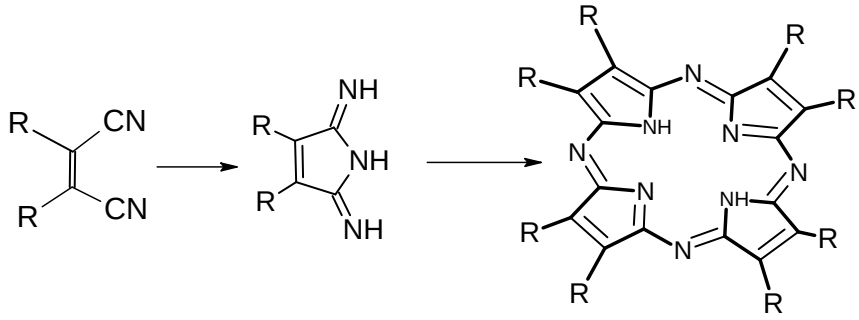


**Figure 2.5** Synthesis of metal free porphyrazine directly from succinoimidine.

Nowadays metal-free porphyrazines are obtained by demetallation of corresponding magnesium porphyrazine with acid such as TFAA or HCl (Fig.2.6).

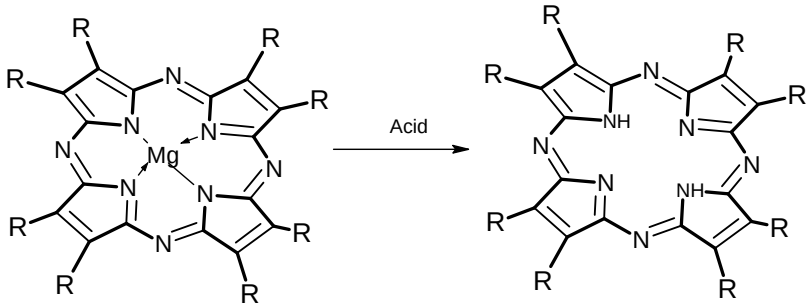


**Figure 2.6** Synthesis of metal free porphyrazine by acid treatment.

Various substituents provide porphyrazines with substantial organic solubility compared to their porphyrin and phthalocyanine counterparts. Peripheral substitution among porphyrazines is becoming an increasingly popular strategy for the design of functional dyes and molecular devices. Porphyrazines with peripheral substitution of the form M[Pz-($A_n$:$B_{4-n}$)], where A and B are functional groups fused to the β-position of the pyrroles, have the potential to exhibit magnetic and electronic properties [9,19,20]. Due to peripheral substitution, these porphyrazines show unusual UV-Visible spectra, redox chemistry and electrochemistry. In addition, they exhibit interesting coordination chemistry for binding of metal ions within the macrocyclic cavity and by peripheral ligating groups (N, S, O) [21]. Substituted amphiphilic and hydrophilic porphyrazines bearing both hydrophilic and hydrophobic moieties can be more potent as photosensitisers in photodynamic therapy [22-24]. With acetylinic units as peripheral substituents, the π-systems of the chromophores are enlarged and bathochromic shifts in the electron absorption and emission spectra are induced. Alkyl groups also serve as

covalent linkers for the assembly of delocalized multichromophore chains or two dimensional polymer networks [25].

The second method involves the macrocyclisation of substituted precursors, which may lead to a cleaner product of known substitution pattern. Peripheral substitution in porphyrazines is achieved by reacting with substituted phthalonitrile and a maleonitrile, or reacting two maleonitriles. However, as shown in Figure 2.7, this method also leads to the formation of isomers due to the symmetry involved in macrocyclisation. While macrocyclisation of substituted precursors has its drawbacks, it is still the method of choice for the synthesis of substituted porphyrazines with improved properties.

*Trans*-substituted porphyrazines can be synthesized by using a phthalonitriles with bulky groups. In this case, the bulky group appears once or twice due to steric hindrance in which the steric groups cannot be adjacent and co-planar (i.e. bulky groups are prevented from being adjacent to each other) as shown in Figure 2.7 [26].

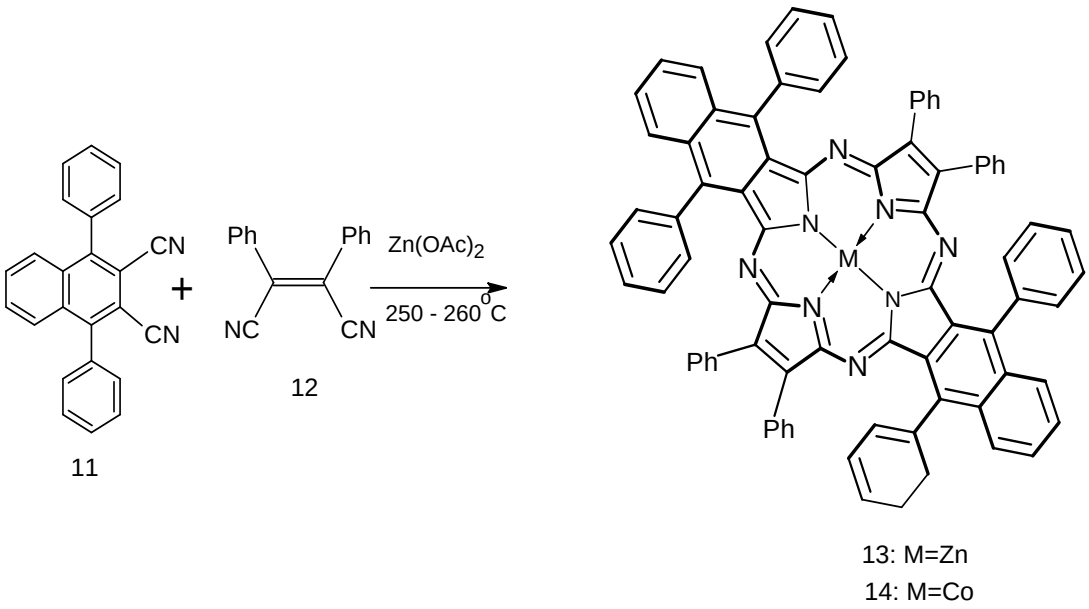


**Figure 2.7** Synthesis of *trans*-substituted porphyrazine.

The most successful pathway of synthesizing unsymmetrical substituted porphyrazines is to a use statistical condensation of two substituted precursors A and B in which the desired product can be isolated by column chromatography. Although the method also gives a mixture of six compounds, required compound can be isolated as a

major product. If, for example, the reaction is done with the precursors A: B at a ratio of 1:8 or above, the major product is that in which A: B is incorporated into the pigment in the ratio of 1:3 (Fig.2.8).

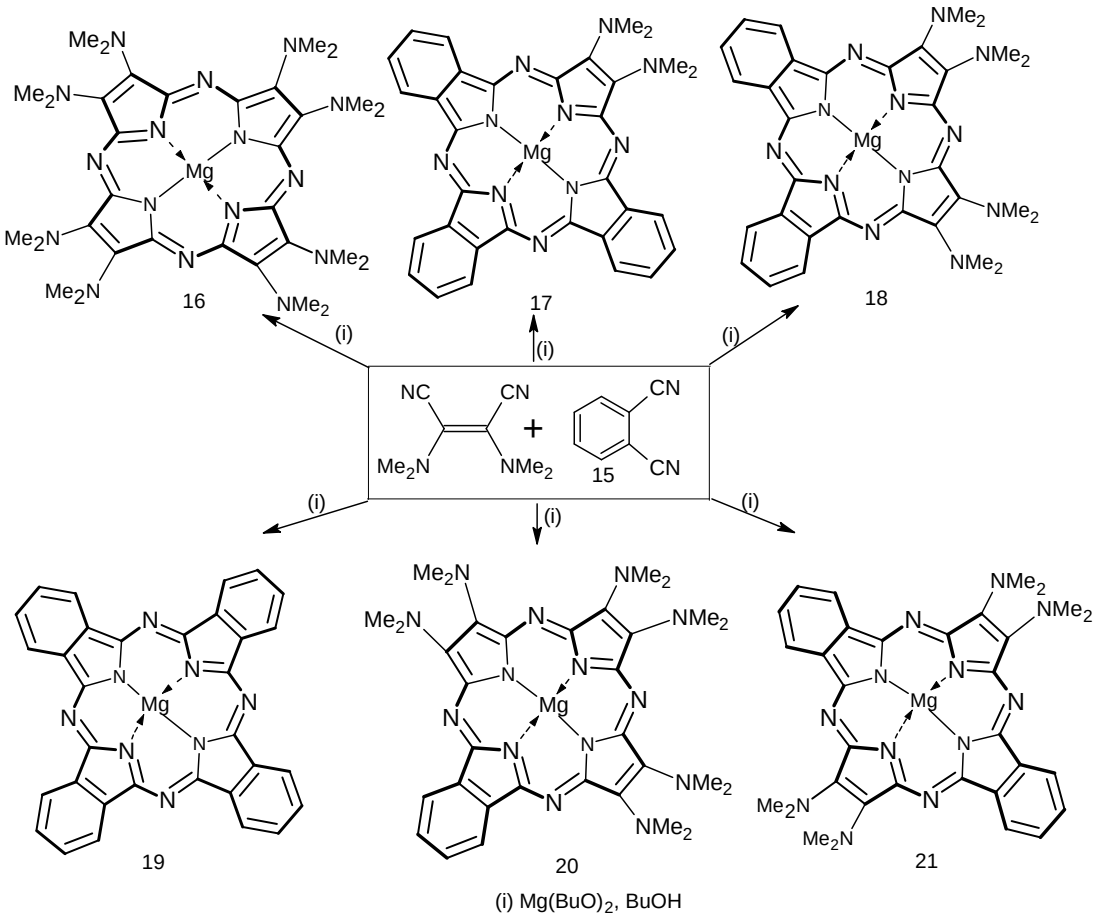


**Figure 2.8** Synthesis of unsymmetrical porphyrazine.

## 2.3 Transition Metal Complexes of Porphyrazines

The porphyrazine macrocycle is a good ligand to most metals even though only few porphyrazine metal complexes have been reported compared to their phthalocyanine and porphyrin counterparts, where most research in this area has been centered. This is because porphyrazines still represent a new field of research, with much research based on the selective incorporation of substituents. Even though metalations can be effected as an integral part of their synthesis, such as in cases in which the macrocyclisation in the presence of a templating transition metal salt or Li or Mg alkoxides, the best method that gives a product of high purity is the metalation reaction of a free-base ligand [27,28].

It has been already determined that a metal in the centre, or metal complexes to peripheral ligating groups can alter the physical and chemical properties of a porphyrin, phthalocyanine or porphyrazine [28,29]. When the central metal is iron or cobalt, phthalocyanines make good electrocatalysts for the reduction of oxygen at a fuel cell cathode [30]. It has also been shown that iron (II) porphyrins decompose oxygen through a mechanism involving two porphyrins acting on oxygen molecule. Metal porphyrins have been also shown to catalyze carbene-type transformations with diazo reagents such as cyclopropanation of alkanes and C-H insertion of alkanes. Recently, it has been reported that iron (II) porphyrin complexes can catalyse the olefination of a selection of aldehydes with diazoacetate in the presence of triphenylphosphine [31]. With porphyrins, phthalocyanines and porphyrazines as photodynamic therapy agents, a metal in the centre may improve their photosensitivity, especially in the instances of the diamagnetic metals like zinc [32].

The normal charge of a porphyrin, porphyrazine or phthalocyanine is (-2). Therefore, the metal ion to be accepted in order to form a stable complex is the one with a (+2) charge. Metal ions with a charge of (+1), requires an additional ion with (+1) charge (Fig.2.9) [30].

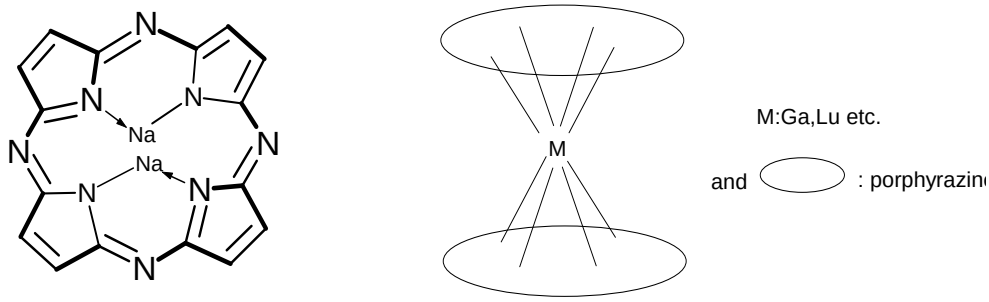


**Figure 2.9** Metal complex formation of porphyrazine.

Metal ions with a charge of (+3) or higher require additional “axial” ligands. In the case of larger ions, the phthalocyanine or porphyrazine or porphyrin cannot fully accommodate these ions within the core cavity and in this case the metal becomes surrounded by two phthalocyanines, porphyrins or porphyrazines, making a “sandwich” complex (Fig.2.9) [30].

Metalation in phthalocyanine and porphyrazine compounds can be incorporated into the synthesis as shown in Figure 2.10 [31,32]. In a metal-free porphyrazine, central metalation is mostly done by heating from 50 ºC to reflux the metal-salt [$Zn(OAc_2)$, $MnCl_2$, etc.] in a mixture of chlorobenzene and DMF or in neat DMF. Peripheral metalation can be effected by heating the porphyrazine in a suitable solvent mixture (mostly using acetonitrile-trichloromethane) [31,34].

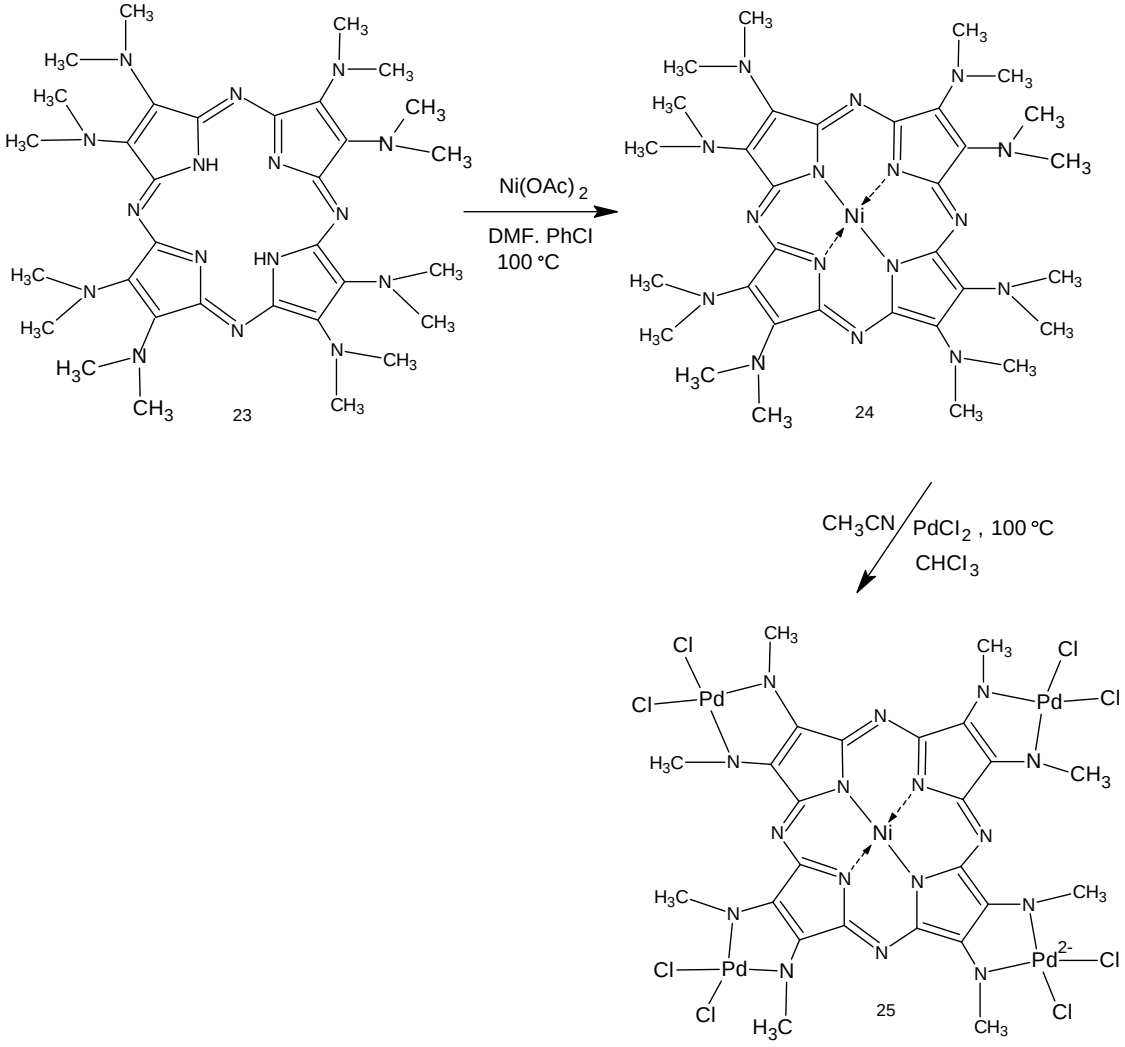


**Figure 2.10** The synthesis of metal complex of porphyrazine **24** with Ni (central) and Pd (peripherally) metals.

Of all the metalloporphyrins listed in Table 2.1 the highest stability is exhibited by complexes of metals $Pd^{2+}$, $A1^{3+}$, $Cr^{3+}$, $Sn^{4+}$, $Si^{4+}$, $Ge^{4+}$, $V^{4+}$, $Ti^{4+}$, $W^{5+}$, $Re^{5+}$ and $Ta^{5+}$, which can be exposed to concentrated $H_2SO_4$ without the metal ion being split off. The use in synthesis reactions of porphyrins made spectroscopically pure by

chromatographic separation or extraction does not require any additional purification of the complex.

If the starting porphyrin contains etherified carboxyl groups, for example $H_2$MP DME or $H_2$PP DME, etherification and chromatographic separation on a column are required after complex formation under stringent conditions, in some cases with subsequent recrystallization. Such procedures are described for vanadyl mesoporphyrin synthesized from $H_2$MP DME and $VCl_4$ in a scaled glass tube at 165 $^oC$ for $Mn^{3+}$ mesoporphyrin synthesized from mesoporphyrin hydrochloride and $MnAc_2$ in glacial HAc with admission of air, and by other investigators.

Many metals form metalloporphyrins with different degrees of oxidation of the central atom. They include $Fe^{2+}$-$Fe^{3+}$, $Co^{2+}$-$Co^{3+}$, $Ag^{+}$-$Ag^{2+}$, $Mn^{2+}$-$Mn^{3+}$-$Mn^{4+}$, $Sn^{2+}$-$Sn^{4+}$, $Cr^{2+}$-$Cr^{3+}$. The least stable of all are $Fe^{2+}$, $Mn^{2+}$, $Ag^{+}$, $Cr^{2+}$ and $Sn^{2+}$ porphyrins. Cobalt usually yields complexes in the form of $Co^{2+}$; special oxidation conditions are required for it to become $Co^{3+}$. However, some porphyrins promote oxidation in air; for example, protoporphyrin with $MnAc_2$ and $CoAc_2$ in hot glacial HAc forms (HO)MnPP and (HO)CoPP in the presence of HCl and air.

A complex of mesoporphyrin DME with $Co^{2+}$ prepared in methanol turns to (HO)CoMP when kept in air. The metal oxidation process is catalyzed with olefins and acetylenes.

**Table 2.1** Conditions for synthesis of metalloporphyrins of multicharge ions.

| **Metal ion** | **Reagent salt** | **Solvent** | **Conditions** | **Metallo Porphyrin** |
|---|---|---|---|---|
| $Al^{3+}$,$Cr^{3+}$, $Mn^{3+}$, $Fe^{3+}$, $Ga^{3+}$, $1n^{3+}$ | $M(Acac)_3$ | Ethanol | Heating in a sealed ampoule | (Acac)MP |
| $Zr^{4+}$, $Hf^{4+}$ | $M(Acac)_4$ | Ethanol | Heating in a sealed ampoule | $(Acac)_2$MP |
| $TiO^{2+}$, $VO^{2+}$ $MoO^{3+}$ | $MO(Acac)_2$ | Ethanol | Heating in a sealed ampoule | O=MP |
| $Ta^{5+}$, $Sb^{5+}$ $Re^{5+}$ | $TaCl_5$, $Sb_2O_5$, $Re_2O_5$ | Ethanol | Heating in a sealed ampoule | $O[(O)MP]_2$ |
| $Co^{3+}$, $Sc^{3+}$ | $M(Acac)_3$ | Imidazole | Heating in a sealed ampoule | (Acac)MP |
| $In^{3+}$, $Cr^{3+}$, $Rh^{3+}$ | $MCl_3$ | Benzonitrile | Heating | (Cl)MP |
| $W^{5+}$, $Nb^{5+}$ | $MCl_5$ | Benzonitrile | Heating | $(C1_3)$MP |
| $Sn^{4+}$, $Si^{4+}$, $Ge^{4+}$ | $SnCl_2$, $SiCl_4$, $GeCl_4$ | Pyridine | Heating | $(C1_2)$MP |
| $Fe^{3+}$, $Mn^{3+}$ | $FeCl_3$, $MnAc_2$ | Glacial HAc | Heating | (X)MP[a] |
| $Re^{4+}$, $V^{4+}$ | $ReCl_5$, $VOSO_4$ | Glacial HAc | Heating | $(C1_2)$ReP, OVP |
| $Rh^{3+}$ | $[Rh(CO)_2C1]$ | Glacial HAc | Heating | (Cl)RhP |
| $Ru^{3+}$ | $RuCl_3$ | Tetramethyl urea | Heating | ClRuP |
| $Ir^{3+}$ | $[Ir(CO)_2C1_2]$ | Methyl cellosolve | Heating | ClIrP |
| $Tl^{3+}$ | $Tl(CF_3COO)_3$ | $CH_2Cl_2$ | Heating | (X)TlP[a] |

[a]X, anion of the respective salt.

## 2.4 Acid Base Properties of Porphyrins

Quite valuable information on the structure of porphyrazines and their analogs can be obtained while studying their behavior in the proton donor media [35,36]. In addition, the possibility of practical application of porphyrazine metal complexes and their analogs significantly depends on their stability in solutions. In this connection, the study of the acid-base interactions of porphyrazines and their complexes is of interest in both theoretical and practical aspects.

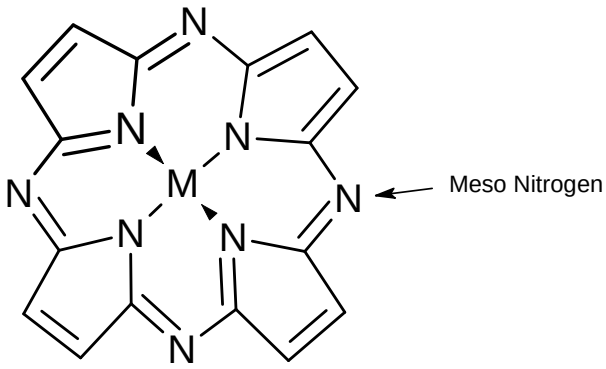


**Figure 2.11** Porphyrazine metal complex.

Porphyrazines are weak multicenter conjugated bases. The number of porphyrazine donor centers involved in the acid–base interaction with acids, the character of the interaction, and the stability of the acidic forms obtained depend on the porphyrazine structure and the properties of the proton donor medium. The π orbitals of endocyclic N atoms in metal complexes of porphyrazines participate in formation of bonds with a central metal atom. Therefore, only the exocyclic meso-nitrogen atoms are involved in the acid–base interaction (Fig.2.11). The long-wavelength region of the electronic absorption spectra of porphyrazine complexes in a neutral solvent contain intense Q-band due to the $\pi \rightarrow \pi^*$ electronic transitions $a_{1u} \rightarrow e_g^*$ of a macrocyclic ligand. The interaction of porphyrazines with acids is attended by the spectral changes in a visible region corresponding to the formation of different acidic-basic forms. In the case of porphyrazine complexes, the acid-base inter-actions occur in two stages, which are attended by bathochromic shift of the Q-band [37-39].

$$MPz + H^+ <=> MPzH^+ \quad (2.1)$$

$$MPzH^+ + H^+ <=> MPzH_2^{2+} \quad (2.2)$$

The transfer of a proton from acid HA to base B: proceeds through the stages of formation of the acid associate, H-associate, ion–ion associate and fully ionized protonated form:

$$B: + HA \Leftrightarrow B^{\cdot}....HA \Leftrightarrow B^{\cdot} ....H....A \Leftrightarrow BH^{+}.... A^{-} \Leftrightarrow BH^{+} + A^{-} \qquad (2.3)$$

Acid associate H-assosiate Ion-ion associate Protonated form

The acidic forms thus obtained differ from one another in a degree of a proton transfer from the acid molecule to the donor center. In media with a low ionizing capability, the electron-donor centers of porphyrazine participate in a weak acid–base interaction and form H-associates and ion–ion associates. The complete transfer of a proton can be observed in strongly ionizing medium only [40].

**2.5 Application Field**

The diversity of useful properties and structures of metalloporphyrins provides favorable conditions for varying the electronic states of the central metal atom which determines the coordination and catalytic properties, as well as searching for new effective catalytic systems that may be compatible with natural biocatalysts and even surpass them. We are speaking of synthesis, on the basis of porphyrin systems, of new effective catalysts, blood substituents, thermo- and photostabilizers, medicinal substances, organic semiconductors, pigments and dyes, solar cells, and inhibitors of homolytic degradation of protein molecules in living organisms exposed to X and gamma rays.

At present, natural porphyrins and their synthetic analogues are finding a host of industrial uses. Phthalocyanine which is a structural synthetic analogue of porphyrins, and its numerous intercomplex salts and functional derivatives arc especially well known pigments.

Their extremely high thermal stability, fastness to light, inertness to acids and alkalis, insolubility in most solvents, high dyeing power, purity, and color intensity have ensured their reputation and wide application in the painting, printing, textile, and paper industries, as well as in chemical fiber and plastic dyeing processes, as superior quality blue, blue-green, and green pigments. Also used as pigments are high-chlorine

derivatives of phthalocyanine and its complexes (e.g. “phthalocyanine green”, which contains up to 15 chlorine atoms in the copper-phthalocyanine nucleus). Sulpho derivatives of copper phthalocyanine arc employed as valuable direct dyes for cotton, known as “Sirius turquoise” and “direct light-fast turquoise”. In addition to the most widely used copper complex, complexes of phthalocyanine with Co, Ni, Al, and other metals are also used industrially.

The introduction of various functional substituents into the benzene nuclei of phthalocyanine, whereby it acquires solubility, new chromophore properties, and the ability to be fixed on fibers from solution, permits numerous dyes of different classes to be obtained on its basis.

A popular process in the textile industry is phthalogenic dyeing of fabrics, based on synthesis of phthalocyanines from intermediate products (so called phthalogens) directly on fibers.

Broad possibilities for using porphyrin complexes are being opened up in the technology of semiconductors and lasers, as well as in quantum-electronics research, because of their exhibition of semiconductor and other valuable properties.

Another promising area of their application as oxidation-reduction catalysts includes industrial synthesis, enzyme catalysis, and electrochemical processes involved in the catalytic reduction of oxygen in fuel cells. Other uses of phthalocyanines include, for example, processes for producing heavy isotopes of some elements and oxidation-reduction indicators.

### 2.5.1 Development of Photosensitisers

Haematoporphyrin derivative and photoporphyrin, both complex mixtures of compounds represent the first-generation of photosensitisers. Second-generation photosensitisers on the other hand are pure single compounds that exhibit photosensitizations properties and they include a number of porphyrins and phthalocyanines derivatives. During the early years in the development of photosensitisers for PDT, certain design criteria for good photosensitisers became apparent [41,44]. These can be summarized as follows:

- Lack of toxicity in the dark.

- Selective uptake by tumor tissue.
- Short-term retention to avoid the persistence of photosensitivity.
- Triplet energy greater than 94 kJ/mol.
- Intermediate lipid water partition coefficient.
- Single substance.
- Light absorption in the red or far red range of the visible spectrum.

The substances that meet these criteria include suitably modified porphyrins, chlorins, porphyrazines and phthalocyanines [45-50]. So far, many photosensitisers have been synthesized and tested; some of them show little or no activity in photo necrosis, sometimes poisonous. But these efforts have not been wasted, for they have provided the basis for the above design criteria and will continue to do so.

*Porphyrin, Porphyrazine and Phthalocyanines as Photosensitisers;* Porphyrins were among the first group of compounds to be used as photodynamic therapy agents. Many of the second generation porphyrins are now in clinical trials for different tumor lesions in different locations. They have improved tumor cell concentration compared to normal cells and also have improved fluid solubility and deep tissue penetration.

Porphyrazine derivatives are showing to be potential candidates as photosensitisers in photodynamic therapy. Recent photophysical studies of some zinc metalated peripherally substituted porphyrazines have shown high triplet quantum yields which are coupled with high oxygen quantum yields. They also absorb strongly in the red region which also makes them capable of deep tissue penetration and their biomedical application will soon be elaborated [46-50].

Phthalocyanines and their derivatives have shown great promise in PDT. They are porphyrin-like second-generation sensitisers for photodynamic therapy [46-50]. The most important attribute that makes phthalocyanines suitable for PDT is the intense absorption in the far red and long-lived excited triplet state [17].

During the past few years, a large number of new sensitisers have been suggested for clinical use, on the basis of experimental studies in animal or in cell cultures. There are several uncertainties and considerable expense related to bringing new agents to the clinic, and these account for the slow incorporation of new sensitisers into medical

practice. While adverse reactions are often considered to be of less than major importance in conventional drug therapy of life-threatening disease, PDT will be applied generally to early lesions with curative intent. The occurrence of unexpected toxicity could seriously impair future trials. A major stumbling block to the use of PDT in the removal of tumor cells is the lack of suitable photosensitisers that can accumulate selectively to the tumor cells and destroy them leaving normal cells unaffected after illumination with light. Although photosensitisers that can accumulate selectively to the tumor cells have been discovered, their major limitation is that they are activated with wavelengths of light that are not capable of penetrating deeply through tissues or blood. Other important limitations of current photosensitisers include the difficulty in the functionalisation and purification of the functionalized compounds. Photosensitisers are generally water insoluble, but they can be made to be water-soluble by functionalisation with hydrophilic groups. Excretion from the body is also one of the most important limitations in the use of photosensitisers. Many that have been synthesized are removed very slowly from the body and therefore cause skin phototoxicity when the patient comes in contact with light. Delayed excretion results, in the patient being forced to stay in the dark for long periods of time to give a sufficient period for the photosensitisers to remove from the normal tissue.

PDT is advantageous over standard therapy since it is not painful and is noninvasive. PDT also has the ability to treat multiple lesions at one sitting, good patient acceptance, excellent cosmetic results and apparent lack of major side effects. Acute effects caused by singlet oxygen include severe damage to various cell membranes including plasma, mitochondrial, lysosomal, endoplasmic reticulum, and nuclear membranes; inhibition of enzymes, including mitochondrial, DNA repair and lysosomal enzymes; and inactivation of membrane transport systems. The diseased tissue in which the photosensitisers is localized should preferable be destroyed with either little or no damage to surrounding normal tissue.

Cancer consists of large group of diseases resulting from uncontrolled proliferation of cells. These diseases can originate in almost any tissue of the body. Symptoms and signs of cancer depend on many factors including the location of the tumors, rate of growth, tendency to invade and divide, and some other individual conditions of patients. The most common cancers originate and spread within the chest,

abdomen, or pelvis. These sites are difficult to treat because of the close positioning of many overlapping organs. Continued cell division leads to the formation of tumors that invade normal tissues and organs. In many cases, the cancer cells become dislodged and spread to other locations within the body where they then take up residence and grow, forming secondary tumors. In these situations, the cancer is frequently advanced and not curable by current approaches.

Several new second-generation photosensitisers are now in clinical trials and are showing promising results since their treatment times, typical light and drug doses are smaller than for HpD. Viewed against photofrin, the new second-generation sensitisers, plus ALA-PDT, are beginning to prove their worth. An important factor with new sensitisers is their ability to enhance selectivity of tumor damage at lower doses of the sensitiser. Whether photosensitivity is an important issue depends on the treatment. In treatment of lethal tumors, it doesn't matter how photosensitive patients become: the priority is to ensure maximum tumor destruction. Today, only a purified form of hematoporphyrin derivative is in therapy, but is not efficient enough for tumor treatment, however, it can be used to treat tumor cells at an early stage. The main disadvantage of Photofrin is its unknown composition for it is still composed of a mixture of porphyrins. Therefore, the synthesis of photosensitisers in which there is certainly regarding the structure and purity thereof is of great importance for the development of new photosensitisers [17].

One of the requirements of new photosensitisers is water solubility, while selective uptake of the photosensitisers by the tumor cells versus healthy tissue is also important. This requires that photosensitisers should be soluble in body fluid and be more concentrated in tumor cells [51]. Although some second generation photosensitisers are water soluble and are less toxic, there is still some problem with selective uptake of the photosensitisers by the tumor cells compared to normal cells.

As a potential solution, synthesis of phosphonic acid substituted porphyrazines is of great interest for cellular recognition and water solubility. A specific objective of this study was to synthesize porphyrazines with phosphonic acid as peripheral substituents. This will be addressed by the development of technology in which phosphonic acid-functionalized porphyrazines will be produced from the corresponding phosphonate ester-substituted maleonitriles.

## 2.6 *Seco*-Type Porphyrazines That Bearing Different Substituents

Novel *seco*-porphyrazines substituted with dimethylamino, 1-naphthyl, 4-*tert*-butylphenyl, *p*-tolyl, *o*-tolyl,4-biphenyl, ect.. These novel compounds have been characterized by elemental analysis, together with FT-IR, $^{1}$H NMR, UV-Vis and mass spectral data.

### 2.6.1 Unsymmetrical *Gemini*-5 and *Solitaire*-Porphyrazines

The other example of *seco*-porphyrazine is that the unsymmetrical *Gemini*-5 and *solitaire*-porphyrazines [52]. Linstead macrocyclization of dinitrile **1** gave [octakis(dimethylamino) porphyrazinato] magnesium-(II) and the *seco*-porphyrazine **4** from adventitious oxidation. The structure of the latter has been unequivocally established by an X-ray crystallographic study. Alternatively, *seco*-porphyrazine **4** compound was obtained in high yield from the manganese dioxide-mediated oxidation of the free base porphyrazine **3**. This convenient method was further extended to core metalated and unsymmetrical porphyrazines. In crystals of zinc-*seco*-porphyrazine **11**, the molecules exist as face-to-face dimers linked via complexation of the zinc center in one molecule to one of the amide oxygen atoms in the other and *vice versa*. The cleaved pyrrole ring in *seco*- and di-*seco*-porphyrazines causes a ~ 50-70 nm red-shifted split Q-band in UV-Vis spectra.

Synthesis of the octakis-(dimethylamino)porphyrazine **2** (MgODMAPz) is described and derivatives of porphyrazinoctaol, two ligands functionalized with nitrogen and oxygen atoms, respectively, in place of sulfur. The free base **3** ($H_2$ODMAPz) is more readily oxidized than ferrocene and forms charge transfer complexes with tetracyanoquinodimethane (TCNQ) and $C_{60}$. It is observed that a minor side product, the *seco*-porphyrazine **4**, was formed during the Linstead macrocyclization of bis(dimethylamino)maleonitrile **1**. Subsequently it is found that acid-mediated demetalation of the magnesium porphyrazine resulted in peripheral oxidation of one pyrrole ring to reveal the *seco*-porphyrazine **4** (Fig.2.12). After report, a related structural type (2,3-*seco*-chlorin-2,3-dione) has been described. It is speculated that this oxidative desymmetrization may have resulted via the formation of singlet oxygen. Full experimental data on the synthesis of MgODMAPz **2** are reported, further studies on

ring oxidation, and the coordination chemistry of the derived macrocycles **6, 7,** and **11** (Fig.2.13).

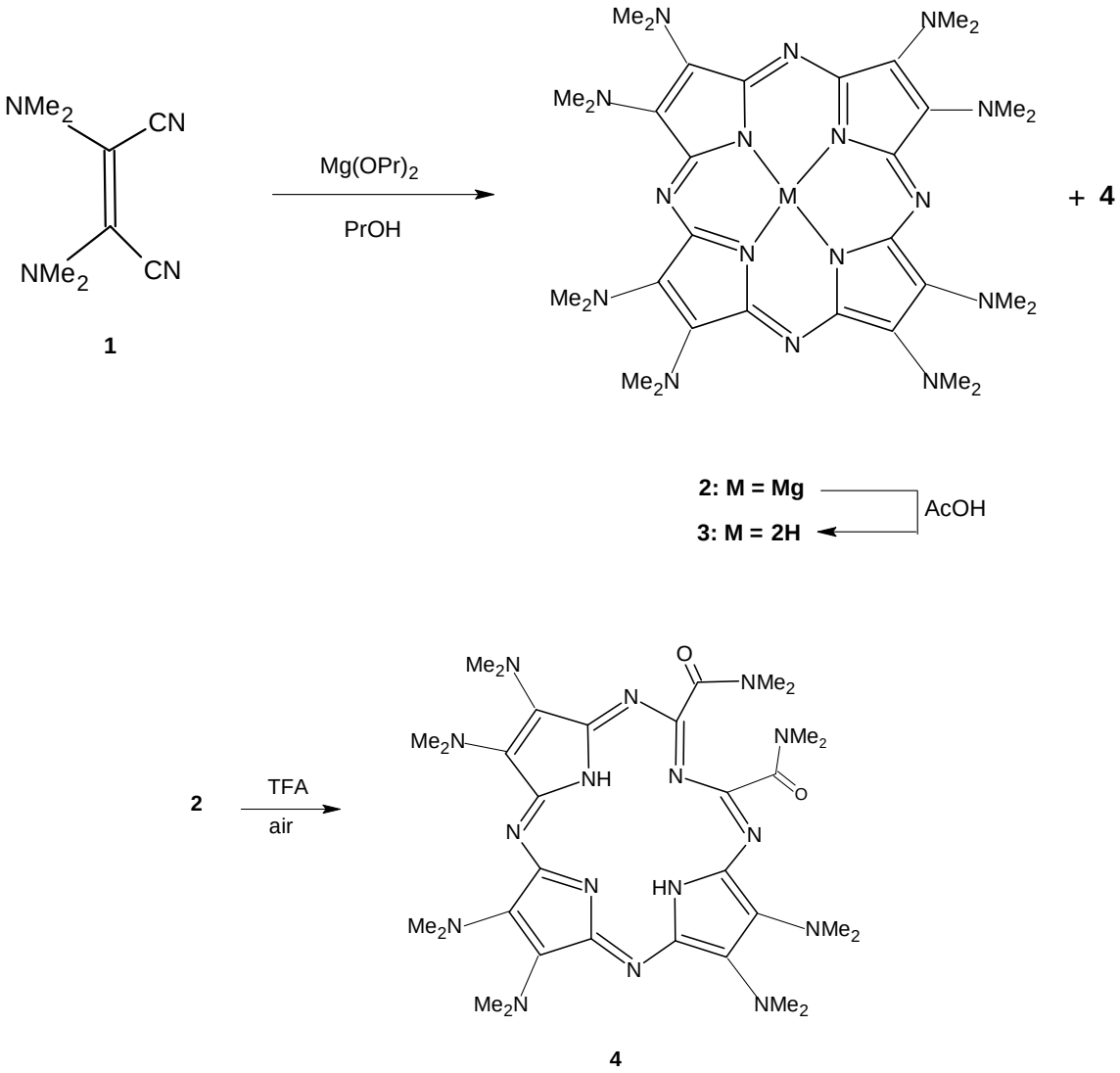


**Figure 2.12** Bis(dimethylamino)maleonitrile **1**, [octakis(dimethylamino) porphyrazinato] magnesium-(II) **2**, free base porphyrazine **3**, *seco*-porphyrazine **4**.

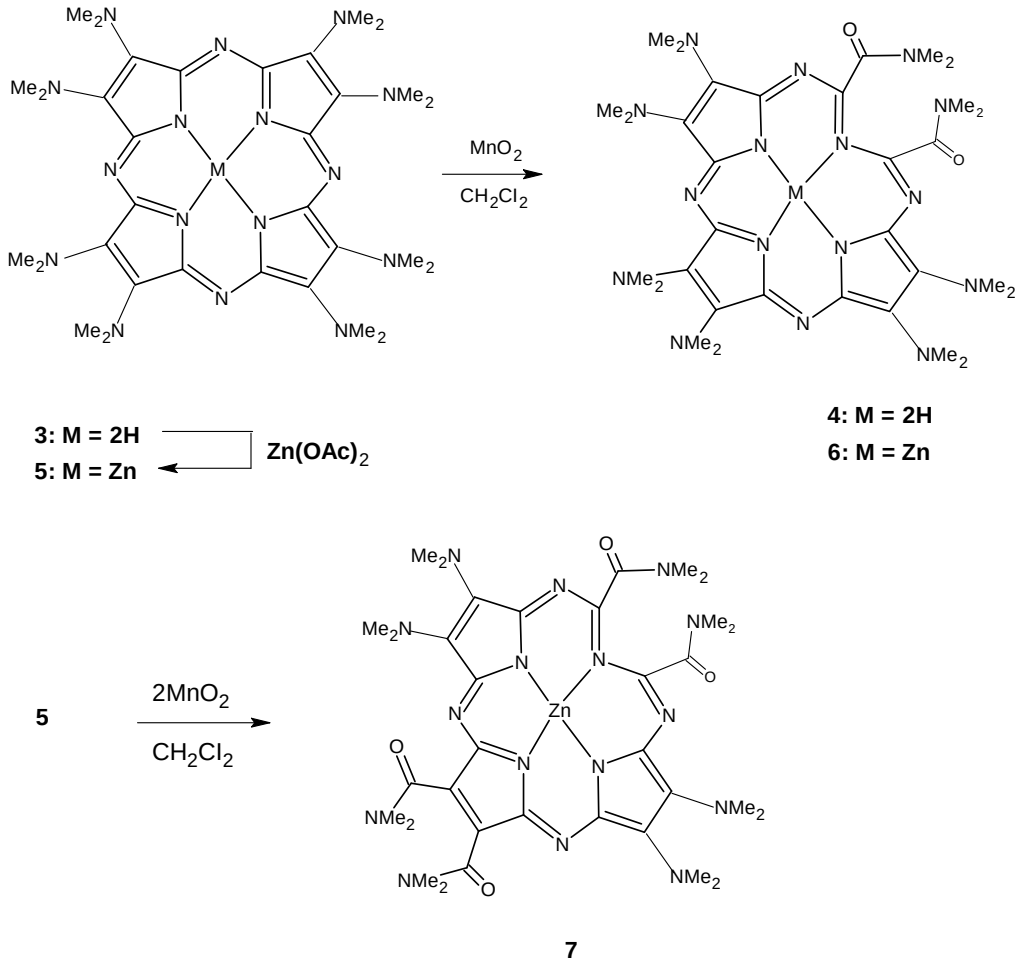


**Figure 2.13** Free base porphyrazine **3**, *seco*-porphyrazine **4**, zinc porphyrazine **5**, zinc-*seco*-porphyrazine **6**, zinc-di-*seco*-porphyrazine **7**.

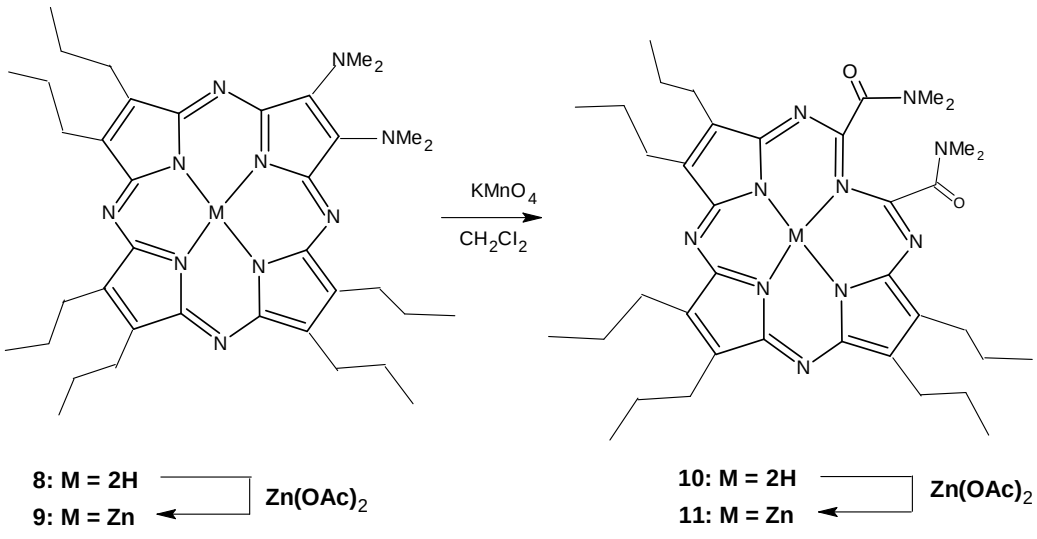


**Figure 2.14** Free base porphyrazine **8**, zinc complex **9**, *seco*-porphyrazine **10**, *seco*-porphyrazine with zinc **11**.

The reaction of the free base porphyrazine **8** with zinc(II) acetate resulted in selective metalation within the macrocyclic cavity to provide the corresponding zinc complex in high yield. Both **8** and **9** were unreactive toward oxidation by manganese dioxide. However, reaction of compounds **8** and **9** with potassium permanganate gave the expected *seco*-porphyrazines **10** and **11** (Fig. 2.14) [52].

### 2.6.2 Partially Oxidized Porphyrazines

The scope of the present work was to prepare metalloporphyrazinates substituted directly with eight (1-naphthyl) groups on the peripheral positions [53]. Magnesium porphyrazinate substituted with eight (1-naphthyl) groups on the peripheral positions has been synthesized by cyclotetramerization of 3,4-(1-naphthyl)pyrroline-2,5-diimine, 4-(1-naphthyl)pyrroline-2,5-diimine in the presence of magnesium butanolate. Its demetalation by treatment with trifluoroacetic acid, resulted in a partially oxidized product, namely, octakis(1-naphthyl)-2-*seco*-porphyrazine-2,3-dione (Fig.2.15). Further reaction of this product with copper(II) acetate, zinc(II) acetate and cobalt(II) acetate led to the metallo derivatives, [octakis(1-naphthyl)-2-*seco*-2,3- dioxoporphyrazinato]M(II) (M = Cu, Zn or Co).

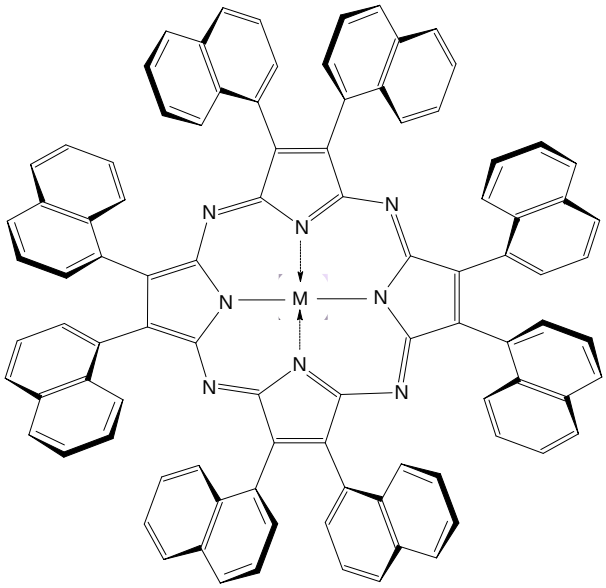


M = Mg **4a**

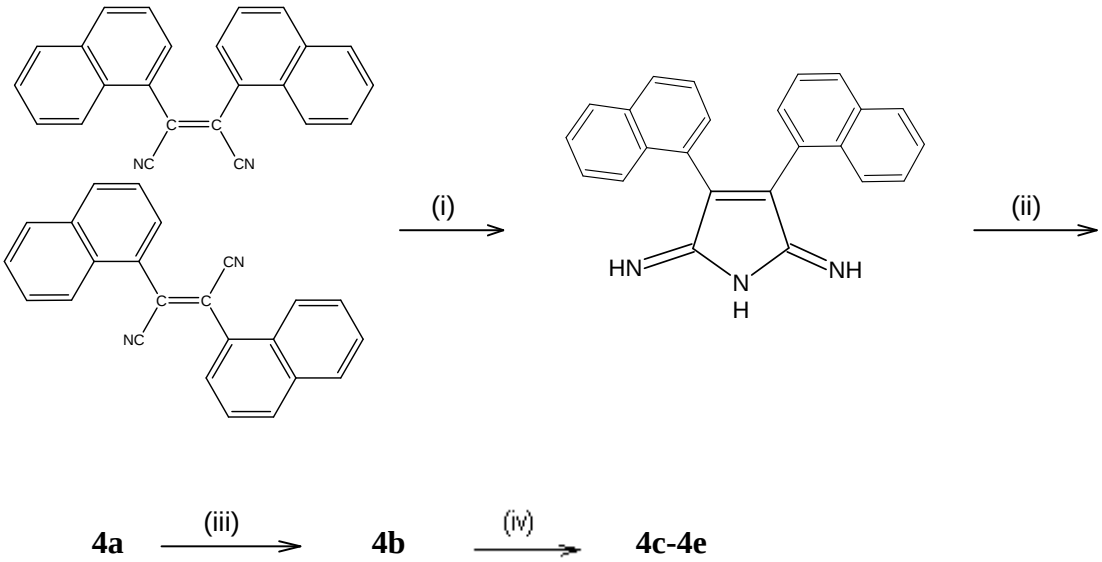


**Figure 2.15** (**i**) Ethylene glycol; (**ii**) Mg turnings, $I_2$, *n*-BuOH; (**iii**) $CF_3CO_2H$; (**iv**) $CHCl_3$, EtOH and $Cu(OAc)_2$, $Zn(OAc)_2$, or $Co(OAc)_2$.

Although, at first glance, the oxidation of the porphyrazine **4a** octakis(1-naphthyl)porphyrazinato magnesium to *seco*-porphyrazine **4b** might not be expected when the dissimilarity of the substituents with those of octakis(dimethylamino)porphyrazine is taken into account, the reasons leading to such a reaction need to be researched by some other mechanism (Fig.2.16) [52,54,55]. First of all, naphthyl groups are not comparable with dimethylamino groups as electron donors to the 18-π electron system of the inner core. This has been verified by the blue shift of the absorption maximum of the Q band in the case of naphthyl-substituted ones.

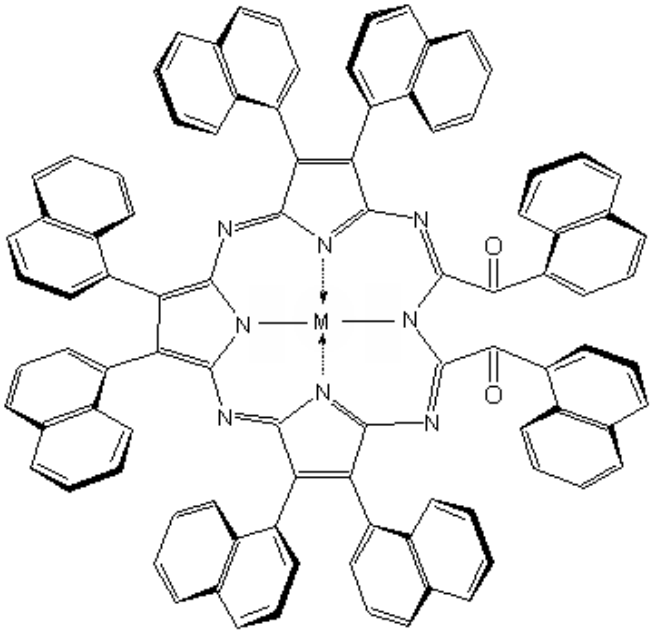

M = 2H **4b**; Cu **4c**; Zn **4d**; Co **4e**

**Figure 2.16** [2,3,7,8,12,13,17,18-octakis(1-naphthyl)-2-*seco*-porphyrazine-2,3-dione] and metal derivatives [M = 2H, Cu(II), Zn(II) or Co(II)].

Moreover, during the demetalation reaction, relatively strong acids (*e.g.* trifluoroacetic acid) inhibit the electron-donating strength of the dimethylamino groups much more than naphthyls. Steric hindrance due to the presence of eight bulky naphthalene units around the core might be the main reason for the cleavage of one of the pyrrole rings. Of course, these can be taken together with the oxidation resulting from singlet-oxygen cycloaddition reactions as described in earlier works [53]. Electronic spectra are especially useful to establish the structure of the porphyrazines (**4a-e**). UV-Vis spectra of the porphyrazine core are dominated by two intense bands, the Q band around 640 nm and the B band in the near UV region of around 348 nm, both correlated to $\pi \rightarrow \pi^*$ transitions [56,57]. In addition to these absorptions of the porphyrazine core, an intense absorption due to the $\pi \rightarrow \pi^*$ transition of naphthalene groups appeared for all these porphyrazine derivatives (**4a-e**) in the UV region at about 284-288 nm [58,59].

### 2.6.3 Decapitation of Dihydroporphyrazinediol Derivatives

The dihydroporphyrazinediol **8**, which was prepared by Linstead macrocyclisation of 2,5-diiminopyrrolidine with 3,4-bis(4-*tert*-butylphenyl)pyrroline-

2,5-diimine, followed by TFA demetallation and $OsO_4$ tetroxide mediated dihydroxylation, underwent reaction with $Ni(OAc)_2$ at 100 °C in the presence of air to give the novel *seco*-porphyrazine, the structure of which was established by an X-ray crystallographic study [55]. It is described the synthesis of *seco*-porphyrazines **1a-d** by the peripheral oxidations of porphyrazines (Fig.2.17).

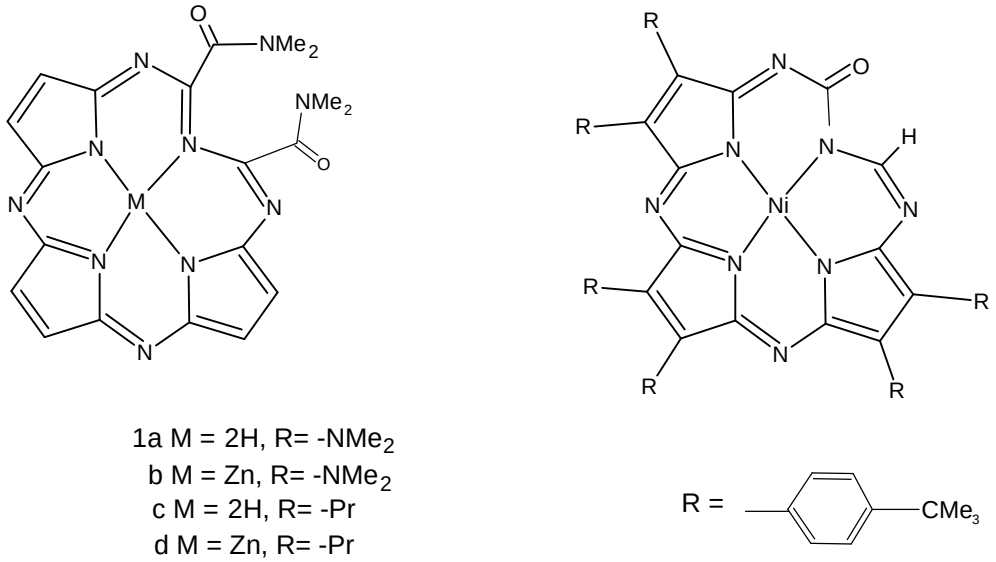


**Figure 2.17** *Seco*-porphyrazines **1a–d** by the peripheral oxidations of porphyrazines and novel *seco*-porphyrazine.

### 2.6.4 Synthesis of a Free Base *Seco*-chlorin from a 2,3-dimethoxy Porphyrin

The interesting nature of symmetric **1** and its acetylated derivative symmetric free base *seco*-chlorins, led us to seek a more efficient synthesis. Here, we were inspired by the realization that **1** could have arisen from an air-based oxidation of the dominant 2,3-dimethoxyporphyrin product **3**. Based on such thinking, we considered that treating porphyrins, such as **3**, with singlet oxygen would effect conversion into the corresponding *seco*-chlorin. On a more practical level, we also thought it might prove useful to start with the bis-acetoxy porphyrin **4**, rather than **3**, so as to simplify purification of the corresponding *seco*-chlorin **2**, assuming it were to be produced. Accordingly, as shown in Figure 2.18, porphyrin **4** (*ca*. 0.1 mol $dm^{-3}$) was dissolved in $O_2$-saturated methanol containing Rose Bengal (*ca*. 150 mg l21) and subject to irradiation using a 250 W projection lamp as a light source for *ca*. 10 h. Under these conditions, wherein singlet oxygen is the dominant oxidant, the $C_2$ symmetric *seco*chlorin was obtained [60].

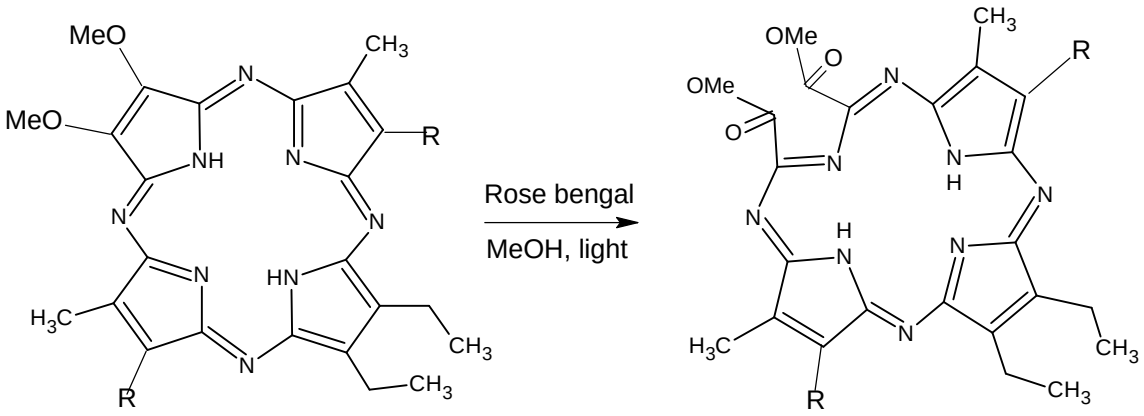


**3: R = $(CH_2)_3OH$**
**4: R = $(CH_2)_3OAc$**

**1: R = $(CH_2)_3OH$**
**2: R = $(CH_2)_3OAc$**

**Figure 2.18 1** and **2** symmetric free base *seco*-chlorins, **3** 2,3-dimethoxyporphyrin product, **4** bis-acetoxy porphyrin.

### 2.6.5 Synthesis of Polyether-Appended Aminoporphyrazines

Linstead co-macrocyclization of dinitriles **5** and **6** in a 1:7 molar ratio resulted in the formation of the Mg-pz **7** along with the Mg-octapropyl pz **10**. Separation of the two macrocycles was easily achieved by chromatography to give compound **7**. Deprotection of the THP groups and concurrent demetallation of macrocycle **7** using glacial acetic acid followed by concentrated HCl gave diol **8** (Fig.2.19). The free base **8** was allowed to react with zinc acetate in DMF to provide the Zn-pz **9**. Subsequent oxidation of pz **9** using an excess of potassium permanganate rapidly afforded the corresponding *seco*-product **11** (Fig.2.20). The incorporation of zinc(II) within the macrocyclic cavity, previously known to enhance the rate of oxidative pyrrole cleavage was also observed in this transformation [61].

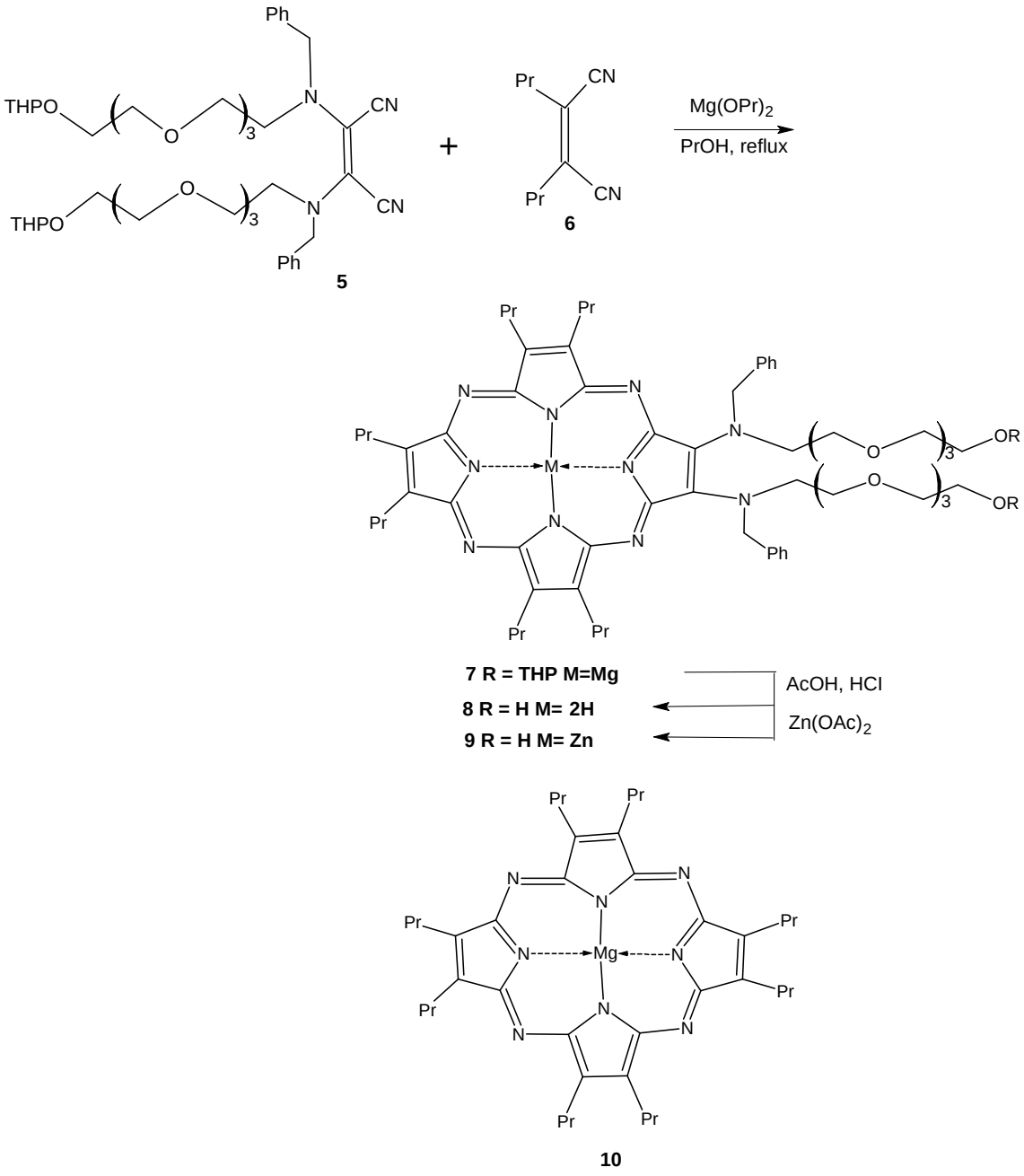


**Figure 2.19** Synthesis of polyether-appended aminoporphyrazines.

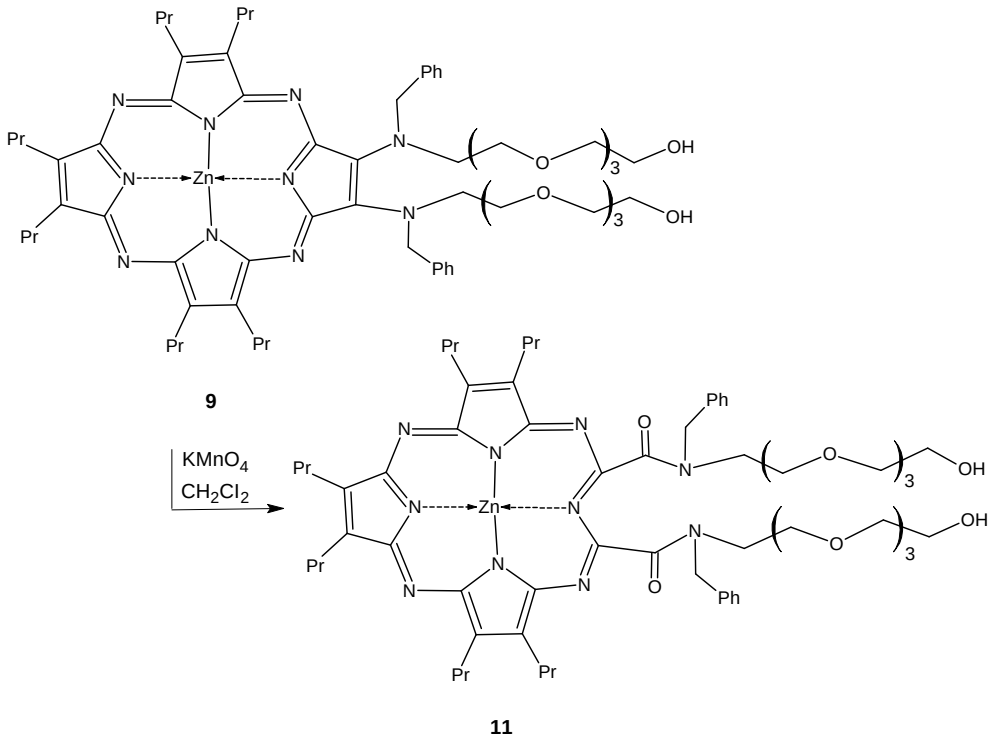


**Figure 2.20** Oxidation of Zn-pz **9** compound by using $KMnO_4$.

### 2.6.6 Synthesis of Symmetrical Porphyrazines with Arenecarboxylate Ester Substituents

In continuation of our efforts towards the synthesis of hydrophilic *seco*-porphyrazines, but with polar groups not directly attached to the amino substituents, the preparation of a second set of macrocycles bearing this time peripheral arenecarboxylate esters was undertaken. Maleodinitrile **14** was prepared via a two-step procedure from the commercially available methyl 4-(bromomethyl)benzoate **12**. Thus, reaction of bromide **12** with potassium cyanide in ethanol at 60 $^{o}$C gave nitrile **13** (Fig.2.21). In turn nitrile **13** was oxidatively dimerized, via the enolate and treatment with iodine in methanolic diethyl ether, to provide the maleonitrile **14**. This was isolated as a single isomer, which was tentatively assigned as the trans isomer. Both trans and cis 2,3-diarylmaleonitriles are known to undergo macrocyclization to produce porphyrazines. Having successfully prepared dinitrile **14**, standard Linstead macrocyclization using magnesium as the template was carried out. Thus, reflux of dinitrile **14** and magnesium butoxide in butanol gave, after chromatography, pz **15** (Fig.2.21). As expected, concurrent transesterification took place during the reaction. Porphyrazine **15** was in turn, demetallated to give the free base pz **16**. Remetallation of ligand **16** with

manganese(II) acetate in DMF at 100 $^{o}$C followed by an aqueous work-up with brine gave the Mn–Cl-pz **17**. Additionally, heating of the free ligand **16** with zinc acetate in DMF resulted in the formation of the Zn-pz **18** [61].

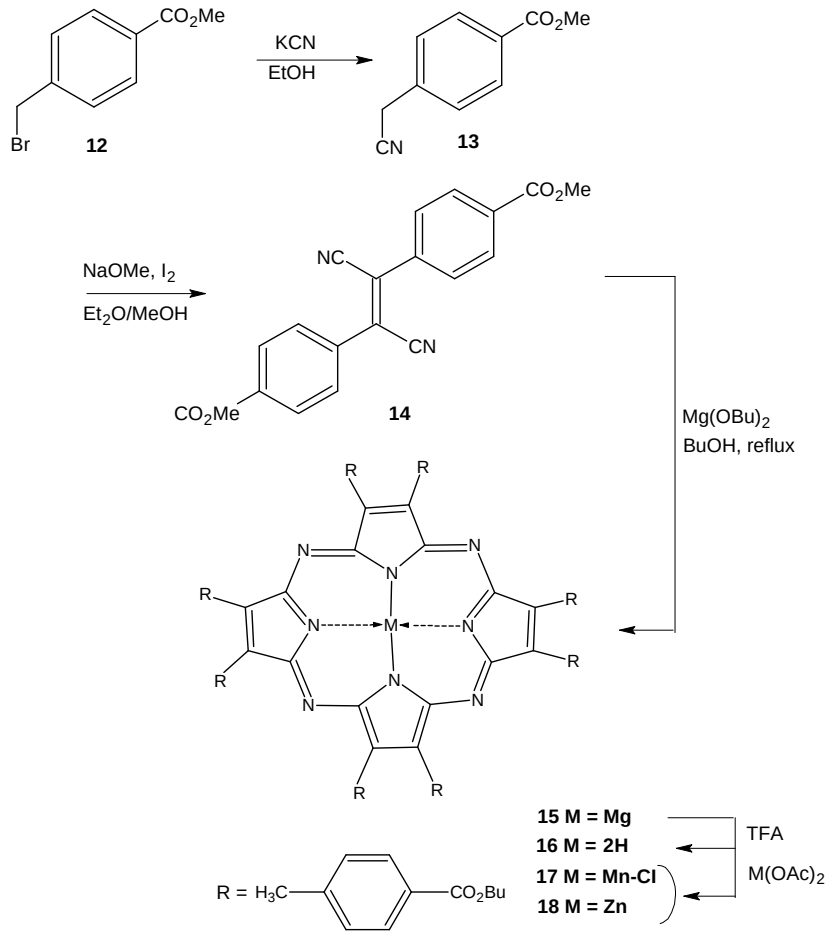


**Figure 2.21** Synthesis of symmetrical porphyrazines with arenecarboxylate ester substituents.

### 2.6.7 Synthesis of Unsymmetrical Porphyrazines with Arenecarboxylate Ester Substituents

In order to obtain the potentially more useful unsymmetrical porphyrazines with ester substituents, the crossover macrocyclization of dinitrile **14** with bis-(dimethylamino)maleonitrile **19** was examined. Thus, when a 7:1 molar ratio of dinitriles **14** and **19** and magnesium butoxide were heated to reflux in butanol, the Mg-pz **20** was obtained along with the Mg-octa-ester-pz **15** (Fig.2.22). Although the formation of both dyes was confirmed by mass spectrometry, separation by chromatography proved extremely difficult and time consuming. This problem was

overcome by the selective demetallation of pz **20** using glacial acetic acid to yield the requisite unsymmetrical pz **21**, which was separated from the Mg-octa-ester-pz **15** using preparative thin layer chromatography (Fig.2.22). Subsequent reaction of ligand **21** with zinc acetate in DMF gave the corresponding Zn-pz **22**. Oxidation of ligand **21** using an excess of potassium permanganate in dichloromethane gave, after 2 h the desired *seco*-pz **23** (Fig.2.22). On the other hand, oxidative cleavage of the Zn-pz **22**, under the same conditions gave, after only 15 min reaction, the desired Zn-*seco*-pz **24**. As observed in previous reports, faster oxidative pyrrole cleavage of the Zn-pz to reveal the corresponding *seco*-compound was observed, relative to the free pz ligand. In consequence of this ease of oxidative scission, it was not possible to completely purify and fully characterize the Zn-pz **22**.

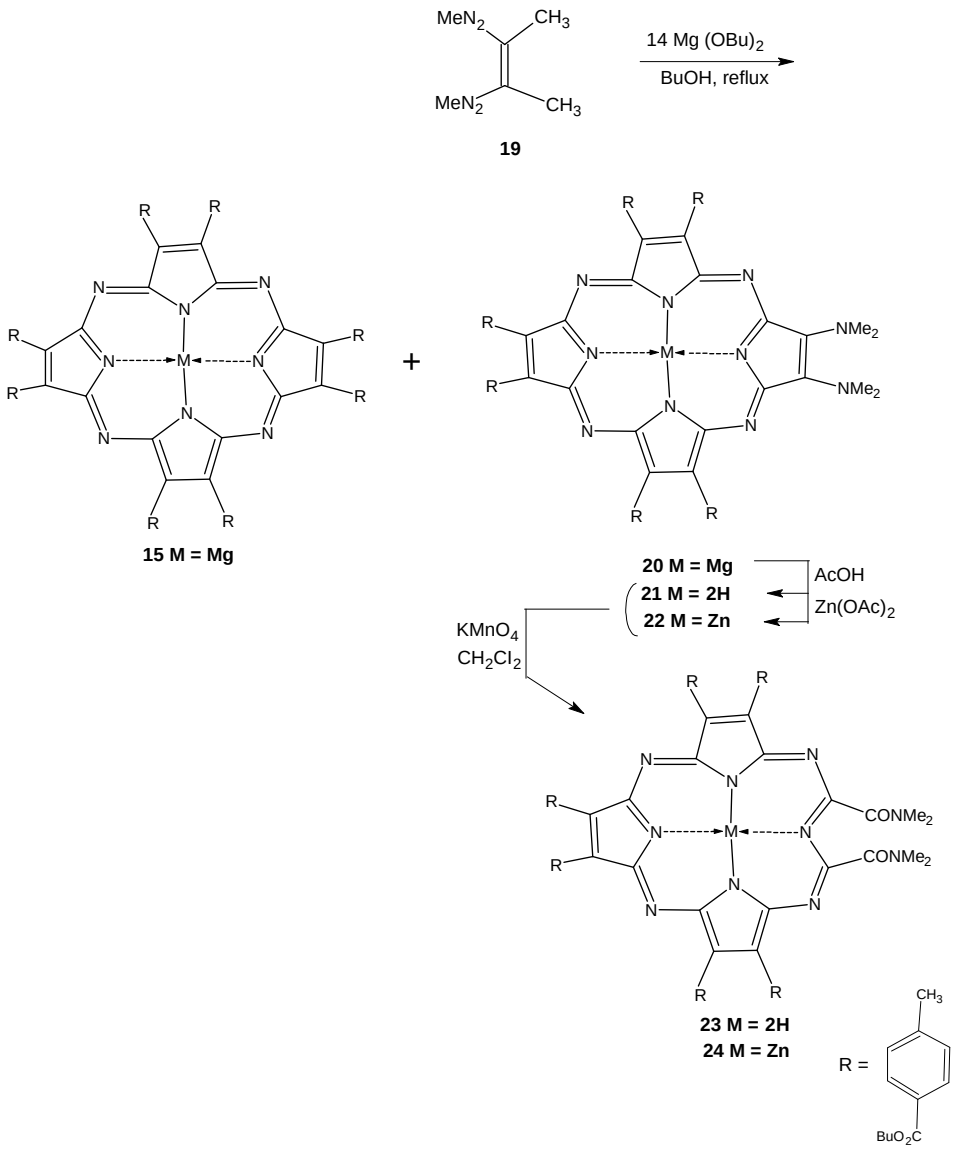


**Figure 2.22** Synthesis of unsymmetrical porphyrazines with arenecarboxylate ester substituents.

### 2.6.8 Studies on *Seco*-Porphyrazines: A Case Study on Serendipity

The conversion of porphyrazine-diamine derivatives into either *seco*-porphyrazines or porphyrazine palladium or platinum complexes has a profound effect on the photophysical and photochemical properties which has relevance to the design of switchable agents for photodynamic therapy and other applications.

The Barrett and Hoffman team began work on the synthesis of porphyrazines in late 1987 at Northwestern University [54]. The first graduate student on the project, Chris Velázquez, started work on the synthesis and characterisation of derivatives of the multidentate ligand porphyrazineoctathiol **3** (Fig.2.23). This was prepared by the Linstead macrocyclisation of the dinitrile **1** followed by transmetallation and sodium in ammonia reduction of octasulfide **2** to provide the very air sensitive octathiolate **3**. Trapping with di-*tert*-butyltin dinitrate *in situ* gave the star porphyrazine **4**. This early success led the group to prepare a myriad of multimetallic complexes of porphyrazine bearing two, four or eight peripheral thiol residues.

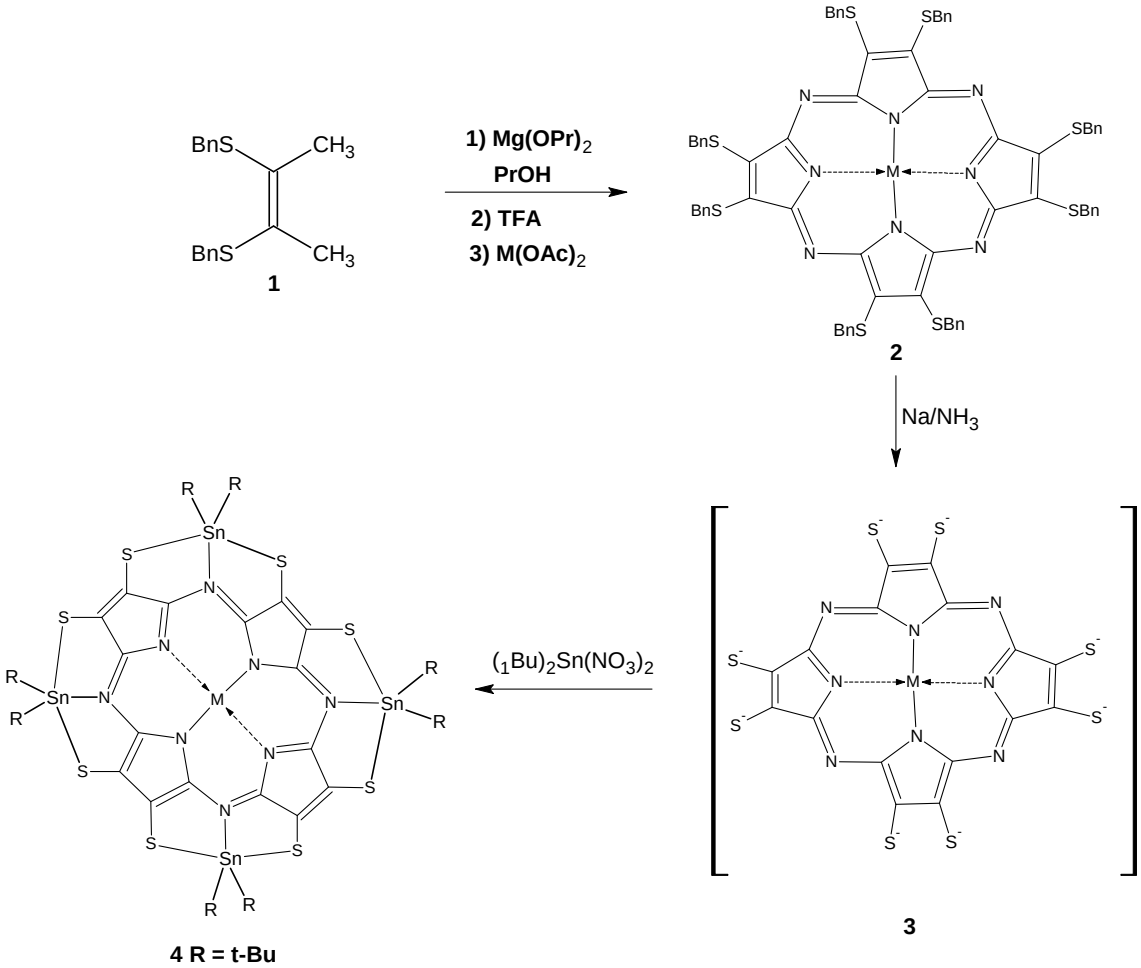


**Figure 2.23** Synthesis of star porphyrazine **4**.

Further west in Fort Collins, CO some years later in 1991 and 1992, two postdoctoral research associates Todd Miller and Neelakandha S. Mani were seeking to prepare derivatives of porphyrazine-octaol **5** and octaamine **6** [54]. At that stage the hydroxylated porphyrazine proved elusive but were prepared some years later due to the insight of Andrew Cook on matters of protecting groups. Both Todd and Neelakandha were successful in preparing derivatives of porphyrazineoctaamine **6** and porphyrazine-diamine **7** (Fig.2.24).

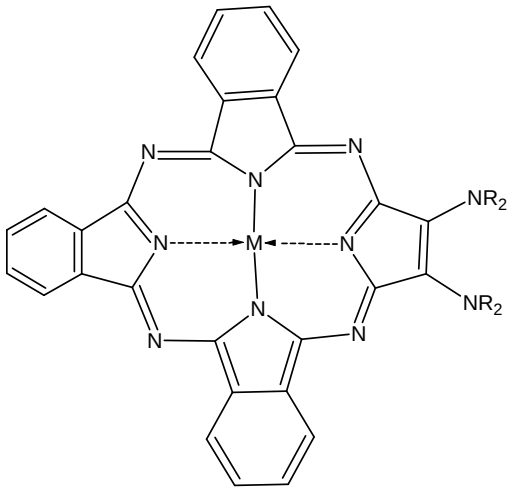


**Figure 2.24** Synthesis of porphyrazine-diamine **7**.

The first cleaved porphyrin-type macrocycle **9** to be structurally characterised was isolated from an unexpected oxidative ring opening of a corrinato nickel(II) complex in 1992 [54]. *Seco*chlorin **9,** diketones **10** and dialdehydes **11** have also been obtained from an analogous oxidative cleavage of the corresponding nickel(II) chlorin diols with lead tetraacetate. However, the first non-metallated derivative **12** was only reported recently by Sessler *et. al.* (Fig.2.25) [54].

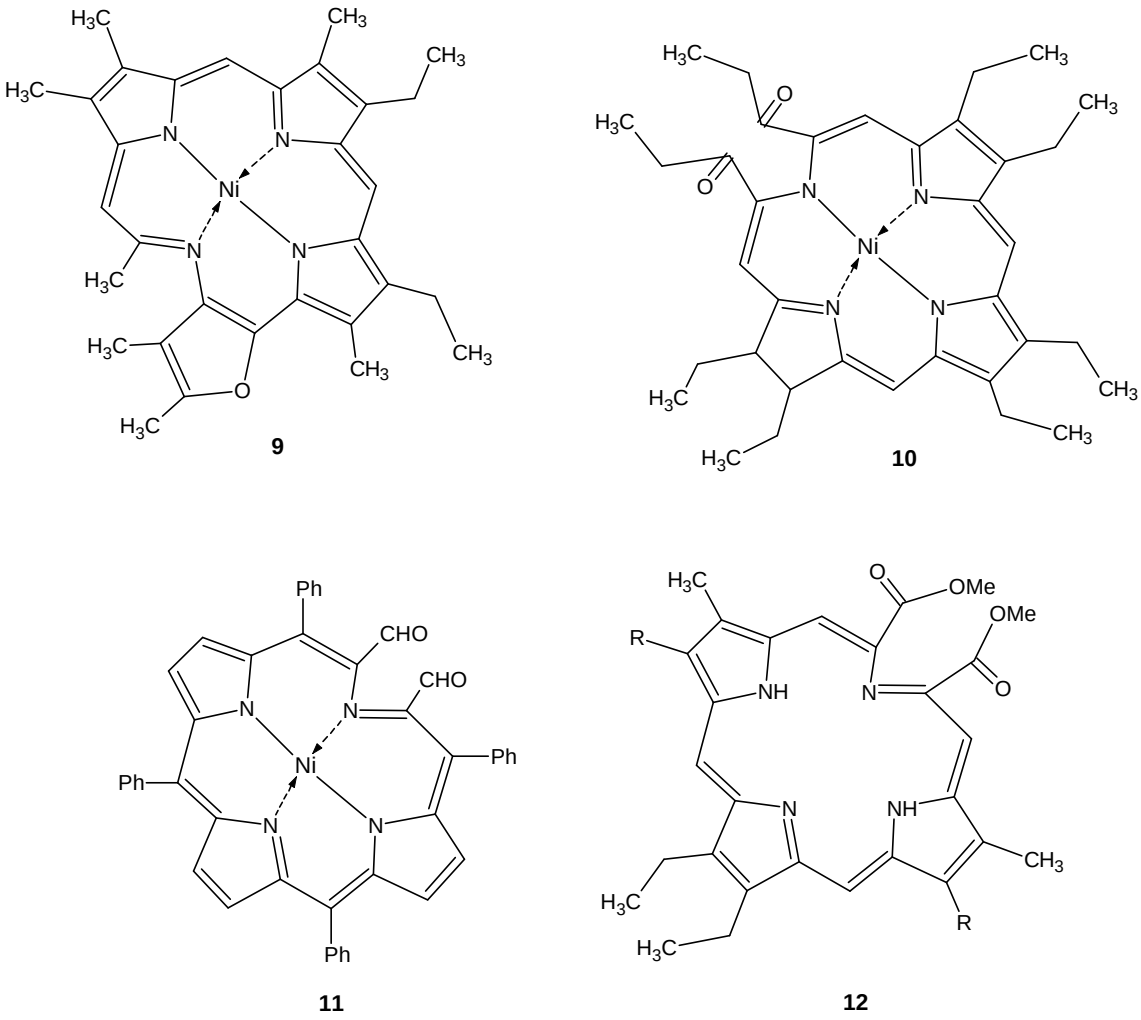


**Figure 2.25** Porphyrin-type macrocycle **9**, *seco*-chlorin diketones **10**, dialdehydes **11**, non-metallated derivative **12**.

The spectral changes for di-*seco*-porphyrazine **16** (Fig.2.26) indicated a low degree of symmetry ($D_{4h} \rightarrow D_{2h}$). We tentatively suggested that the peaks centered at 789 and 579 nm corresponded to the red-shifted split Q band, and that the n–π* peak was reduced to a small shoulder centered at 470 nm. In accordance with Gouterman's four orbital model, the Soret region was also split into two absorbances which appeared at 363 and 314 nm.

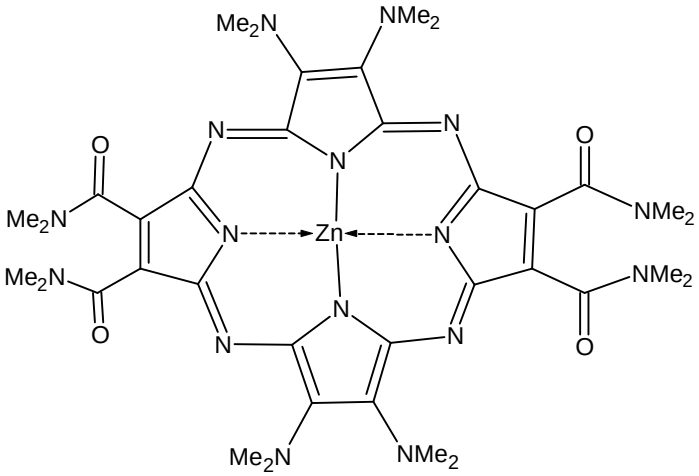


**Figure 2.26** Di-*seco*-porphyrazine **16**.

This convenient method was further extended to unsymmetrical porphyrazines. Thus, reaction of the free base porphyrazine **17** with zinc(II) acetate resulted in selective metallation within the macrocyclic cavity to provide the corresponding zinc complex **18**. Both, **17** and **18** were unreactive towards oxidation by manganese dioxide. However, reaction of compounds **17** and **18** with potassium permanganate gave the expected *seco*-porphyrazines **19** and **20** (Fig. 2.27).

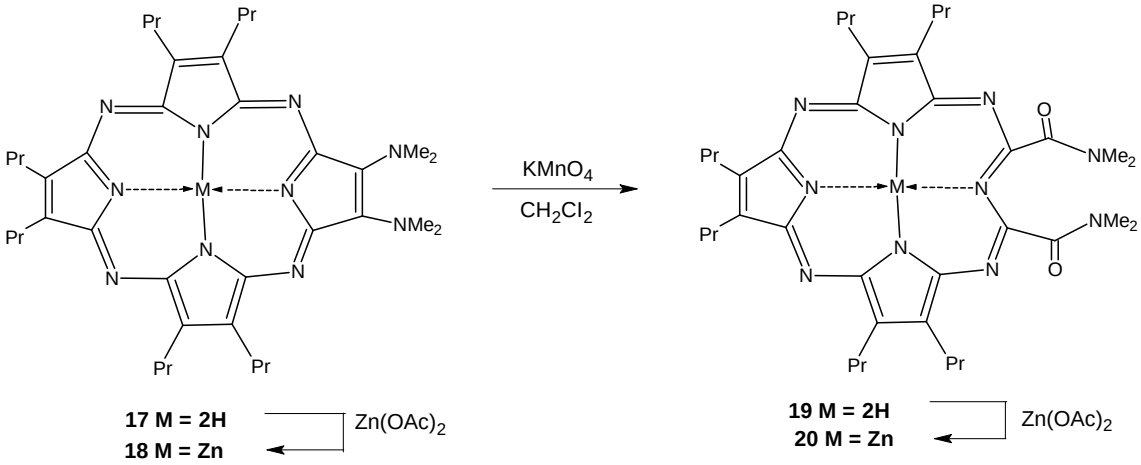


**Figure 2.27** Unsymmetrical porphyrazines.

Efstathia Sakellariou readily prepared the palladium solitaire porphyrazine **21** through reaction of equimolar amounts of Zn-porphyrazine **18** with $PdCl_2$ in chloroform and acetonitrile (3:1) at reflux (Fig.2.28) [54]. Similarly, treatment of the free ligand **18** with a stoichiometric amount of bis(benzonitrile) platinum(II) chloride in 1,2-dichloroethane at reflux gave the corresponding solitaire porphyrazine **22** (Fig.2.28).

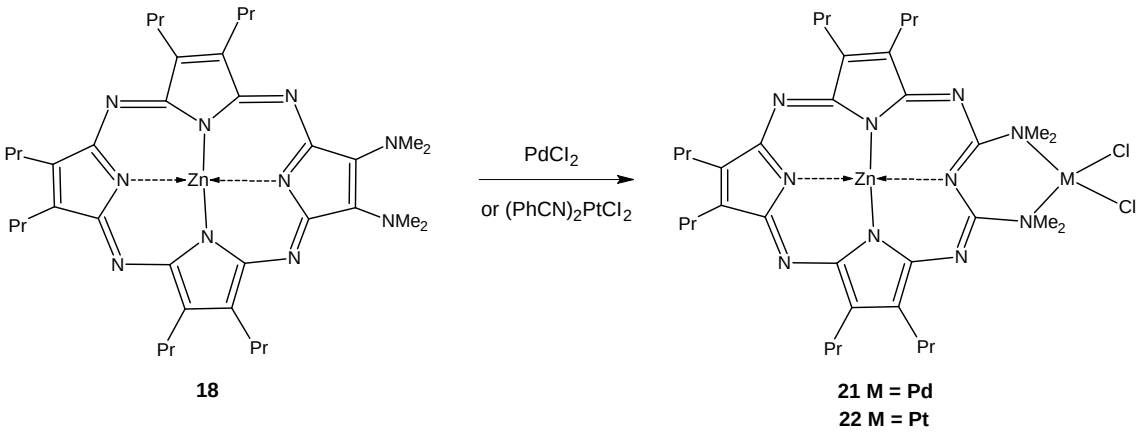


**Figure 2.28** Synthesis of corresponding solitaire porphyrazine.

Upon treatment of porphyrazine **27** with $Pt(PhCN)_2Cl_2$ in 1,2-dichloroethane, the desired metallated product **28a**. Similarly, reflux of **27** with palladium(II) chloride in acetonitrile and chloroform (4:1) gave the *seco*-solitaire-porphyrazine **28b** (Fig.2.29).

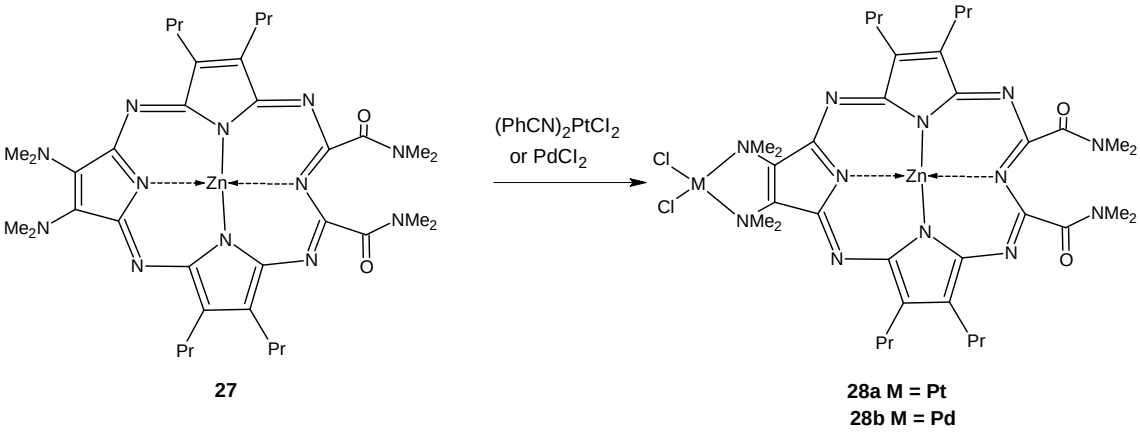


**Figure 2.29** Synthesis of *seco*-solitaire-porphyrazines.

Reaction of the free base porphyrazine **32** with zinc(II) acetate resulted in selective metallation within the macrocyclic cavity to provide the corresponding zinc complex **33**. All attempts to oxidise the free base porphyrazine **32** to its corresponding *seco*-derivative failed. On the other hand, treatment of the zinc-complex **33** with one equivalent of potassium permanganate gave the requisite novel *seco*-porphyrazine **34** (Fig.2.30).

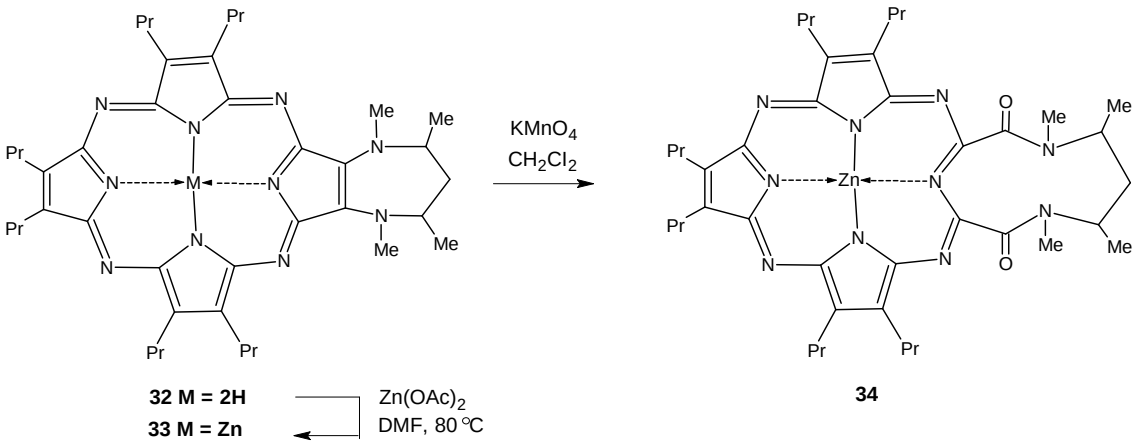


**Figure 2.30** Synthesis of *seco*-porphyrazine **34**.

## 2.7 Group Works in Porphyrazine Chemistry

Tetrapyrrole macrocycles modified by attachment of substituents at the periphery have long been widely studied as building blocks for materials displaying interesting catalytic, electronic and optical properties, e.g. phthalocyanines with fused macrocycles on the periphery show selective interaction with metal ions, lead to ordered structures such as ion-channels and mesogens, act as sensitive in chemical sensors and show electrocatalytic activity in redox reactions. At the same time, peripherally substituted ones are much more soluble than the parent molecules. Although to a lesser extent when compared with phthalocyanines, porphyrazines are receiving considerable interest as substitutes for phthalocyanines in many respects recently. Having similar delocalized p systems, the resulting compounds are expected to have the same distinct electrical and chemical properties.

The synthetic methodology developed during the last decades for symmetrical octa-substituted porphyrazines has been the tetramerization of substituted unsaturated 1,2-dinitriles in the presence of magnesium alkoxide. A wide range of porphyrazines with peripheral substituents from alkyl chains to simple aromatic groups has been prepared. When 1,2-dinitrile group is an integral part of a macrocycle, then the product will carry this macrocycle at the periphery (e.g. dithia-15-crown-5, trithiacycloheptane, etc.). When extremely bulky groups are bound to the dinitrile moiety, then cyclotetramerization might be hindered sterically. A possible solution to this problem will be first to prepare the porphyrazine structure with reactive end groups, subsequently adding the bulky substituents afterwards through the reactive sites. This

method has been utilised with hydroxyalkyl groups as reactive points and unsaturated cinnamoyl groups, as the substituents successfully.

### 2.7.1 Porphyrazines with Tosylamine Functional Groups

Metal-free and metallo-porphyrazines (M= Mg, Ni and Co) carrying eight functional tosylaminoethylthia- groups on peripheral positions have been synthesised for the first time from cyclotetramerization of 1,2-bis (2 tosylaminoethylthia)maleonitrile in the presence of magnesium propoxide; the metal-free derivative was obtained by treatment of with trifluoroacetic acid and it was further converted into Co(II) and Ni(II) derivatives by using acetate salts of corresponding metal ions. The reactivity of tosylamino-groups was verified by its alkylation to yield octakis[(tosyl)(hexyl)amino-ethylthia]porphyrazinatomagnesium(II) (Fig.2.31) [62].

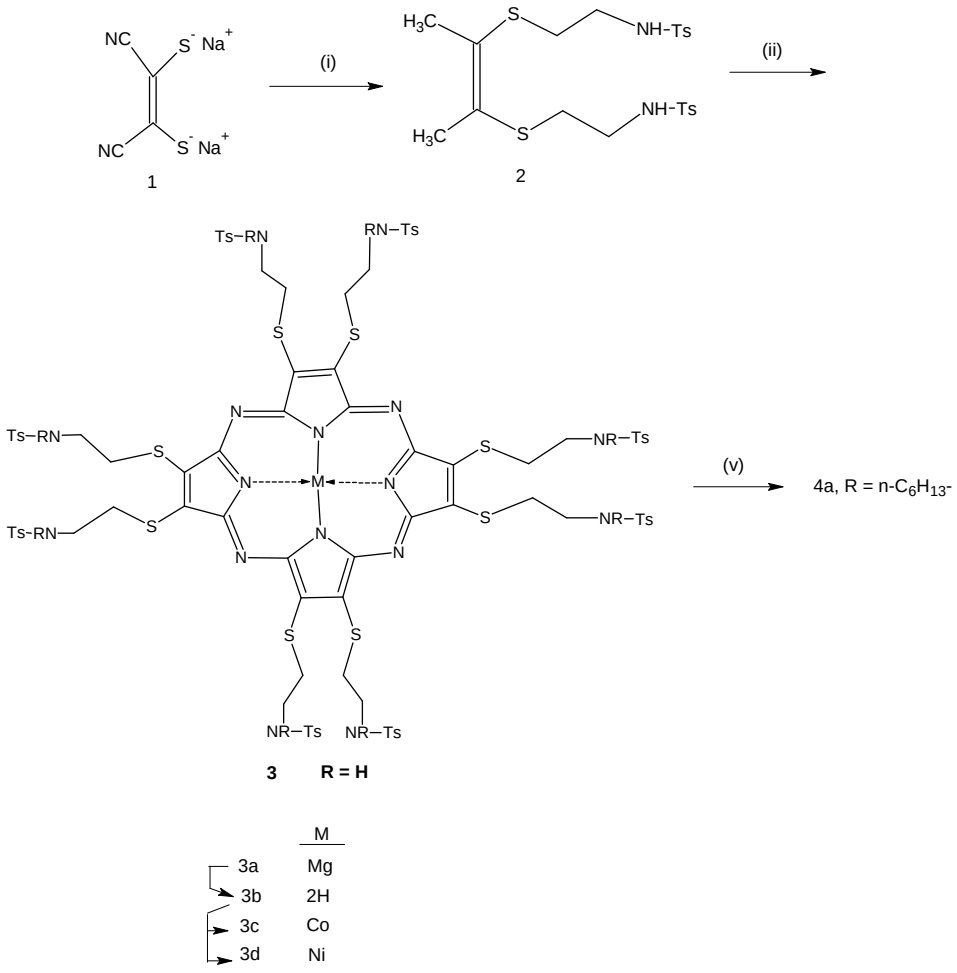


**Figure 2.31** Synthesis route to novel porphyrazines. (**i**) di(tosyl)aminoethanol; (**ii**) magnesium, $I_2$ propanol; (**iii**) trifluoroacetic acid; (**iv**) cobalt(II) acetate or nickel(II) acetate; (**v**) *n*-hexylbromide.

### 2.7.2 Synthesis of New Porphyrazines with Tertiary or Quaternized Aminoethyl Substituents

Metal-free and metallo-porphyrazines (M=Mg or Co) carrying eight dimethylaminoethylthia-groups on peripheral positions have been synthesized from the disodium salt of dithiomaleonitrile and the hydrochloride of dimethyl-aminoethylchloride [63]. The magnesium derivative (MgPza) was converted into quaternized product (MgPzq) (Fig.2.32) by reaction with methyl iodide. The metal-free derivative was obtained by treatment with trifluoroacetic acid and its reaction with cobalt (II) acetate led to the cobalt derivative (CoPza). Aggregation of MgPzq molecules (Fig.2.33) has been observed in aqueous solution by the blue-shift of the Q-band absorption with an accompanying decrease in intensity.

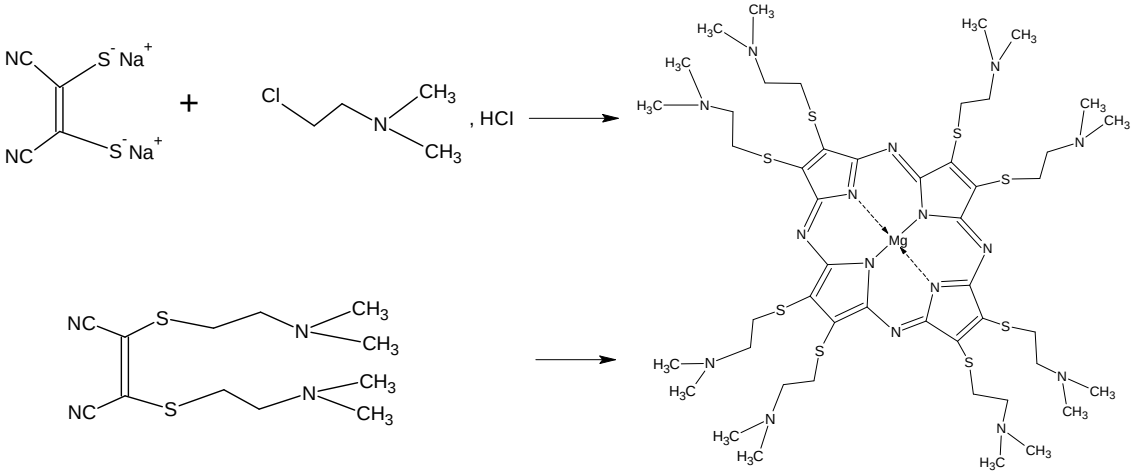


**Figure 2.32** Octakis(2-dimethylaminoethylthio) porphyrazinato-magnezyum (MgPza).

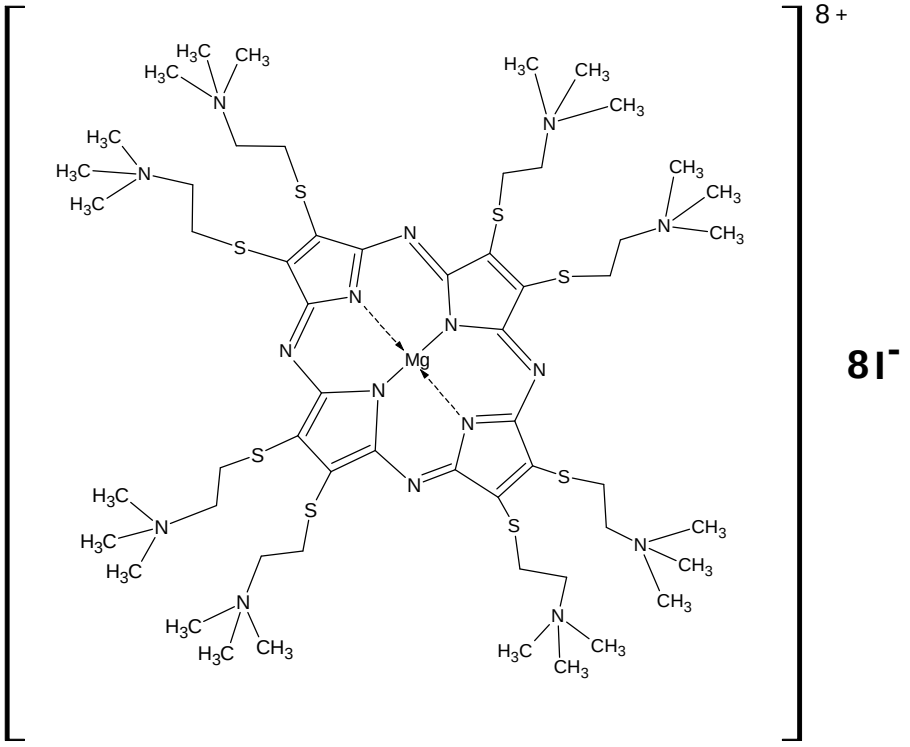


**Figure 2.33** [Octakis (2-trimethylammoniumethylthio) porphyrazinato-magnesium] octaiodide (MgPzq).

### 2.7.3 Magnesium Porphyrazinate with Eight Triphenylphosphonium Moieties Attached Through (2-Sulfanyl-Ethoxycarbonyl-2-Propyl) Bridges

A new magnesium porphyrazinate with eight [triphenyl-(2-sulfanyl-ethoxycarbonyl-2 propyl)phosphonium]bromide groups has been prepared from octakis (2-hydroxyethylthio)porphyrazinatomagnesium and (2-carboxy-1-methylethyl) triphenylphosphonium bromide {[$(Ph)_3PCH_2CH(Me)CO_2H$]Br}( Fig.2.34) [64].

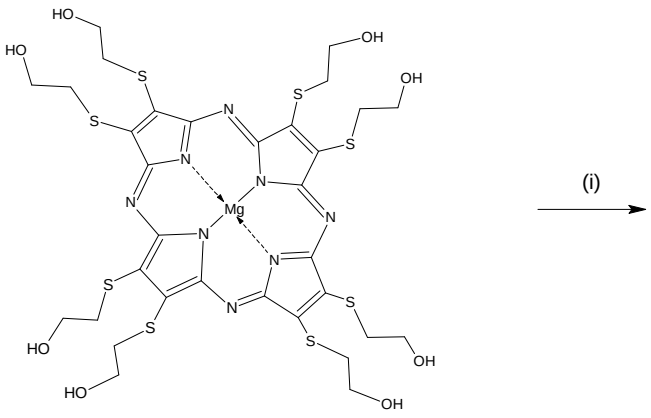

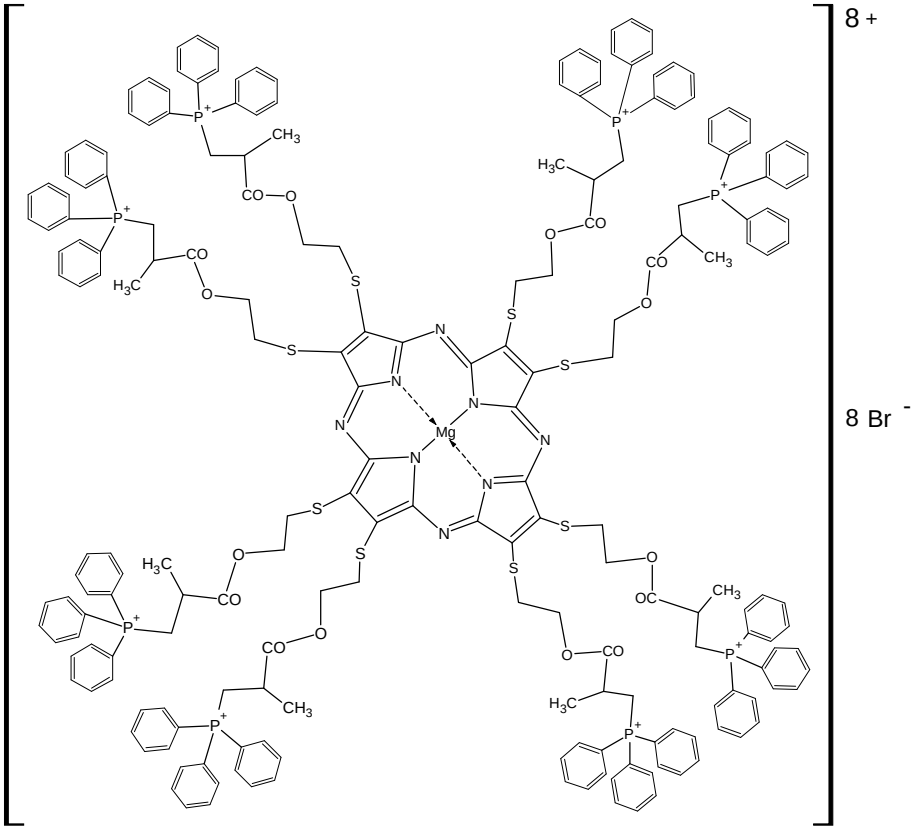


**Figure 2.34** Synthetic route to {octakis[triphenyl-(2-sulfanyl-ethoxycarbonyl-2-propyl) phosphonium]yl-porphyrazinatomagnesium}octabromide.
(**i**) $[(Ph)_3PCH_2CH(Me)CO_2H]Br$, DCCI, toluene-p-sulfonic acid and dry pyridine.

### 2.7.4 Octakis (9-anthracenylmethylthio) Iron Porphyrazine Derivatives

Chloro[octakis(9-anthracenylmethylthio)porphyrazinato]iron(III), [FePzCl] (Fig.2.35), was prepared by the reaction of metalfree porphyrazine with iron(II) acetate and further treatment with HCl solution. The monomeric bisaxial complex $[FePz(py)_{2}]$ as well as the bridged complex $[FePz(pyz)]_n$ (Fig.2.36) were formed as stable complexes by reacting [FePzCl] with pyridine or pyrazine, respectively [65].

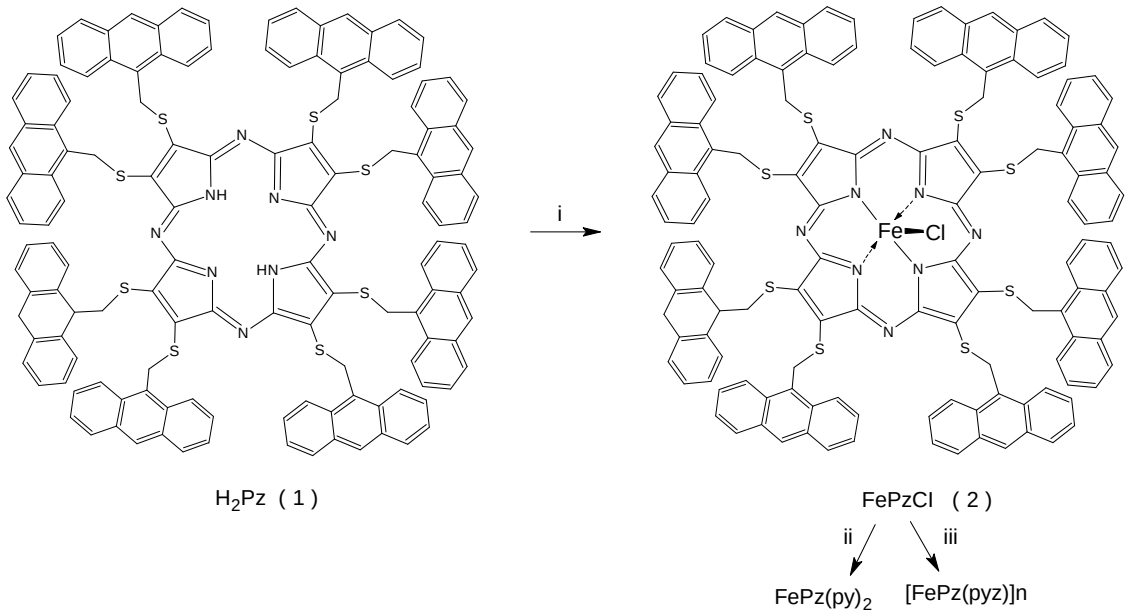


**Figure 2.35** Synthesis route to new compounds: (**i**) $Fe(OAc)_2$, acetic acid, HCl; (**ii**) pyridine; (**iii**) pyrazine.

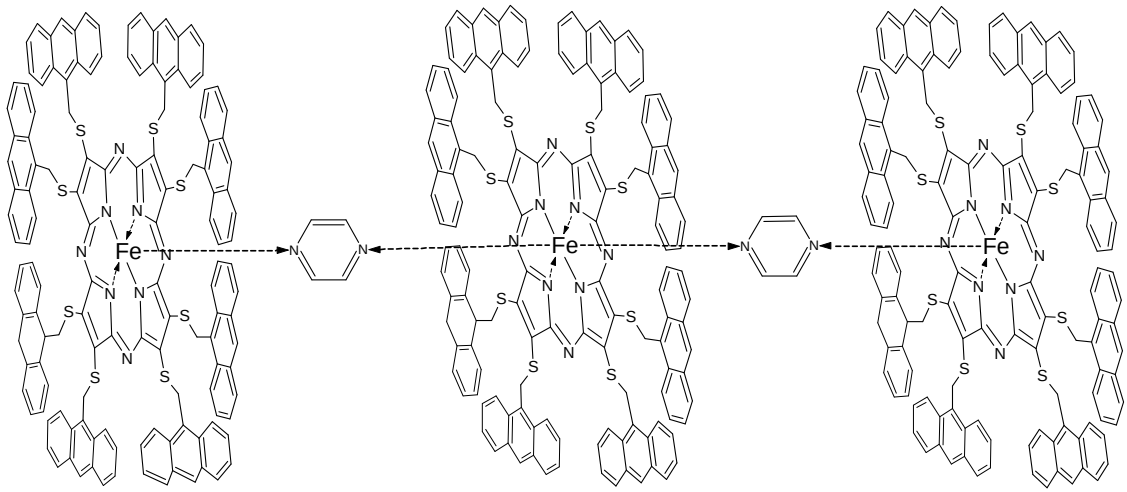


**Figure 2.36** μ-Pyrazine[octakis(9-anthracenylmethylthio)porphyrazinato]iron(II) $[FePz(pyz)]_n$.

### 2.7.5 Synthesis and Characterization of a Phthalocyanine-Porphyrazine Hybrid and its Palladium(II) Complex

A phthalocyanine-porphyrazine hybrid molecule composed of three phthalonitrile units and one maleonitrile moiety was prepared by cyclomerization of the reactants in the presence of magnesium butoxide. Two thioether groups fused to -pyrrol positions were complexed with $PdCl_2$ (Fig.2.37) [66].

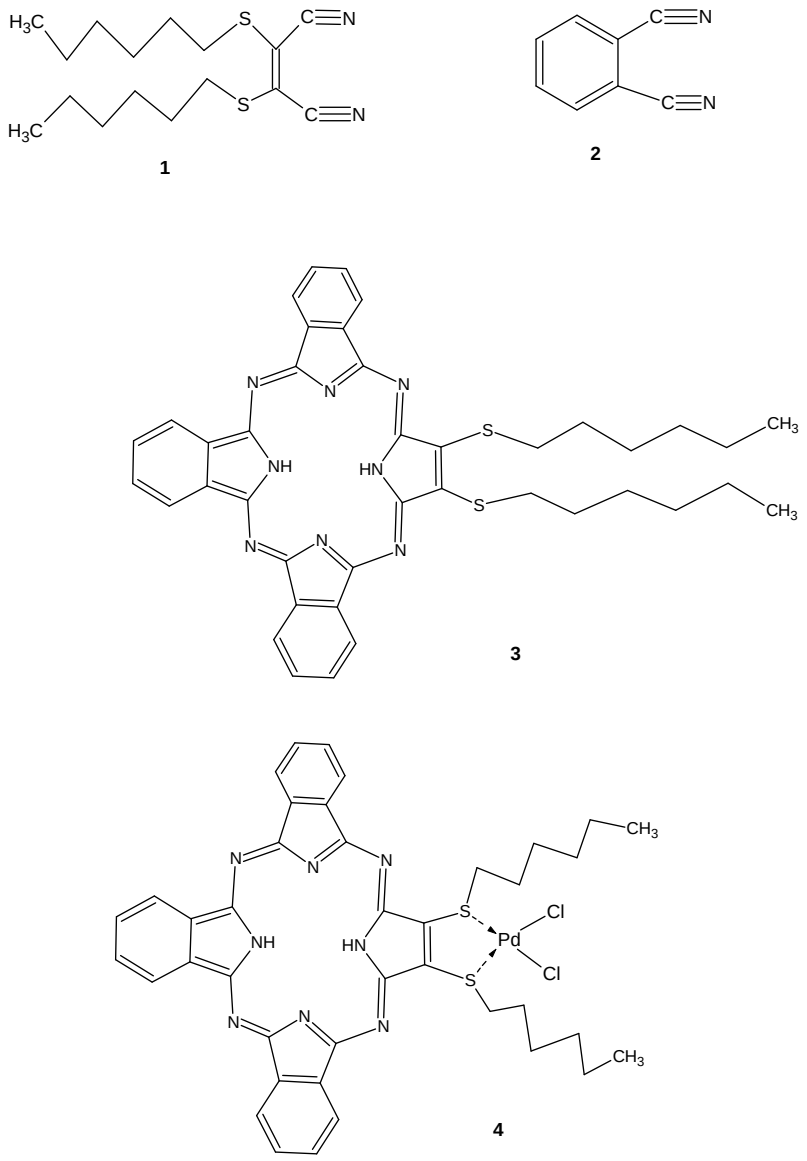


**Figure 2.37** Bis-hexylthio-maleonitrile **1**, phthalonitrile **2**, phthalocyanineporphyrazine hybrid **3**, and the four-coordinate palladium complex **4**.

### 2.7.6 Porphyrazines with Appending Eight Crown Ethers

Porphyrazines (M= 2H, Mg, Cu, Co or Zn) with eight crown ether groups appending on the periphery through flexible alkylthio-bridges have been synthesized through esterification of octakis (hydroxyethylthio)-porphyrazinatomagnesium with a carboxylic acid derivative of benzo-15-crown-5 in the presence of dicyclohexyl-carbodiimid (Fig.2.38). Alkali metal interaction of the crown ethers on the magnesium porphyrazinate are shown to form intramolecular sandwich type adducts by the changes

occurring after gradual portionwise addition of these salts into the porphyrazine solutions [67].

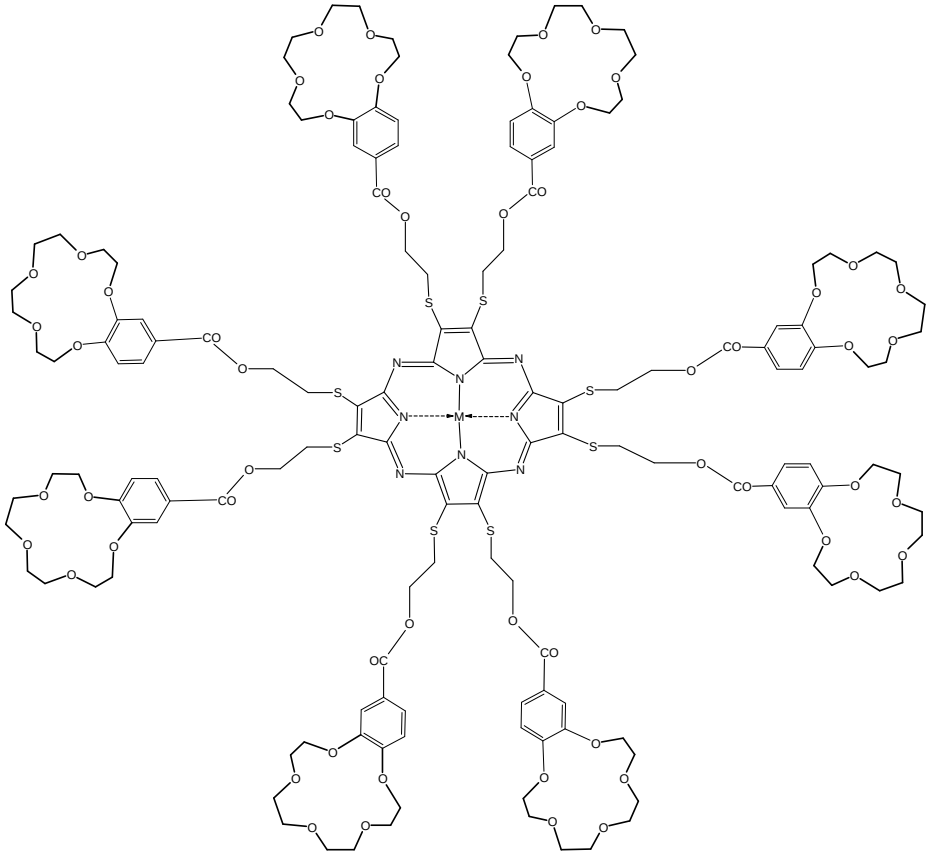

| M: | Mg | 2H | Co | Cu | Zn |
|---|---|---|---|---|---|
| | 4 | 5 | 6 | 7 | 8 |

**Figure 2.38** Octakis (crown ether) substituted phthalocyanines.

### 2.7.7 Octakis(1-naphthylmethylthio) Substituted Porphyrazine Derivatives

Magnesium porphyrazinate substituted with eight (1-naphthylmethylthio)groups on the peripheral positions has been synthesized by cyclotetramerization of 1,2-bis(1-naphthylmethylthio)maleonitrile in the presence of magnesium butanolate. The metal-free derivative was obtained by its treatment with trifluoroacetic acid and further reaction of this product with copper(II) acetate, zinc(II) acetate and cobalt(II) acetate led to the metal porphyrazinates (M=Cu, Zn, Co) (Fig.2.39) [59].

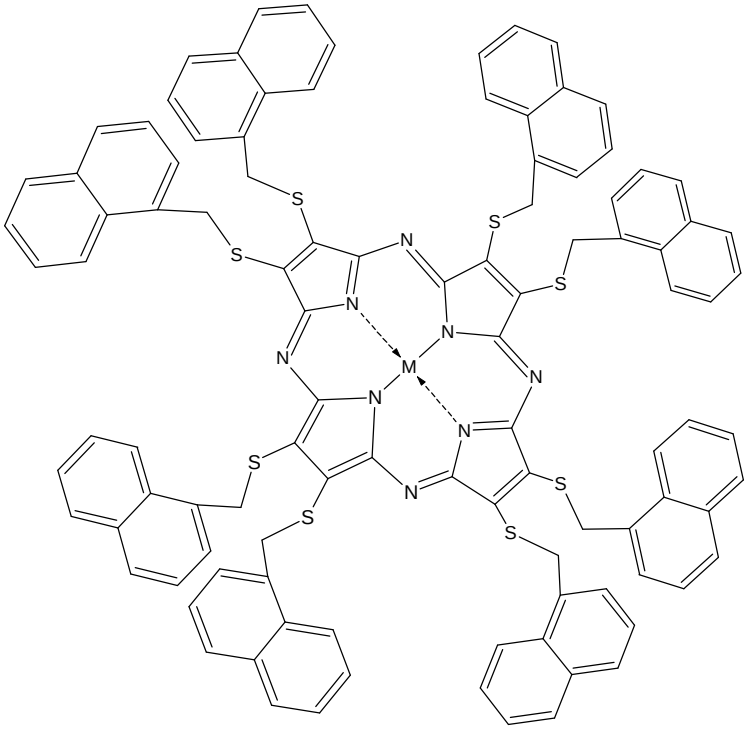


**Figure 2.39** Octakis (1-naphthylmethylthio) substituted porphyrazines (M=Mg; 2H; Cu; Zn; Co).

### 2.7.8 Synthesis and EPR Studies of Porphyrazines with Bulky Substituents

Magnesium porphyrazinate substituted with eight 4-tert-butylphenylthio-groups on the peripheral positions has been synthesized by cyclotetramerization of 1,2-bis(4-tert-butylphenylthio)maleonitrile in the presence of magnesium butanolate. The metal-free derivative was obtained by its treatment with trifluoroacetic acid and further reaction of this product with copper(II) acetate, zinc(II) acetate and cobalt(II) acetate led to the metal porphyrazinates (M = Cu, Zn, Co) (Fig.2.40). By using EPR technique, room temperature paramagnetic properties of Cu(II) doped porphyrazine sample as powder and solution forms were measured. The first-derivative EPR signals taken from as powder and solution forms shows that the sample is axially symmetric. The trend $g_{ll} > g_{\perp} > 2$ indicates that the unpaired electron is located mainly in the $d_{x2\_y2}$ orbital ($^2B_1$ as ground state) [68].

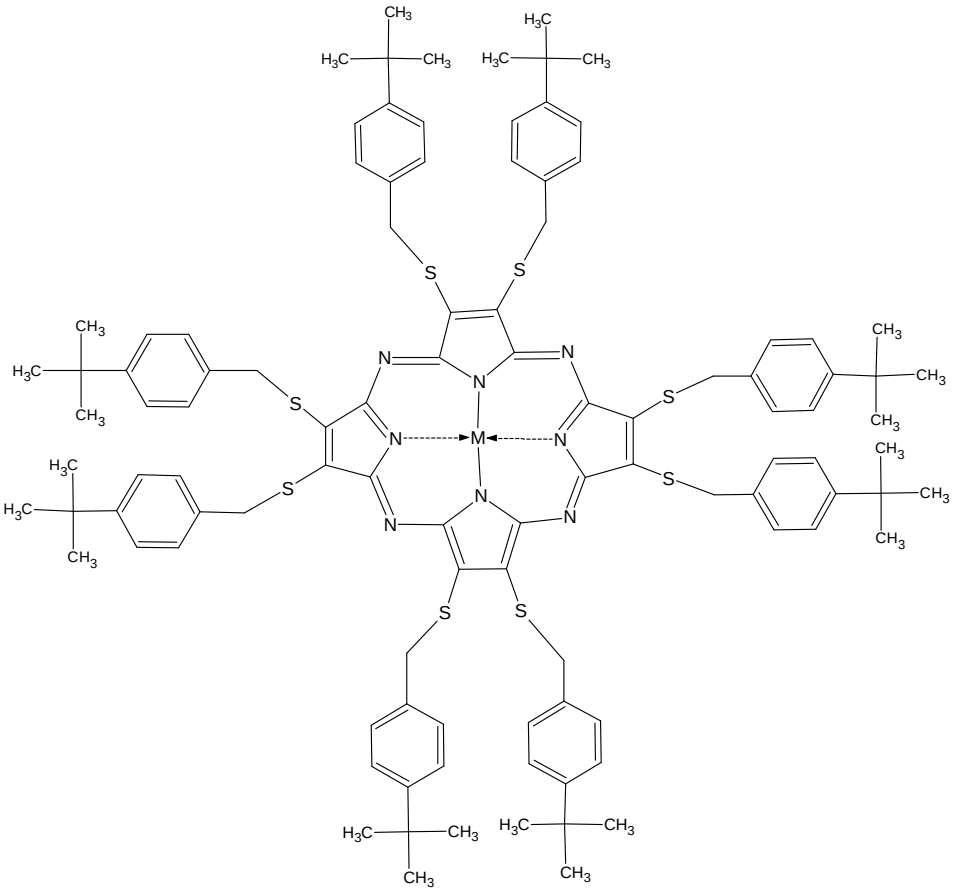

**Figure 2.40** Octakis(4-tert-butylbenzylthio) substituted porphyrazines (M =Mg; 2H; Cu; Co; Zn ).

### 2.7.9 Construction of Nonanuclear Supramolecular Structures from Simple Modular Units

A porphyrazine based supramolecule with a nonanuclear structure has been prepared by the ready coordination of pyridine donor sites in octakis(4-pyridoxyethylthio) porphyrazinatomagnesium with vanadyl bis(acetylacetonate) (Fig.2.41) [69].

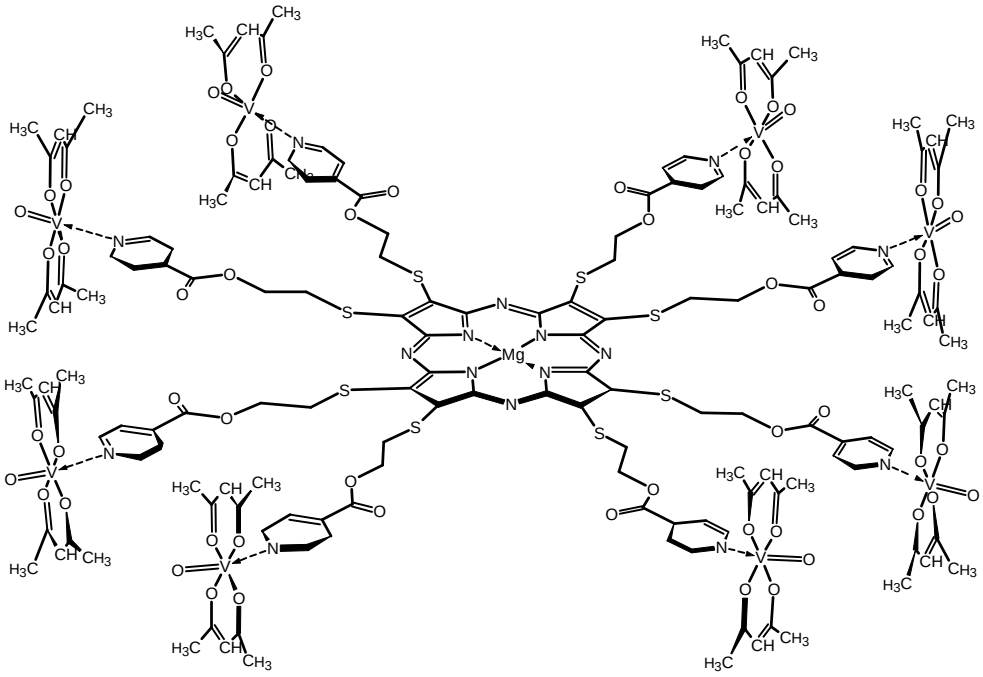

**Figure 2.41** Octakis (4-pyridoxyethylthio) porphyrazinatomagnesium with vanadyl bis(acetylacetonate) $[VO(acac)_2(4\text{-}pyCOOCH_2CH_2S)]_8$ MgPz.

### 2.7.10 Synthesis and Characterization of Octakis-(9-anthracenylmethylthio) Substituted Novel Porphyrazines

A magnesium porphyrazinate carrying eight (9-anthracenyl) units on the periphery through flexible methylthio bridges has been synthesized by cyclotetramerization of 3,4-(9-anthracenylmethylthio) pyrroline-2,5-diimine (Fig.2.42) in the presence of magnesium butanolate. The metal-free derivative was obtained by treatment with trifluoroacetic acid and further reaction of this product with copper(II) acetate, zinc(II) acetate, and cobalt(II) acetate led to the metal porphyrazinates (M = Cu, Zn, Co) [70].

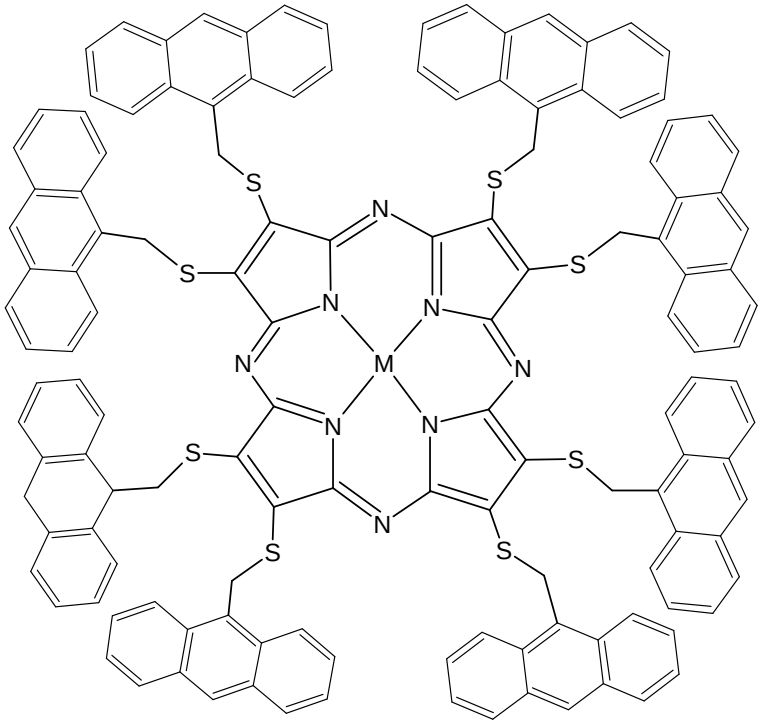

M= Mg; 2H; Cu; Zn; Co

**Figure 2.42** Octakis(9-anthracenylmethylthio)substituted porphyrazines.

### 2.7.11 Octakis(ferrocene)-Substituted Porphyrazines

Metal-free porphyrazine and metal porphyrazinates (M= Mg, Cu, Co or Zn) substituted with eight ferrocene moieties on the periphery through flexible alkylthio-bridges have been synthesised in a multi-step reaction sequence (Fig.2.43) [71].

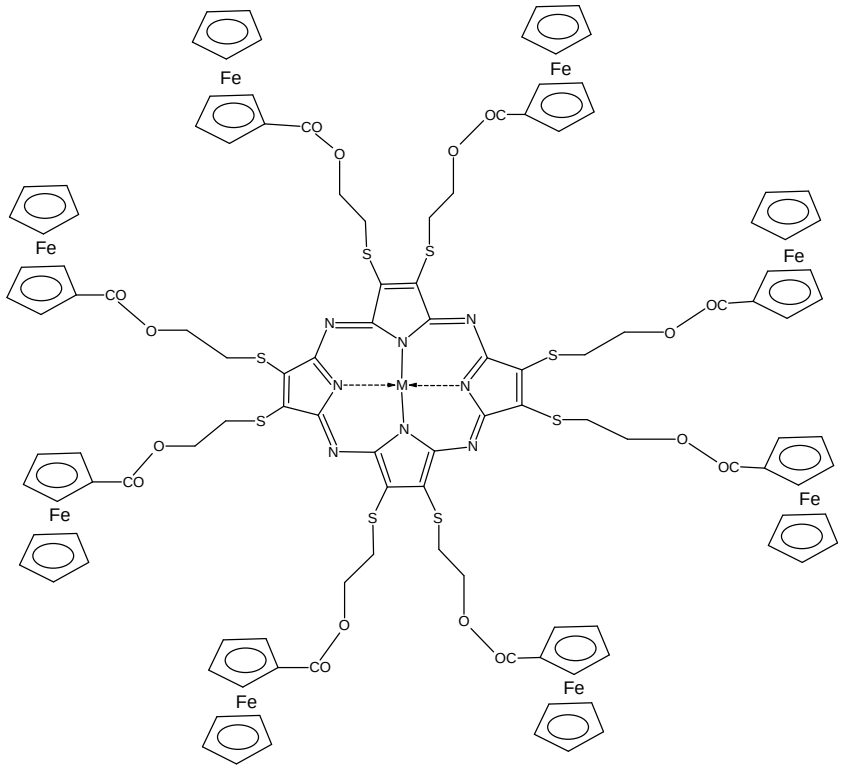


**Figure 2.43** Octakis(ferrocene)substituted porphyrazines.

### 2.7.12 Synthesis and Characterization of Phosphonic Acid-Substituted Porphyrazines

It is synthesized phosphonate-substituted maleonitrile **1** by the reaction of dithiomaleonitrile disodium salt with diethyl(2-bromoethyl)phosphonate in absolute ethanol under nitrogen at ambient temperature for 12 h (Fig.2.44). The phosphonate-substituted porphyrazine molecule **2** has been prepared by the Linstead macrocyclization of 1,2-bis{2-(diethylphosphonate) ethylthio}maleonitrile with freshly prepared $Mg(OPr)_2$ in 1-propanol under reflux for 12 h (Fig.2.45). The proposed structures of maleonitrile **1** and porphyrazine **2** are consistent with their spectral characterizations; the phosphonate groups were easily identified by FT-IR, $^{31}P$ and $^{13}C$ NMR spectroscopy. Because of the macrocyclization, the phosphorous peak of the $P{=}O(OR)_2$ groups of maleonitrile shifts from doublet 26.5 to 29.8 ppm in $^{31}P$ NMR spectrum [72].

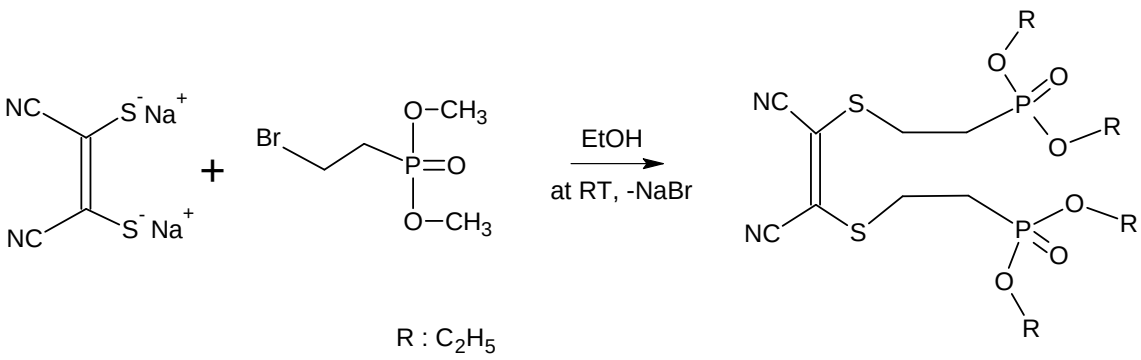


**Figure 2.44** Synthesis of 1,2-bis{2-(diethyl phosphonate) ethylthio}maleonitrile **1**.

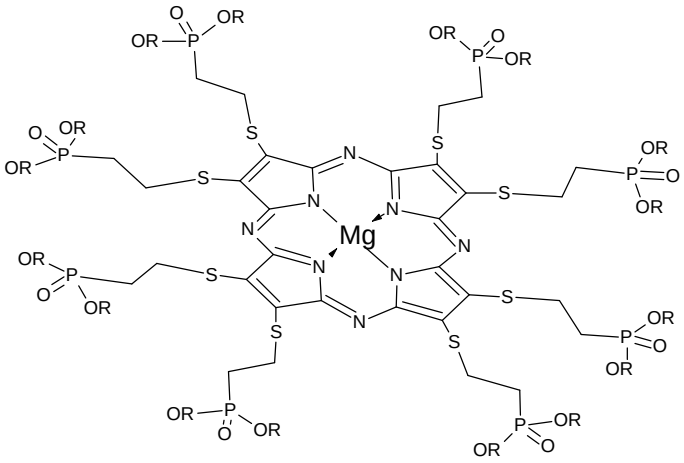


**Figure 2.45** Phosphonate-substituted **2** and phosphonic acid-substituted **3** porphyrazines.

## 2.8 The Aim and Scope of This Work

Porphyrazines may be considered to be structural hybrids of the well-studied porphyrins and phthalocyanines. As such, they provide an excellent opportunity to explore the subtle effects of ligand structure on the properties of coordinated metal ions in porphyrinic complexes. In addition, porphyrazines show several unique properties (optical, electrochemical, and catalytic), which make them of interest in their own right.

Despite the structural similarities, porphyrazines are virtually unstudied compared to the related macrocycles, partly due to the lack of an efficient synthesis of soluble derivatives. Octakis (phenyl) derivative, first reported by Linstead, have received scattered attention.

The synthesis of novel porphyrazines with eight (*p*-tolyl) and (*o*-tolyl) and (4-biphenyl) substituents derivatives has been the main scope of this work. Magnesium porphyrazinates have been synthesized for the first time by cyclotetramerization of 1,2-bis(*p*-tolyl)maleonitrile and 1,2-bis(*o*-tolyl)maleonitrile and 1,2-bis(4-biphenyl)maleonitrile in the presence of magnesium butanolate. Their demetalation by treatment with trifluoroacetic acid resulted in partially oxidized products, namely, octakis(*p*-tolyl)-2-*seco*-porphyrazine-2,3-dione, octakis(*o*-tolyl)-2-*seco*-porphyrazine-2,3-dione and octakis(4-biphenyl)-2-*seco*-porphyrazine-2,3-dione. Further reaction of these products with copper(II) acetate, zinc(II) acetate and cobalt(II) acetate has led to the metallo derivatives, [octakis(*p*-tolyl)-2-*seco*-2,3-dioxoporphyrazinato] M(II), [octakis(*o*-tolyl)-2-*seco*-2,3-dioxoporphyrazinato] M(II) and [octakis(4-biphenyl)-2-*seco*-2,3-dioxoporphyrazinato] M(II) (M = Cu, Zn, Co) [73,74].

The synthesis along with the spectroscopic properties of the novel compounds will be described.

# CHAPTER 3

# CHEMICALS AND EQUIPMENT

## 3.1. Chemicals

α-chloro-o-xylol ($C_9H_{11}Cl$), α-chloro-p-xylol ($C_9H_{11}Cl$), 4-chloromethyl-biphenyl ($C_{13}H_{11}Cl$), Potassium Cyanide (KCN), Methanol ($CH_3OH$), Ethanol ($C_2H_5OH$), Sodium (Na), Iodine ($I_2$), Magnesium (Mg), Sodium Sulfate ($Na_2SO_4$), Chloroform ($CHCl_3$), Dichloromethane ($CH_2Cl_2$), Ammonia ($NH_3$), Trifluoroaceticacid ($CF_3COOH$), *n*-Buthanol ($C_4H_9OH$), Diethylether ($C_4H_{10}O$), Benzene ($C_6H_6$), Acetone ($C_3H_6O$), Paraffin Oil, *n*-hexane, Cobalt Acetate ($Co(OAc)_2$), Copper Acetate ($Cu(OAc)_2$ ), Zinc Acetate ($Zn(OAc)_2$ ), Silica Gel 60 (0.063-0.200 mm), TLC Aluminum Sheets, Parafilm, Distilled water ($H_2O$).

## 3.2. Equipment

| | |
|---|---|
| IR (infrared) Spectrophotometer | Perkin Elmer Spectrum One FT-IR |
| UV/ VIS Spectrophotometer | UNICAM UV2-100 |
| Magnetic Stirrer and Heater | IKA |
| Elemental Analyses | Thermo Finnigan Flash EA 1112 |
| $^1$H-NMR Spectrophotometer | Varian INOVA 500 MHz |
| Mass Spectrophotometer | Bruker Daltonics MicrOTOF LC-MS |

# CHAPTER 4

# EXPERIMENTAL PART

## 4.1 Synthesis of (*o*-tolyl)acetonitrile (O1) [75]

To a stirred solution of 2 g (14.2 mmol) of α-chloro-*o*-xylol in 20 mL of absolute ethanol was added in one portion 1.85 g (28.4 mmol) of potassium cyanide in 5 mL of water. The reaction mixture was refluxed for 8 h. After the reaction mixture was treated with sea sand and filtered through a pad of fisher alumina, all of the alcohol was distilled at reduced pressure. The aqueous mixture remaining was extracted with ether which was in turn washed, dried and evaporated. The product was oily and red brown colored (Fig.4.1). The yield was 1.49 mg (80%) of (*o*-tolyl)acetonitrile.

## 4.2 Synthesis of (*p*-tolyl)acetonitrile (P1) [76]

5 g (35.5 mmol) α-chloro-*p*-xylol in the diluted 50 mL of absolute ethanol was refluxed with 4.56 g (69.92 mmol) KCN for 4 h. After the reflux, all of the ethyl alcohol was distilled at reduced pressure. The oily product was red brown colored (Fig.4.1). The yield was 3.17 g (85%).

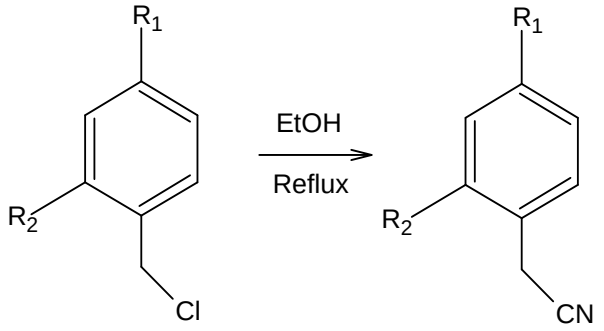


**O** ($R_1$: H, $R_2$: $CH_3$) **O1** ($R_1$: H, $R_2$: $CH_3$)
**P** ($R_1$: $CH_3$, $R_2$: H) **P1** ($R_1$: $CH_3$, $R_2$: H)

**Figure 4.1** Synthesis of (*o*-tolyl)acetonitrile **O1** and (*p*-tolyl)acetonitrile **P1**.

### 4.3 Synthesis of 1,2-bis(*o*-tolyl)maleonitrile (O2)

A slurry of **O1** (1.60 g, 12.20 mmol) and iodine (3.10 g, 12.20 mmol) in 1:1 $Et_2O$-MeOH (20 mL) was allowed to reflux under nitrogen for 1 h. The solution was cooled to room temperature, and sodium methoxide (2.2 equiv, 2.0 M, 13.4 mL) in methanol was added drop by drop (over a period of 30 min) into the reaction medium under a nitrogen atmosphere. The reaction mixture was stirred for another 3-4 h. During this time, more and more precipitation was formed in the solution. The solution was filtered at room temperature and the solid product was washed with water. The product was green colored and was very soluble in chloroform and dichloromethane, but insoluble in *n*-hexane (Fig.4.2). Yield: 1.15 g (73%). FT-IR: $\nu_{max}$, $cm^{-1}$: 3058 (CH, aromatic), 2937 (CH, aliphatic), 2246 (C≡N), 1620 (C=C, aromatic), 1515, 1390, 1170, 1128, 1020, 846, 750 (Appendix A). $^1H$ NMR ($CDCl_3$, 500 MHz): δ, ppm 7.46-7.43 (t, 2H, Ar-H), 7.39-7.35 (m, 4H, Ar-H), 7.32-7.26 (t, 2H, Ar-H), 2.51 (s, 6H, $-CH_3$) (Appendix D). MS (ESI): *m/z* 258.2 $[M]^+$ (Appendix B). Anal. calcd. for $C_{18}H_{14}N_2$: C, 83.69; H, 5.46; N, 10.84%. Found: C, 83.48; H, 5.54; N, 10.96%.

### 4.4 Synthesis of 1,2-bis(*p*-tolyl) maleonitrile (P2)

A slurry of **P1** (1.60 g, 12.20 mmol) and iodine (3.10 g, 12.20 mmol) in 1:1 $Et_2O$-MeOH (20 mL) was allowed to reflux under nitrogen for 1 h. The solution was cooled to room temperature, and sodium methoxide (2.2 equiv, 2.0 M, 13.4 mL) in methanol was added drop by drop (over a period of 30 min) into the reaction medium under a nitrogen atmosphere. The reaction mixture was stirred for another 3-4 h. During this time, more and more precipitation was formed in the solution. The solution was filtered at room temperature and the solid product was washed with water. The product was a yellow-green color and was very soluble in chloroform and dichloromethane, but insoluble in *n*-hexane (Fig.4.2). Yield: 1.23 g (78%). FT-IR: $\nu_{max}$, $cm^{-1}$: 3047 (CH, aromatic), 2918 (CH, aliphatic), 2219 (C≡N), 1606 (C=C, aromatic), 1509, 1386, 1184, 1115, 1017, 802, 766 (Appendix E). $^1H$ NMR (500 MHz; $CDCl_3$): δ, ppm 7.75-7.70 (m, 4H, Ar-H), 7.35 7.30 (m, 4H, Ar-H), 2.44 (s, 6H, $-CH_3$) (Appendix F). MS (ESI): *m/z* 258.6 $[M]^+$ (Appendix C). Anal. calcd. for $C_{18}H_{14}N_2$: C, 83.69; H, 5.46; N, 10.84%. Found: C, 83.43; H, 5.62; N, 10.69%.

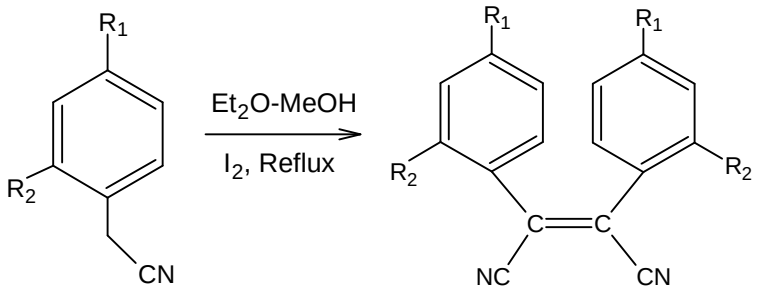


**O1** ($R_1$: H, $R_2$: $CH_3$) **O2** ($R_1$: H, $R_2$: $CH_3$)
**P1** ($R_1$: $CH_3$, $R_2$: H) **P2** ($R_1$: $CH_3$, $R_2$: H)

**Figure 4.2** Synthesis of 1,2-bis(*o*-tolyl)maleonitrile **O2** and 1,2-bis(*p*-tolyl)maleonitrile **P2**.

### 4.5 [2,3,7,8,12,13,17,18-octakis(*o*-tolyl)porphyrazinato] Mg(II) (O3)

Mg turnings (24.3 mg, 1 mmol) and a small $I_2$ crystal were refluxed in *n*-BuOH (20 mL) for about 8 h to obtain $Mg(BuO)_2$. **O2** (516.6 mg, 2 mmol) was added to this solution and the mixture was refluxed for about 8 h. The blue-green colored product was filtered, washed with ethanol and water and dried in a vacuum. The crude product was dissolved in $CHCl_3$ and filtered. The $CHCl_3$ solution was dried over anhydrous $Na_2SO4$. When the solvent was evaporated, a blue-green colored product was obtained. Finally, pure porphyrazine was obtained by chromatography on silica gel using methanol/chloroform (1:50) mixture as eluent. The product was soluble in chloroform, dichloromethane, acetone and toluene, but insoluble in *n*-hexane (Fig.4.3). Yield: 349 mg (66%). FT-IR: $\nu_{max}$, $cm^{-1}$: 3050 (CH, aromatic), 2925 (CH, aliphatic), 1620 (C=C, aromatic), 1468, 1350, 1190, 1144, 982, 824, 765. $^1H$ NMR ($CDCl_3$, 500 MHz): δ, ppm 7.56-7.20 (m, 4H, aromatic H), 2.58 (s, 3H, $CH_3$). MS (ESI): *m/z* 1057.7 $[M]^+$. Anal. calcd. for $C_{72}H_{56}N_8Mg$: C, 81.77; H, 5.34; N, 10.60%. Found: C, 81.58; H, 5.43; N, 10.53%.

### 4.6 [2,3,7,8,12,13,17,18-octakis(*p*-tolyl)porphyrazinato] Mg(II) (P3)

Mg turnings (24.3 mg, 1 mmol) and a small $I_2$ crystal were refluxed in *n*-BuOH (20 mL) for about 8 h to obtain $Mg(BuO)_2$. **P2** (516.6 mg, 2 mmol) was added to this solution and the mixture was refluxed for about 8 h. The dark green product was filtered, washed with ethanol and water and dried in a vacuum. The crude product was

dissolved in $CHCl_3$ and filtered. The $CHCl_3$ solution was dried over anhydrous $Na_2SO_4$. When the solvent was evaporated, a dark green product was obtained. Finally, pure porphyrazine was obtained by chromatography on silica gel using methanol/chloroform (1:50) mixture as eluent. The product was soluble in chloroform, dichloromethane, acetone and toluene, but insoluble in *n*-hexane (Fig.4.3). Yield: 375 mg (71%). FT-IR: $\nu_{max}$, $cm^{-1}$: 3025 (CH, aromatic), 2957 (CH, aliphatic), 1609 (C=C, aromatic), 1463, 1363, 1182, 1136, 976, 820, 767 (Appendix H). $^1H$ NMR ($CDCl_3$, 500 MHz): δ, ppm 7.65-7.26 (m, 4H, Ar-H), 2.64 (s, 3H, $-CH_3$) (Appendix K). MS (ESI): *m/z* 1057.5 $[M]^+$ (Appendix J). Anal. calcd. for $C_{72}H_{56}N_8Mg$: C, 81.77; H, 5.34; N, 10.60%. Found: C, 81.61; H, 5.25; N, 10.75%.

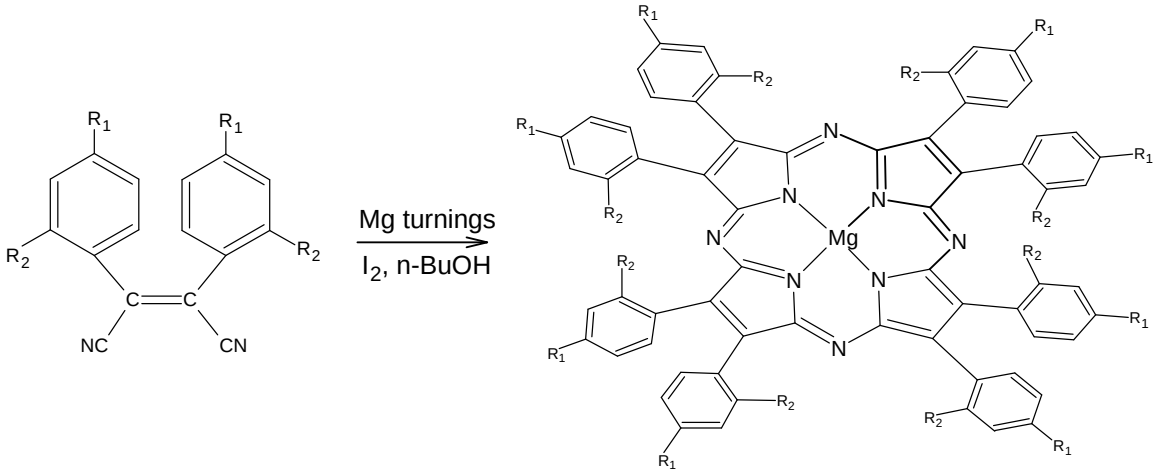


M= Mg (**O3**) ($R_1$: H, $R_2$: $CH_3$)
M= Mg (**P3**) ($R_1$: $CH_3$, $R_2$: H)

**Figure 4.3** Synthesis of [2,3,7,8,12,13,17,18-octakis(*o*-tolyl)porfirazinato] Mg(II) **O3** and [2,3,7,8,12,13,17,18-octakis(*p*-tolyl)porfirazinato] Mg(II) **P3**.

### 4.7 [2,3,7,8,12,13,17,18-octakis(*o*-tolyl)-2-*seco*-porphyrazine-2,3-dione] (O4)

**O3** (106 mg, 0.1 mmol) was dissolved in the minimum amount of trifluoroacetic acid (~ 4 mL) and stirred for 3 h at room temperature. When the reaction mixture was added to ice, drop by drop, and neutralized with 25% ammonia solution, precipitation occurred and it was filtered. The precipitate was extracted into the chloroform and the chloroform solution was extracted with water twice. After drying over anhydrous $Na_2SO_4$, the solvent was evaporated to obtain a violet colored metal-free porphyrazine

(Fig.4.4). The crude product **O4** was purified by chromatography on silica gel using methanol/chloroform (1:50) mixture as the eluent. Yield: 51 mg (48%). FT-IR: $\nu_{max}$, $cm^{-1}$: 3320 (N-H), 3052 (CH, aromatic), 2923-2855 (CH, aliphatic), 1725 (C=O), 1655 (C=C, aromatic), 1445, 1362, 1195, 1128, 993, 842, 755. $^1$H NMR ($CDCl_3$, 500 MHz): δ, ppm 7.60-7.24 (m, 4H, aromatic H), 2.55 (s, 3H, $-CH_3$), -0.95 (br s, 2H, NH). MS (ESI): *m/z* 1067.8 $[M]^+$. Anal. calcd. for $C_{72}H_{58}N_8O_2$: C, 81.03; H, 5.48; N, 10.50%. Found: C, 80.87; H, 5.40; N, 10.62%.

### 4.8 [2,3,7,8,12,13,17,18-octakis(*p*-tolyl)-2-*seco*-porphyrazine- 2,3-dione] (P4)

**P3** (106 mg, 0.1 mmol) was dissolved in the minimum amount of trifluoroacetic acid (~ 4 mL) and stirred for 3 h at room temperature. When the reaction mixture was added to ice, drop by drop, and neutralized with 25% ammonia solution, precipitation occurred and it was filtered. The precipitate was extracted into the chloroform and the chloroform solution was extracted with water twice. After drying over anhydrous $Na_2SO_4$, the solvent was evaporated to obtain a green colored metal-free porphyrazine (Fig.4.4). The crude product **P4** was purified by chromatography on silica gel using methanol/chloroform (1:50) mixture as the eluent. Yield: 57 mg (53%). FT IR: $\nu_{max}$, $cm^{-1}$: 3335 (N-H), 3048 (CH, aromatic), 2923-2855 (CH, aliphatic), 1718 (C=O), 1625 (C=C, aromatic), 1445, 1318, 1168, 1120, 960, 852, 758. $^1$H NMR ($CDCl_3$, 500 MHz): δ, ppm 7.75-7.28 (m, 4H, Ar-H), 2.68 (s, 3H, $-CH_3$), -1.05 (br s, 2H, NH). MS (ESI): *m/z* 1067.1 $[M]^+$ (Appendix M). Anal. calcd. for $C_{72}H_{58}N_8O_2$: C, 81.03; H, 5.48; N, 10.50%. Found: C, 80.89; H, 5.61; N, 10.58%.

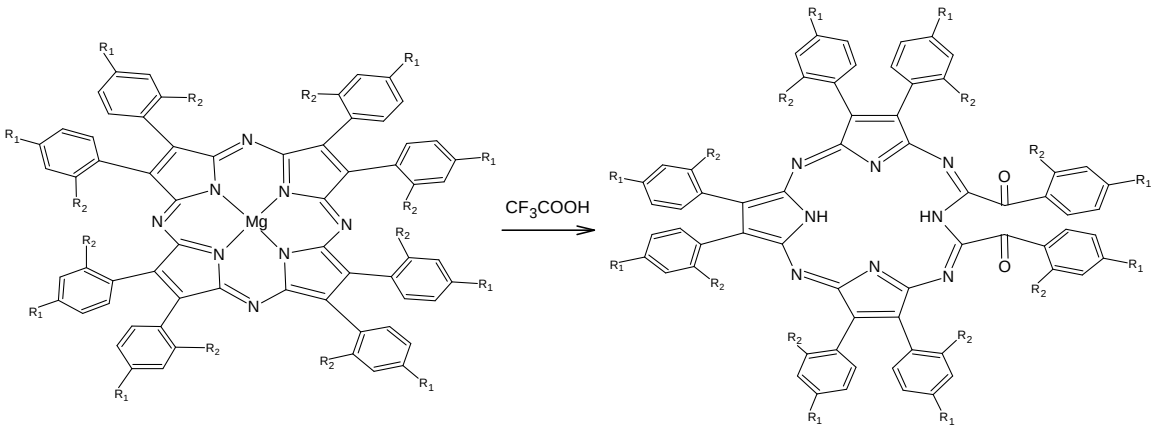


M= 2H (**O4**) ($R_1$: H, $R_2$: $CH_3$)
M= 2H (**P4**) ($R_1$: $CH_3$, $R_2$: H)

**Figure 4.4** Synthesis of [2,3,7,8,12,13,17,18-octakis(*o*-tolyl)-2-*seco*-porphyrazine-2,3-dione] (M= 2H) or [2,3,7,8,12,13,17,18-octakis (*p*-tolyl)-2-*seco*-porphyrazine-2,3-dione] (M= 2H).

### 4.9 General procedure for metallo *seco*-porphyrazines (O5-O7, P5-P7)

**O4 or P4** (107 mg, 0.1 mmol) in $CHCl_3$ (10 mL) was stirred with the metal salt [$Cu(OAc)_2$ (181.6 mg, 1 mmol), $Zn(OAc)_2$ (183.4 mg, 1 mmol) or $Co(OAc)_2$ (177 mg, 1 mmol)] in ethanol (15 mL) and refluxed under nitrogen for about 4 h. Then, the precipitate composed of the crude product and the excess metal salt was filtered. The precipitate was treated with $CHCl_3$ and the insoluble metal salts were removed by filtration (Fig.4.5). The filtrate was reduced to the minimum volume under reduced pressure and then added into *n*-hexane (100 ml) drop by drop to realize the precipitation. Finally, pure porphyrazine derivatives were obtained by chromatography on silica gel using methanol/chloroform (1:20) mixture as the eluent.

### 4.10 [2,3,7,8,12,13,17,18-octakis(o-tolyl)-2-seco-2,3-dioxoporphyrazinato] Cu(II) (O5)

Yield: 55 mg (49%). FT-IR, $\nu_{max}$, $cm^{-1}$: 3052 (CH, aromatic), 2928-2868 (CH, aliphatic), 1718 (C=O), 1628 (C=C, aromatic), 1453, 1365, 1183, 1132, 978, 833, 757. MS (ESI): *m/z* 1128.65 $[M]^+$. Anal. calcd. for $C_{72}H_{56}N_8O_2Cu$: C, 76.61; H, 5.00; N, 9.93%. Found: C, 76.49; H, 4.91; N, 9.99%.

### 4.11 [2,3,7,8,12,13,17,18-octakis(o-tolyl)-2-seco-2,3-dioxoporphyrazinato] Zn(II) (O6)

Yield: 51 mg (45%). FT-IR, $\nu_{max}$, $cm^{-1}$: 3048 (CH, aromatic), 2925-2855 (CH, aliphatic), 1722 (C=O), 1622 (C=C, aromatic), 1440, 1348, 1188, 1139, 973, 813, 762. $^1H$ NMR ($CDCl_3$, 500 MHz): δ, ppm 7.62-7.23 (m, 4H, aromatic H), 2.53 (s, 3H, $-CH_3$). MS (ESI): *m/z* 1130.24 $[M]^+$. Anal. calcd. for $C_{72}H_{56}N_8O_2Zn$: C, 76.48; H, 4.99; N, 9.91%. Found: C, 76.36; H, 5.12; N, 10.03%.

### 4.12 [2,3,7,8,12,13,17,18-octakis(o-tolyl)-2-seco-2,3-dioxoporphyrazinato] Co(II) (O7)

Yield: 47 mg (42%). FT-IR, $\nu_{max}$, $cm^{-1}$: 3045 (CH, aromatic), 2932-2874 (CH, aliphatic), 1724 (C=O), 1635 (C=C, aromatic), 1444, 1350, 1176, 1142, 988, 839, 768. MS (ESI): *m/z* 1124.53 $[M]^+$. Anal. calcd. for $C_{72}H_{56}N_8O_2Co$: C, 76.92; H, 5.02; N, 9.97%. Found: C, 76.81; H, 5.15; N, 9.85%.

### 4.13 [2,3,7,8,12,13,17,18-octakis(p-tolyl)-2-seco-2,3-dioxoporphyrazinato] Cu(II) (P5)

Yield: 52 mg (46%). FT-IR, $\nu_{max}$, $cm^{-1}$: 3052 (CH, aromatic), 2924-2880 (CH, aliphatic), 1726 (C=O), 1653 (C=C, aromatic), 1444, 1385, 1188, 1128, 988, 834, 755. MS (ESI): *m/z* 1128.13 $[M]^+$. Anal. calcd. for $C_{72}H_{56}N_8O_2Cu$: C, 76.61; H, 5.00; N, 9.93%. Found: C, 76.52; H, 5.09; N, 9.84%.

### 4.14 [2,3,7,8,12,13,17,18-octakis(p-tolyl)-2-seco-2,3-dioxoporphyrazinato] Zn(II) (P6)

Yield: 59 mg (52%). FT-IR, $\nu_{max}$, $cm^{-1}$: 3044 (CH, aromatic), 2932-2865 (CH, aliphatic), 1720 (C=O), 1672 (C=C, aromatic), 1438, 1348, 1178, 1123, 984, 832, 762. $^1H$ NMR ($CDCl_3$, 500 MHz): δ, ppm 7.62-7.24 (m, 4H, aromatic H), 2.52 (s, 3H, $-CH_3$). MS (ESI): *m/z* 1130.27 $[M]^+$. Anal. calcd. for $C_{72}H_{56}N_8O_2Zn$: C, 76.48; H, 4.99; N, 9.91%. Found: C, 76.59; H, 4.88; N, 9.99%.

### 4.15 [2,3,7,8,12,13,17,18-octakis(p-tolyl)-2-seco-2,3-dioxoporphyrazinato] Co(II)(P7)

Yield: 62 mg (55%). FT-IR, $\nu_{max}$, $cm^{-1}$: 3052 (CH, aromatic), 2934-2858 (CH, aliphatic), 1722 (C=O), 1665 (C=C, aromatic), 1442, 1350, 1166, 1142, 972, 839, 748. MS (ESI): *m/z* 1124.63 $[M]^+$. Anal. calcd. for $C_{72}H_{56}N_8O_2Co$: C, 76.92; H, 5.02; N, 9.97%. Found: C, 76.79; H, 5.13; N, 9.88%.

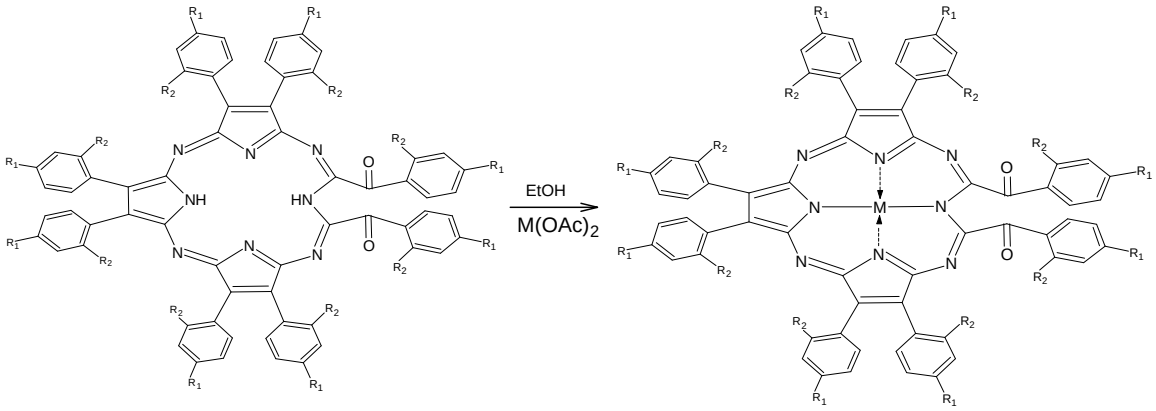


M= Cu (**O5**); Zn (**O6**); Co (**O7**) ($R_1$: H, $R_2$: $CH_3$)
M= Cu (**P5**); Zn (**P6**); Co (**P7**) ($R_1$: $CH_3$, $R_2$: H)

**Figure 4.5** Synthesis of [2,3,7,8,12,13,17,18-octakis(o-tolyl)-2-seco-2,3-dioxoporphyrazinato] {M=Cu(II), Zn(II) or Co(II)} and [2,3,7,8,12,13,17,18-octakis(p-tolyl)-2-seco-2,3-dioxoporphyrazinato] {M=Cu(II), Zn(II) or Co(II)}.

### 4.16 Synthesis of (4-biphenyl)acetonitrile (B1) [77]

A solution of 8,1 g (40 mmol) of (4-chloromethyl-biphenyl) 4-phenylbenzyl chloride, in 100 mL of acetone was added dropwise over 20 min to a stirred refluxing solution of 10 g of potassium cyanide in 80 mL of 70% aqueous acetone. After refluxing for 20 h, most of the aqueous acetone was removed by distillation and replaced with a 4 to 1 mixture of benzene and ether. The cooled organic phase was washed several times with water, dried, and the solvent was removed on a steam bath. The residue was crystallized from cyclohexane to yield 7 g (90%) of 4-biphenylylacetonitrile (Fig.4.6).

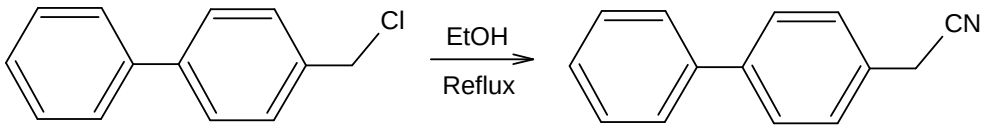


**Figure 4.6** Synthesis of (4-biphenyl)acetonitrile **B1**.

### 4.17 Synthesis of 1,2-bis(4-biphenyl)maleonitrile (B2)

A slurry of 4-biphenylacetonitrile (1.0 g, 5.2 mmol) and iodine (1.313 g, 5.200 mmol) in 1:1 $Et_2O$-MeOH (20 mL) was allowed to reflux under nitrogen for 1 h. The solution was cooled to room temperature, and sodium methoxide (2.2 equiv, 2.0 M, 5.7 mL) in methanol was added drop by drop (over a period of 30 min) into the reaction medium under a nitrogen atmosphere. The reaction mixture was stirred for another 3 h. During this time, more and more precipitation was formed in the solution. The solution was filtered at room temperature and the solid product was washed with water. The product was yellow colored and was very soluble in chloroform, dichloromethane and acetone, but insoluble in n-hexane (Fig.4.7). Yield was 0.316 g (32%). FT-IR, $\nu_{max,}$ $cm^{-1}$: 3070-3030 (CH, aromatic), 2218 (C≡N), 1604 (C=C, aromatic), 1486, 1405, 1209, 1140, 1005, 845, 766, 724, 691 (Appendix N). $^1H$ NMR ($CDCl_3$, 500 MHz): δ, ppm 7.99-7.93 (m, 4H, Ar-H), 7.80-7.75 (m, 4H, Ar-H), 7.68-7.26 (m, 10H, Ar-H) (Appendix O). MS (ESI): *m/z* 382.2 $[M]^+$ (Appendix P). Anal. calcd. for $C_{28}H_{18}N_2$: C, 87.93; H, 4.74; N, 7.32%. Found: C, 87.77; H, 4.66; N, 7.45%.

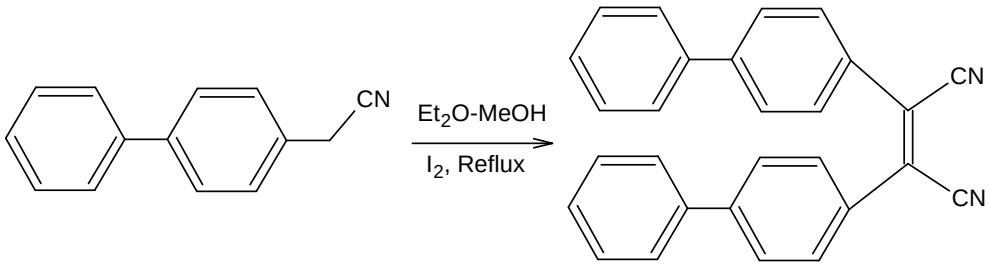


**Figure 4.7** Synthesis of 1,2-bis(4-biphenyl)maleonitrile **B2**.

### 4.18 [2,3,7,8,12,13,17,18-octakis(4-biphenyl)porphyrazinato] Mg(II) (B3)

Mg turnings (24.3 mg, 1.00 mmol) and a small $I_2$ crystal were refluxed in n-BuOH (20 mL) for about 8 h to obtain $Mg(BuO)_2$. 1,2-bis(4-biphenyl)maleonitrile (**B2**) (765

mg, 2.00 mmol) was added to this solution and the mixture was refluxed for about 8 h. The dark green product was filtered, washed with ethanol and water and dried in a vacuum. The crude product was dissolved in $CHCl_3$ and filtered. The $CHCl_3$ solution was dried over anhydrous $Na_2SO_4$. When the solvent was evaporated, a dark green product was obtained. Finally, pure porphyrazine was obtained by chromatography on silica gel using methanol/chloroform (1:50) mixture as eluent. The product was soluble in chloroform, dichloromethane, acetone and toluene, but insoluble in n-hexane (Fig.4.8). Yield: 326 mg (42%). FT-IR, $\nu_{max}$, $cm^{-1}$: 3075-3025 (CH, aromatic), 1602 (C=C, aromatic), 1484, 1404, 1208, 1139, 1004, 843, 763, 722, 689 (Appendix R). UV-Vis ($CHCl_3$) $\lambda_{max}$ (nm) (log ε / $dm^3$ $mol^{-1}$ $cm^{-1}$): 380 (4.86), 652 (4.64) (Appendix Q). $^1H$ NMR ($CDCl_3$, 500 MHz): δ, ppm 7.97-7.75 (m, 4H, Ar-H), 7.67-7.26 (m, 5H, Ar-H) (Appendix U). MS (ESI): *m/z* 1554.7 $[M]^+$ (Appendix S). Anal. calcd. for $C_{112}H_{72}N_8Mg$: C, 86.56; H, 4.67; N, 7.21%. Found: C, 86.39; H, 4.54; N, 7.33%.

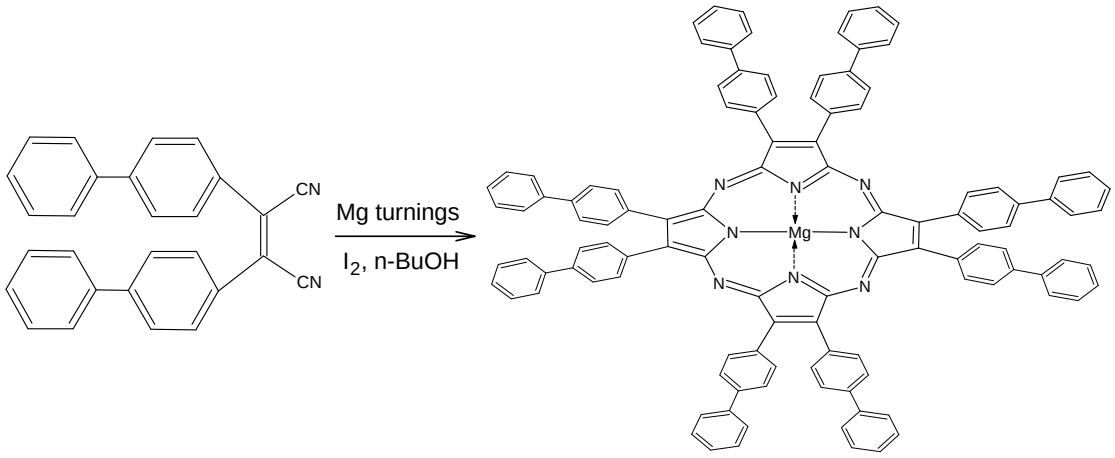


**Figure 4.8** Synthesis of [2,3,7,8,12,13,17,18-octakis(4-biphenyl)porphyrazinato] Mg(II) **B3**.

### 4.19 [2,3,7,8,12,13,17,18- octakis(4-biphenyl)-2-*seco*-porphyrazine-2,3-dione] (B4)

**B3** (155 mg, 0.100 mmol) was dissolved in the minimum amount of trifluoroacetic acid (~4 mL) and stirred for 5 h at room temperature. When the reaction mixture was added to ice drop by drop and neutralized with 25% ammonia solution, precipitation occurred and it was filtered. The precipitate was extracted into the chloroform and the chloroform solution was extracted with water twice. After drying over anhydrous $Na_2SO_4$, the solvent was evaporated to obtain the green colored metal-free porphyrazine (Fig.4.9). The crude product was purified by chromatography on

silica gel using methanol/chloroform (1:50) mixture as the eluent. Yield: 100 mg (64%). FT-IR, $\nu_{max}$, $cm^{-1}$: 3339 (N-H), 3072-3035 (CH, aromatic), 1721 (C=O), 1615 (C=C, aromatic), 1475, 1400, 1212, 1128, 1012, 838, 765, 718, 680. UV-Vis ($CHCl_3$) $\lambda_{max}$ (nm) (log ε / $dm^3$ $mol^{-1}$ $cm^{-1}$): 368 (4.77), 650 (4.41), 712 (4.49) (Appendix T). $^1H$ NMR ($CDCl_3$, 500 MHz): δ, ppm 7.91-7.70 (m, 4H, Ar-H), 7.61-7.22 (m, 5H, Ar-H), -0.95 (br s, 2H, NH). MS (ESI): *m/z* 1563.2 $[M]^+$ (Appendix V). Anal. calcd. for $C_{112}H_{74}N_8O_2$: C, 86.02; H, 4.55; N, 7.17%. Found: C, 86.15; H, 4.41; N, 7.29%.

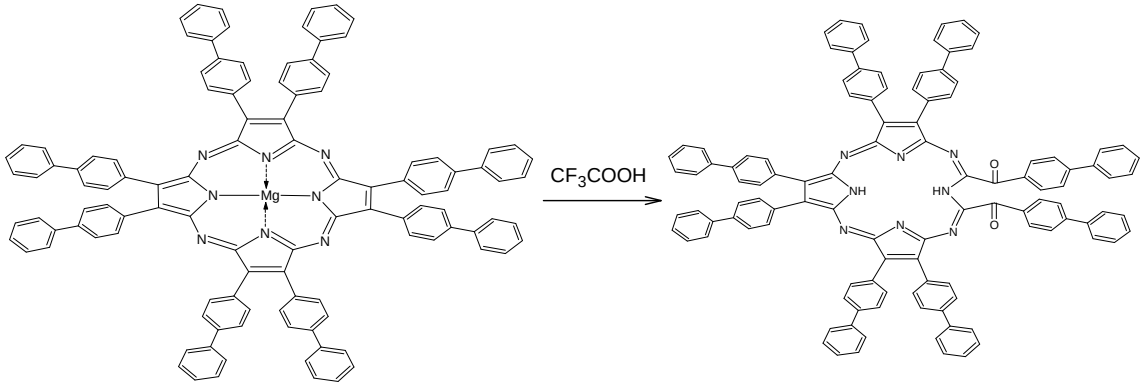


**Figure 4.9** Synthesis of [2,3,7,8,12,13,17,18-octakis(4-biphenyl)-2-*seco*-porphyrazine-2,3-dione] **B4**.

### 4.20 General procedure for metallo *seco*-porphyrazines (B5-B7)

**B4** (156 mg, 0.100 mmol) in $CHCl_3$ (10 mL) was stirred with the metal salt [$Cu(OAc)_2$ (182 mg, 1.00 mmol), $Zn(OAc)_2$ (183 mg, 1.00 mmol) or $Co(OAc)_2$ (177 mg, 1.00 mmol)] in ethanol (15 mL) and refluxed under nitrogen for about 4 h. Then, the precipitate composed of the crude product and the excess metal salt were filtered. The precipitate was treated with $CHCl_3$ and the insoluble metal salts were removed by filtration (Fig.4.10). The filtrate was reduced to the minimum volume under reduced pressure and then added into n-hexane (100 ml) drop by drop to realize the precipitation. Finally, pure porphyrazine derivatives were obtained by chromatography on silica gel using methanol/chloroform (1:20) mixture as the eluent.

**4.21 [2,3,7,8,12,13,17,18-octakis(4-biphenyl)-2-*seco*-2,3-dioxoporphyrazinato] Cu(II) (B5)**

Yield: 72 mg (44%). FT-IR, $\nu_{max}$, $cm^{-1}$: 3075-3030 (CH, aromatic), 1718 (C=O), 1622 (C=C, aromatic), 1445, 1410, 1215, 1133, 1018, 868, 753, 715, 688. UV-vis ($CHCl_3$) $\lambda_{max}$ (nm) (log ε / $dm^3$ $mol^{-1}$ $cm^{-1}$): 348 (4.82), 658 (4.58). MS (ESI): *m/z* 1625.8 $[M]^+$. Anal. calcd. for $C_{112}H_{72}N_8O_2Cu$: C, 82.76; H, 4.46; N, 6.89%. Found: C, 82.64; H, 4.59; N, 6.78%.

**4.22 [2,3,7,8,12,13,17,18-octakis(4-biphenyl)-2-*seco*-2,3-dioxoporphyrazinato] Zn(II) (B6)**

Yield: 78 mg (48%). FT-IR, $\nu_{max}$, $cm^{-1}$: 3055-3025 (CH, aromatic), 1722 (C=O), 1652 (C=C, aromatic), 1440, 1248, 1118, 1023, 848, 752, 724, 685. UV-vis ($CHCl_3$) $\lambda_{max}$ (nm) (log ε / $dm^3$ $mol^{-1}$ $cm^{-1}$): 356 (4.80), 654 (4.60). $^1H$ NMR ($CDCl_3$, 500 MHz): 7.92-7.81 (m, 4H, aromatic H), 7.65-7.24 (m, 5H, Ar-H). MS (ESI): *m/z* 1627.6 $[M]^+$. Anal. calcd. for $C_{112}H_{72}N_8O_2Zn$: C 82.67; H 4.46; N 6.89%. Found: C 82.78; H 4.39; N 6.98%.

**4.23 [2,3,7,8,12,13,17,18-octakis(4-biphenyl)-2-*seco*-2,3-dioxoporphyrazinato] Co(II) (B7)**

Yield: 62 mg (38%). FT-IR, $\nu_{max,}$ $cm^{-1}$: 3065-3020 (CH, aromatic), 1723 (C=O), 1625 (C=C, aromatic), 1476, 1408, 1215, 1146, 1009, 879, 758, 725, 684. UV-vis ($CHCl_3$) $\lambda_{max}$ (nm) (log ε / $dm^3$ $mol^{-1}$ $cm^{-1}$): 352 (4.84), 656 (4.56). MS (ESI): *m/z* 1620.3 $[M]^+$. Anal. calcd. for $C_{112}H_{72}N_8O_2Co$: C 83.00; H 4.48; N 6.91%. Found: C 82.89; H 4.59; N 6.79%.

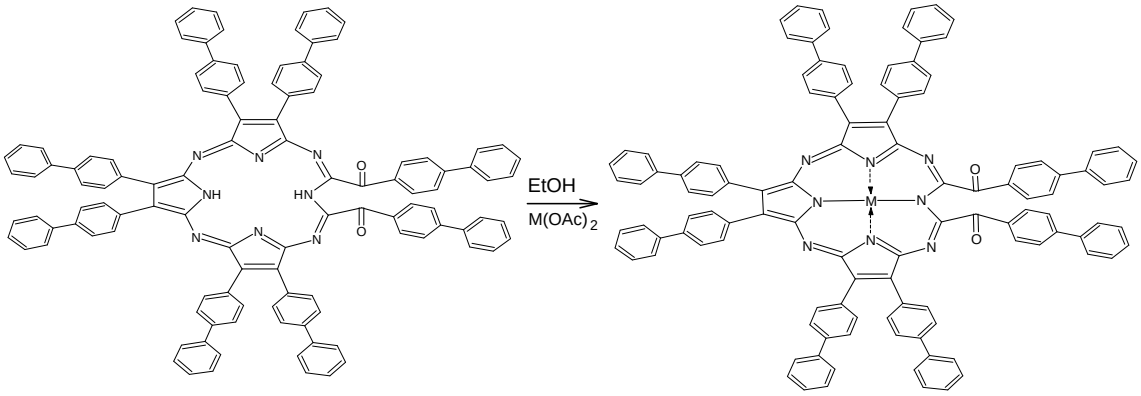


M= Cu (**B5**); Zn (**B6**); Co (**B7**)

**Figure 4.10** Synthesis of [2,3,7,8,12,13,17,18-octakis(4-biphenyl)-2-*seco*-2,3-dioxoporphyrazinato] {M= Cu(II), Zn(II) or Co(II)}.

# CHAPTER 5

# RESULTS AND DISCUSSIONS

Porphyrins (P) and their structural relatives phthalocyanines (Pc) and porphyrazines (Pz) constitute a distinct class of macrocyclic tetrapyrrolic systems with unique physico-chemical properties. Due to their chemical diversity, these compounds, and in particular porphyrins and phthalocyanines, have been at the focus of multidisciplinary interest for many years. However, although the molecular structures of all three types of macrocycles are very similar, benzo- and especially aza substitution have a strong impact on the overall chemical behavior of the corresponding tetrapyrrolic ligands [64].

Peripherally functionalized porphyrazines (tetraazaporphyrins) and related macrocycles can bind multiple metal ions, have the potential to exhibit novel magnetic and electronic properties, and serve as building blocks in the assembly of higher order polymetallic arrays [55].

## 5.1 Synthesis of *p*-tolyl and *o*-tolyl Porphyrazines

The starting point for these novel porphyrazine structures with eight (*p*-tolyl) and (*o*-tolyl) groups bound to the periphery is α-chloro-*p*-xylol **P** and α-chloro-*o*-xylol **O** which were modified to (*p*-tolyl)acetonitrile **P1** and (*o*-tolyl)acetonitrile **O1** by adding potassium cyanide. (Fig.5.1) The red brown colored products **P1** and **O1** were obtained in yield 85%, and 80%, respectively.

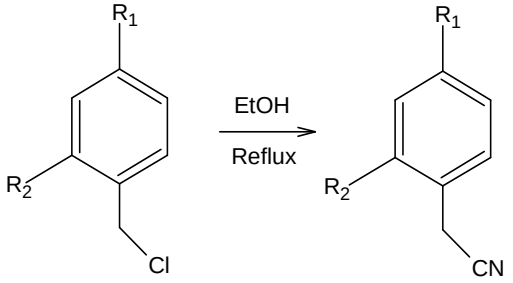


**O** ($R_1$: H, $R_2$: $CH_3$) **O1** ($R_1$: H, $R_2$: $CH_3$)

**P** ($R_1$: $CH_3$, $R_2$: H) **P1** ($R_1$: $CH_3$, $R_2$: H)

**Figure 5.1** Synthesis of (*o*-tolyl)acetonitrile (**O1**) and (*p*-tolyl)acetonitrile (**P1**).

1,2-bis(*p*-tolyl)maleonitrile **P2** and 1,2-bis(*o*-tolyl)maleonitrile **O2** which were obtained from (*p* tolyl)acetonitrile **P1** and (*o*-tolyl) acetonitrile **O1**, respectively and $I_2$ (Fig.5.2). The yellow-green colored product **P2** and the green colored product **O2** were obtained in yield 78%, and 73%, respectively.

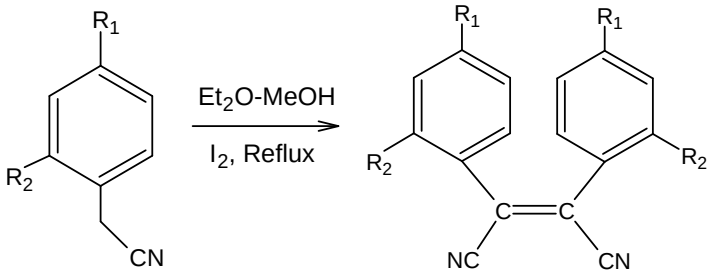


**O1** ($R_1$: H, $R_2$: $CH_3$) **O2** ($R_1$: H, $R_2$: $CH_3$)

**P1** ($R_1$: $CH_3$, $R_2$: H) **P2** ($R_1$: $CH_3$, $R_2$: H)

**Figure 5.2** Synthesis of 1,2-bis(*o*-tolyl)maleonitrile (**O2**) and 1,2-bis(*p*-tolyl)maleonitrile **P2**.

The conversion of **P2** and **O2** into **P3** and **O3** were achieved by the template effect of magnesium butanolate. The cyclotetramerization gave the dark green colored **P3** in yield 71% and the blue-green colored **O3** in yield 66% (Fig.5.3). In the conversion of **P3** and **O3** into **P4** and **O4** (Fig.5.4) by treatment with relatively strong acids (*e.g.* trifluoroacetic acid), a *seco*-porphyrazine type macrocycle in which one of the four pyrrole rings has been oxidized was the main product. Formation of oxidized species was almost inevitable even when the reaction was carried out under inert conditions.

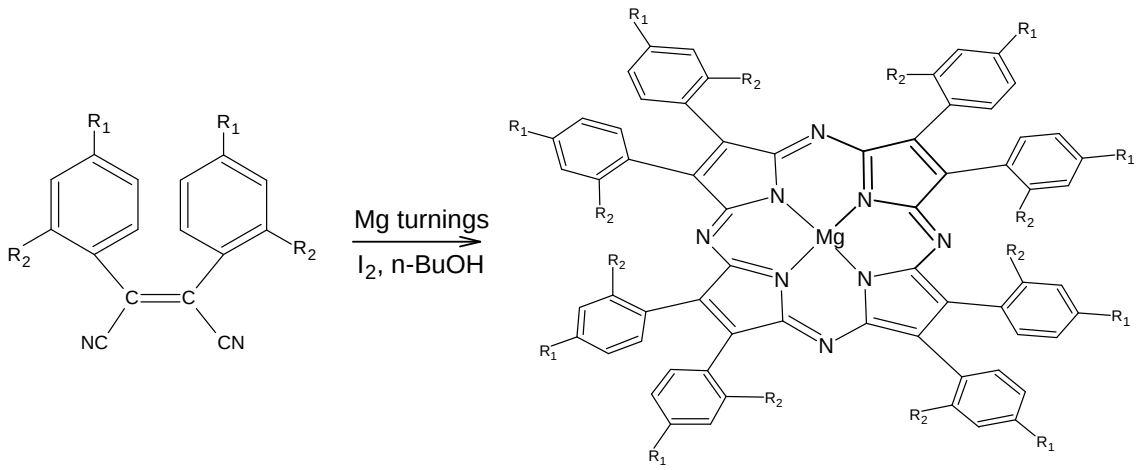


M= Mg (**O3**) ($R_1$: H, $R_2$: $CH_3$)
M= Mg (**P3**) ($R_1$: $CH_3$, $R_2$: H)

**Figure 5.3** Synthesis of [2,3,7,8,12,13,17,18-octakis(*o*-tolyl)porfirazinato] Mg(II) **O3** and [2,3,7,8,12,13,17,18-octakis(*p*-tolyl)porfirazinato] Mg(II) **P3**.

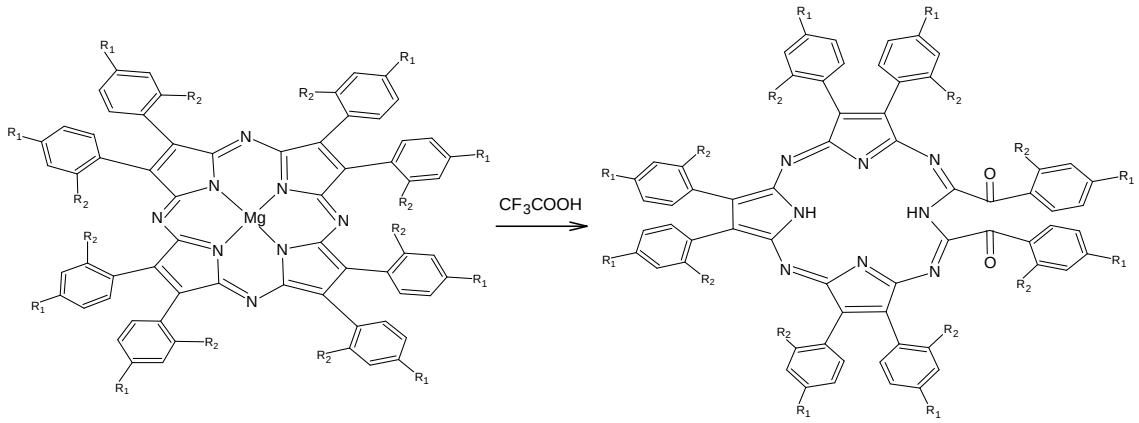


M= 2H (**O4**) ($R_1$: H, $R_2$: $CH_3$)
M= 2H (**P4**) ($R_1$: $CH_3$, $R_2$: H)

**Figure 5.4** Synthesis of [2,3,7,8,12,13,17,18-octakis(*o*-tolyl)-2-*seco*-porphyrazine-2,3-dione] (M= 2H) or [2,3,7,8,12,13,17,18-octakis(*p*-tolyl)-2-*seco*-porphyrazine-2,3-dione] (M= 2H).

*P*-tolyl and *o*-tolyl units are not comparable with dimethylamino groups, but are comparable with naphthyl groups as electron donors to the 18-π electron system of the inner core. In the present case, the tendency of *p*-tolyl and *o*-tolyl substituted porphyrazines to oxidize to the *seco*-porphyrazine derivatives should be higher than

dimethylamino substituted ones because the reactions were carried under inert atmospheres during these experiments, but still no product corresponding to the metal-free derivatives of **P3** and **O3** could be isolated. The mass spectral results have clearly indicated the change of the structure from magnesium porphyrazinates **P3** and **O3** to the demetalated *seco*-porphyrazines **P4** and **O4**. In addition to the mass spectral results, the intense C=O absorption peaks clearly differentiates oxidized products from the symmetrically octakis(*p*-tolyl) and octakis(*o*-tolyl) substituted magnesium porphyrazinates.

The metalation reactions of the demetalated *seco*-porpyrazines **P4** and **O4** with metal salts gave the metalated species **P5-P7** and **O5-O7**. (Fig.5.5).

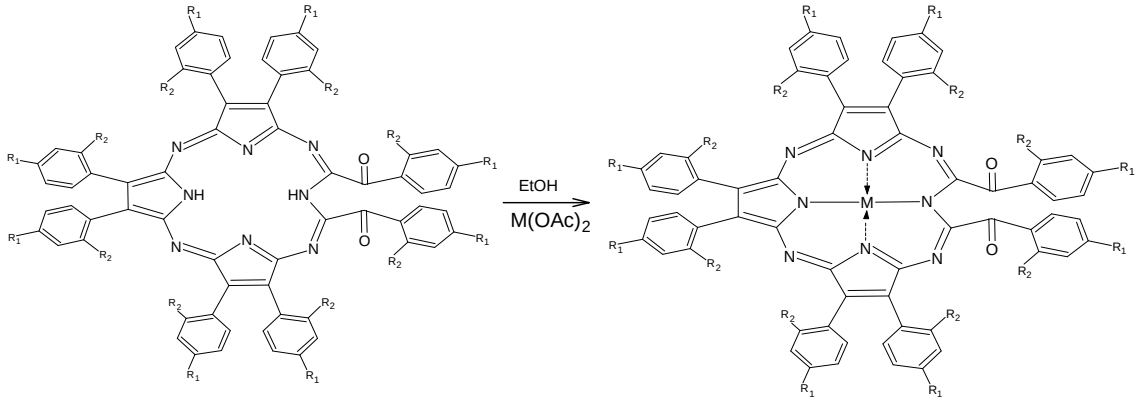


M= Cu (**O5**); Zn (**O6**); Co (**O7**) ($R_1$: H, $R_2$: $CH_3$)
M= Cu (**P5**); Zn (**P6**); Co (**P7**) ($R_1$: $CH_3$, $R_2$: H)

**Figure 5.5** Synthesis of [2,3,7,8,12,13,17,18-octakis(o-tolyl)-2-seco-2,3 dioxoporphyrazinato] {M=Cu(II), Zn(II) or Co(II)} and [2,3,7,8,12,13,17,18-octakis(p-tolyl)-2-seco-2,3- dioxoporphyrazinato] {M=Cu(II), Zn(II) or Co(II)}.

Elemental analyses correspond closely with the values calculated for (**P2, O2, P3-P7** and **O3-O7**. (Table 5.1).

**Table 5.1** Elemental analyses results of the porphyrazines*

| Compound | C | H | N |
|---|---|---|---|
| **P2** | 83.43 (83.69) | 5.62 (5.46) | 10.69 (10.84) |
| **O2** | 83.48 (83.69) | 5.54 (5.46) | 10.96 (10.84) |
| **P3** | 81.61 (81.77) | 5.25 (5.34) | 10.75 (10.60) |
| **P4** | 80.89 (81.03) | 5.61 (5.48) | 10.58 (10.50) |
| **P5** | 76.52 (76.61) | 5.09 (5.00) | 9.84 (9.93) |
| **P6** | 76.59 (76.48) | 4.88 (4.99) | 9.99 (9.91) |
| **P7** | 76.79 (76.92) | 5.13 (5.02) | 9.88 (9.97) |
| **O3** | 81.58 (81.77) | 5.43 (5.34) | 10.53 (10.60) |
| **O4** | 80.87 (81.03) | 5.40 (5.48) | 10.62 (10.50) |
| **O5** | 76.49 (76.61) | 4.91 (5.00) | 9.99 (9.93) |
| **O6** | 76.36 (76.48) | 5.12 (4.99) | 10.03 (9.91) |
| **O7** | 76.81 (76.92) | 5.15 (5.02) | 9.85 (9.97) |

* Required values are given in parentheses.

**IR spectra**

In the FT-IR spectrum of **P2**, the stretching vibration of C≡N is observed at 2219 $cm^{-1}$, the aromatic and aliphatic C-H peaks are around 2918-3047 $cm^{-1}$ and the characteristic substituted (p-tolyl) peak is at 802 $cm^{-1}$ and in the FT-IR spectrum of **O2**, the stretching vibration of C≡N is observed at 2246 $cm^{-1}$, the aromatic and aliphatic C-H peaks are around 2937-3058 $cm^{-1}$ and the characteristic substituted (*o*-tolyl) peak is at 750 $cm^{-1}$. These values comply with those reported in the literature for similar compounds. After the conversion of **P2** and **O2** to **P3** and **O3**, the sharp C≡N vibrations around 2219 and 2246 $cm^{-1}$ disappeared. The N-H stretching absorptions of the inner core of the metal-free porphyrazines **P4** and **O4** were observed around 3335 and 3320 $cm^{-1}$. Furthermore, during acid-mediated demetalation of the magnesium porphyrazines **P3** and **O3**, peripheral oxidation of one pyrrole ring was confirmed with an intense

absorption around 1718-1725 $cm^{-1}$. The FT-IR spectra of all porphyrazines derivatives **P3-P7** and **O3-O7** showed that the aromatic and aliphatic C-H peaks are around 2855-3052 $cm^{-1}$, the characteristic substituted *p*-tolyl peaks are around 820-852 $cm^{-1}$ and the characteristic substituted *o*-tolyl peaks are around 755-768, indicating the presence of *p*-tolyl and *o*-tolyl substituents as well as the *seco*-porphyrazine derivatives.

**NMR Spectra**

The N–H protons of the metal-free porphyrazines **P4** and **O4** were also identified in the $^1H$ NMR spectra with the broad peaks at δ= -1.05 and δ= -0.95 ppm, presenting the typical shielding of inner core protons, which is a common feature of the $^1H$ NMR spectra of metal-free porphyrazines. In the $^1H$ NMR spectra of diamagnetic porphyrazines **P3**, **P4**, **P6, O3, O4** and **O6**, two different types of protons are clearly seen: a multiplet around 7-8 ppm corresponding to phenyl protons and a singlet around 2.52-2.68 ppm for methylene protons. The ratio of the integral values 4:3 also confirms the proposed structures.

**Electronic Spectra**

Electronic spectra are especially useful to establish the structure of the porphyrazines **P3-P7** and **O3-O7**. UV-Vis spectra of porphyrazine core are dominated by two intense bands, the Q band around 640 nm and the B band in the near UV region around 348 nm, both correlated to $\pi \rightarrow \pi^*$ transitions. The presence of an electron-donating group on the periphery causes a bathochromic shift on Q bands. The UV-Vis spectra of porphyrazines (**P3, P5-P7, O3, O5-O7** in $CHCl_3$) prepared in the present work exhibited intense single Q band absorption of the $\pi \rightarrow \pi^*$ transitions around 640-648 nm and B bands in the near UV region around 348-380 nm (Table 5.2). As a consequence of the lowering of the symmetry of porphyrazine core, the electronic absorption spectra of the *seco*-porphyrazines **P4** and **O4** display a split in the Q band at 632 and 704 nm and at 636 and 712 nm, respectively. UV-Vis spectra of **P3** and **P4** at a concentration of $1x10^{-5}$ M in chloroform are shown in (Fig.5.6). An absorbance *vs.* concentration study indicated that due to the bulky *p*-tolyl and *o*-tolyl substituents, no aggregation occurred either for **P3, P4, O3** or **O4**.

**Table 5.2** UV–Vis data for the porphyrazines in chloroform.

| Compound | **λ/nm ( log ε / dm$^3$ mol$^{-1}$ cm$^{-1}$)** | | |
|---|---|---|---|
| **5a** | 380 (4.82) | 644 (4.91) | |
| **5b** | 376 (4.87) | 632 (4.71) | 704 (4.78) |
| **5c** | 372 (4.76) | 648 (4.81) | |
| **5d** | 366 (4.74) | 640 (4.83) | |
| **5e** | 364 (4.80) | 644 (4.86) | |
| **6a** | 352 (4.91) | 648 (4.70) | |
| **6b** | 352 (4.49) | 636 (4.15) | 712 (3.82) |
| **6c** | 356 (4.38) | 640 (4.32) | |
| **6d** | 348 (4.42) | 644 (4.38) | |
| **6e** | 354 (4.46) | 648 (4.36) | |

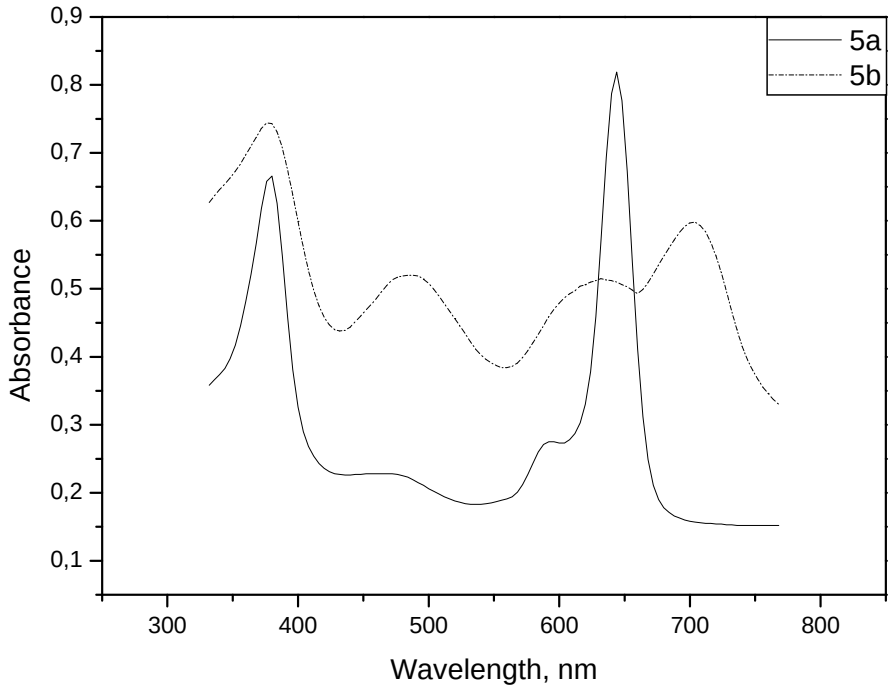


**Figure 5.6.** UV-Vis Spectra of **P3** and **P4** in Chloroform.

## 5.2 Synthesis of Biphenyl Porphrazine

The starting point for these novel porphyrazine structures with eight 4-biphenyl groups bound to the periphery is (4-chloromethyl-biphenyl) 4-phenylbenzyl chloride which were modified to 1,2-bis(4-biphenyl)maleonitrile by adding potassium cyanide. (Fig.5.7) The white colored products **B1** were obtained in yield 90%, respectively.

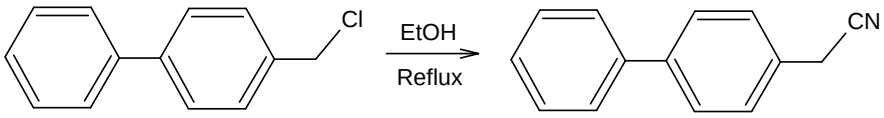


**Figure 5.7** Synthesis of (4-biphenyl)acetonitrile **B1**.

1,2-bis(4-biphenyl)maleonitrile **B2** which was obtained from (4-biphenyl)acetonitrile **B1** and $I_2$. The yellow colored product **B2** was obtained in yield 32% (Fig.5.8).

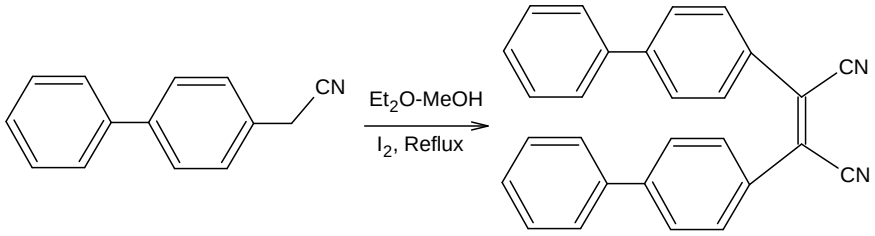


**Figure 5.8** Synthesis of 1,2-bis(4-biphenyl)maleonitrile **B2**.

The conversion of **B2** into **B3** was achieved by the template effect of magnesium butanolate. The cyclotetramerization gave the dark green colored **B3** (Fig.5.9) in yield 42%. It was soluble in chloroform, dichloromethane, acetone and toluene, but insoluble in apolar hydrocarbon solvents such as *n*-hexane.

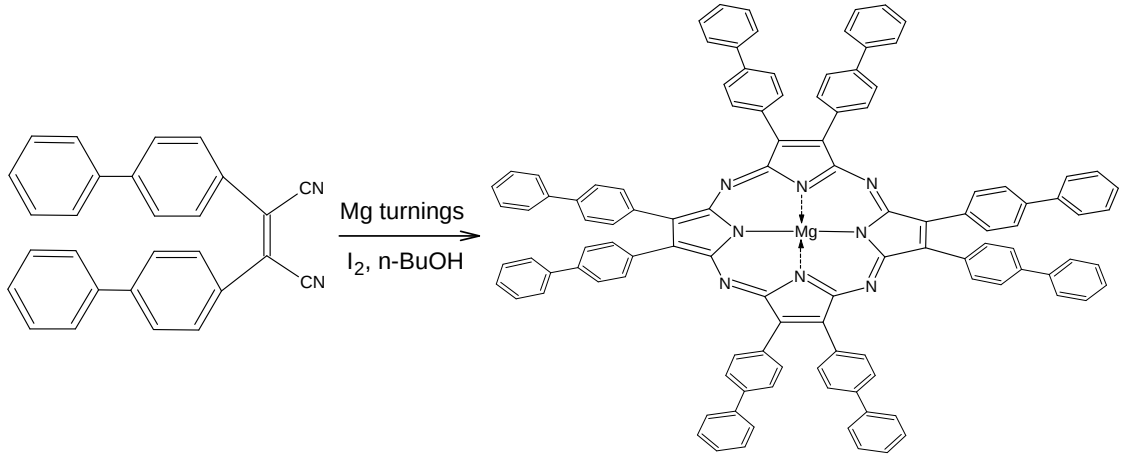


**Figure 5.9.** Synthesis of [2,3,7,8,12,13,17,18-octakis(4-biphenyl)porphyrazinato] Mg(II) (**B3**)

In the conversion of **B3** into **B4** (Fig.5.10) by treatment with relatively strong acids (*e.g.* trifluoroacetic acid), a *seco*-porphyrazine type macrocycle in which one of the four pyrrole rings has been oxidized has been the main product. Sterical tension due to the presence of eight bulky 4-biphenyl units around the core might be the main reason for the cleavage of one of the pyrrol rings. 4-biphenyl units are not comparable with dimethylamino groups, but are comparable with naphthyl groups as electron donors to the 18-π electron system of the inner core.

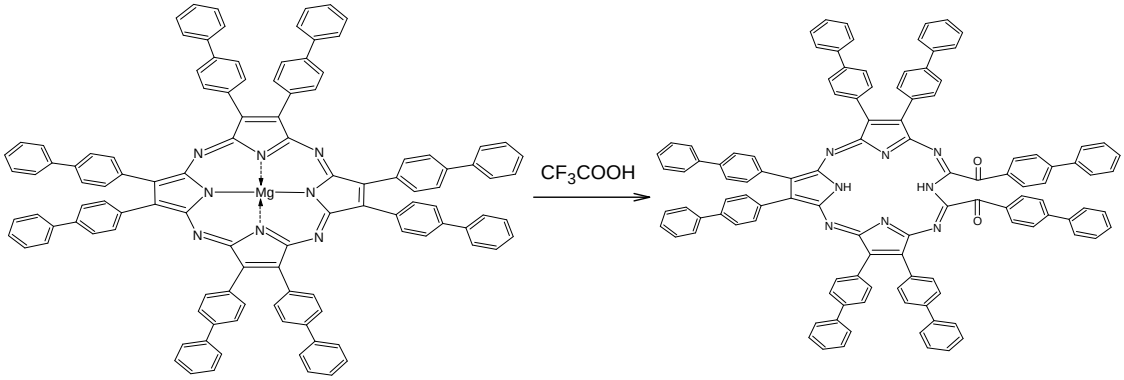


**Figure 5.10** Synthesis of [2,3,7,8,12,13,17,18-octakis(4-biphenyl)-2-*seco*-porphyrazine-2,3-dione] **B4**.

In the present case, the tendency of 4-biphenyl substituted porphyrazine to oxidize to the *seco*-porphyrazine derivative should be higher than dimethylamino substituted ones because the reactions were carried under inert atmospheres during these experiments, but still no product corresponding to the metal-free derivative of **B3** could

be isolated. The mass spectral results have clearly indicated the change of the structure from magnesium porphyrazinate **B3** to the demetalated *seco*-porphyrazine **B4** (Fig.5.11 and Fig.5.12). In addition to the mass spectral results, the intense C=O absorption peak clearly differentiates oxidized products from the symmetrically octakis(4-biphenyl) substituted magnesium porphyrazinate.

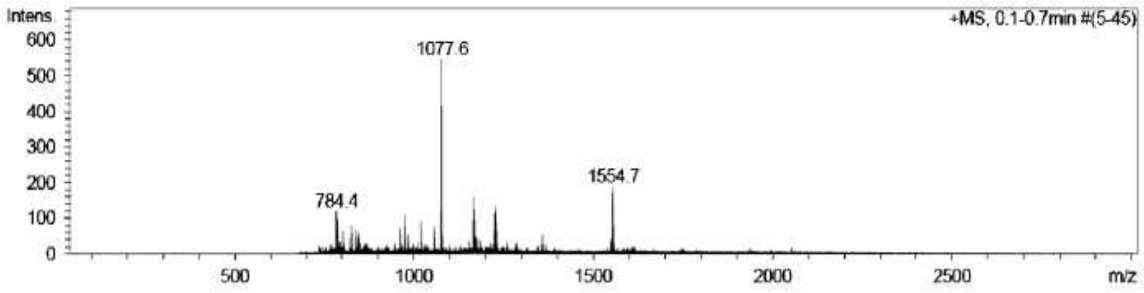


**Figure 5.11** Mass spectrum of **B3**.

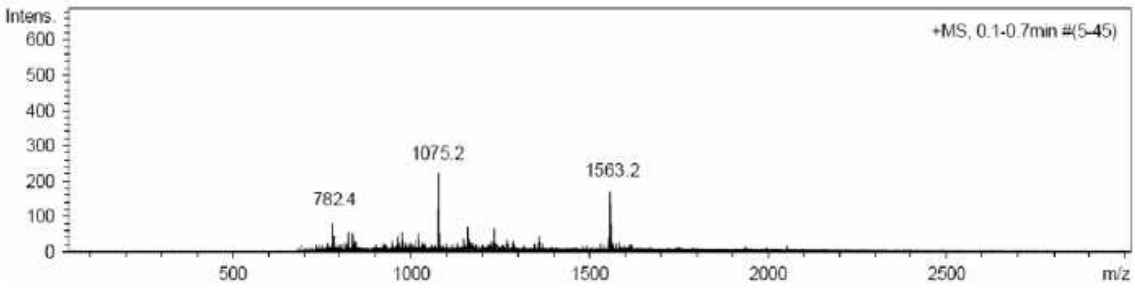


**Figure 5.12** Mass spectrum of **B4**.

The metalation reactions of the demetalated *seco*-porpyrazine **B4** with metal salts gave the metalated species **B5-B7**. (Fig.5.13).

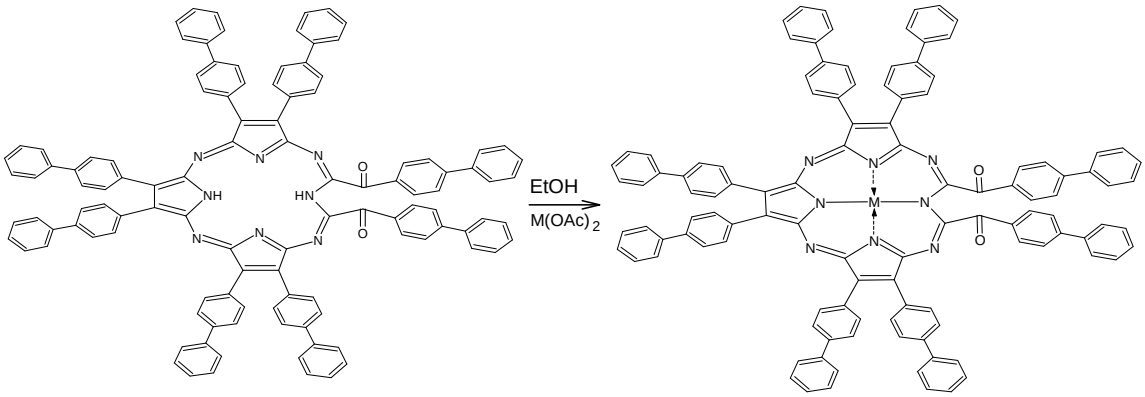


M= Cu (**B5**); Zn (**B6**); Co (**B7**)

**Figure 5.13** Synthesis of [2,3,7,8,12,13,17,18-octakis(4-biphenyl)-2-*seco*-2,3 dioxoporphyrazinato] {M= Cu(II), Zn(II) or Co(II)}.

All new compounds were identified through several spectroscopic techniques such as $^{1}$H NMR, FT-IR, UV-Vis, mass and elemental analysis. The spectroscopic data of desired products were in accordance with the assigned structures.

Elemental analyses correspond closely with the values calculated for **B2** and **B3-B7**. (Table 5.3).

**Table 5.3** Elemental analyses results of the porphyrazines*

| Compound | **C** | **H** | **N** |
|---|---|---|---|
| **B2** | 87.77 (87.93) | 4.66 (4.74) | 7.45 (7.32) |
| **B3** | 86.39 (86.56) | 4.54 (4.67) | 7.33 (7.21) |
| **B4** | 86.15 (86.02) | 4.41 (4.55) | 7.29 (7.17) |
| **B5** | 82.64 (82.76) | 4.59 (4.46) | 6.78 (6.89) |
| **B6** | 82.78 (82.67) | 4.39 (4.46) | 6.98 (6.89) |
| **B7** | 82.89 (83.00) | 4.59 (4.48) | 6.79 (6.91) |

* Required values are given in parentheses

**IR Spectra**

In the FT-IR spectrum of **B2**, the stretching vibration of C≡N peak is observed at 2218 $cm^{-1}$, the aromatic C-H peaks are around 3030-3070 $cm^{-1}$ and the aromatic C=C peak is at 1604 $cm^{-1}$. These values comply with those reported in the literature for similar compounds [20-23]. After the conversion of dinitrile derivative **B2** to porphyrazine **B3**, the sharp C≡N vibration around 2218 $cm^{-1}$ disappeared. The N-H stretching absorption of the inner core of the metal-free porphyrazine **B4** was observed around 3339 $cm^{-1}$. Furthermore, during acid-mediated demetalation of the magnesium porphyrazine **B3**, peripheral oxidation of one pyrrole ring was confirmed with an intense absorption around 1718-1723 $cm^{-1}$. The FT-IR spectra of all porphyrazines derivatives **B3-B7** showed that the aromatic C-H peaks are around 3020-3075 $cm^{-1}$, indicating the presence of 4-biphenyl substituents as well as the *seco*-porphyrazine derivatives.

**NMR Spectra**

The N–H protons of the metal-free porphyrazine **B4** were also identified in the $^{1}$H NMR spectra with the broad peak at $\delta$= -0.95 ppm, presenting the typical shielding of inner core protons, which is a common feature of the $^{1}$H NMR spectra of metal-free

porphyrazines. In the $^{1}$H NMR spectra of diamagnetic porphyrazines **B3**, **B4** and **B6**, only one chemical shift is clearly seen: a multiplet around 7-8 ppm corresponding to the phenyl protons.

**Electronic Spectra**

Electronic spectra are especially useful to identify the structure of the porphyrazines **B3-B7**. UV-Vis spectra of porphyrazine core are dominated by two intense bands, the Q band around 652 nm and the B band in the near UV region around 380 nm, both correlated to $\pi \rightarrow \pi^*$ transitions. The presence of an electron-donating group on the periphery causes a bathochromic shift on Q bands. The UV-Vis spectra of porphyrazines (**B3, B5-B7** in $CHCl_3$) prepared in the present study exhibited intense single Q band absorption of the $\pi \rightarrow \pi^*$ transitions around 652-658 nm and B bands in the near UV region around 348-380 nm (Table 5.4). As a consequence of the lowering of the symmetry of porphyrazine core, the electronic absorption spectrum of the *seco*-porphyrazine **B4** displays a split in the Q band at 650 and 712 nm. UV-Vis spectra of **B3** and **B4** in chloroform are shown in Figure 5.14.. An absorbance *vs.* concentration study indicated that due to the bulky 4-biphenyl substituents, no aggregation occurred either for **B3, B4**.

**Table 5.4** UV-Vis data for the porphyrazines in chloroform.

| Compound | **λ/nm ( log ε / dm$^3$ mol$^{-1}$ cm$^{-1}$)** | | |
|---|---|---|---|
| **B3** | 380 (4.86) | 652 (4.64) | |
| **B4** | 368 (4.77) | 650 (4.41) | 712 (4.49) |
| **B5** | 348 (4.82) | 658 (4.58) | |
| **B6** | 356 (4.80) | 654 (4.60) | |
| **B7** | 352 (4.84) | 656 (4.56) | |

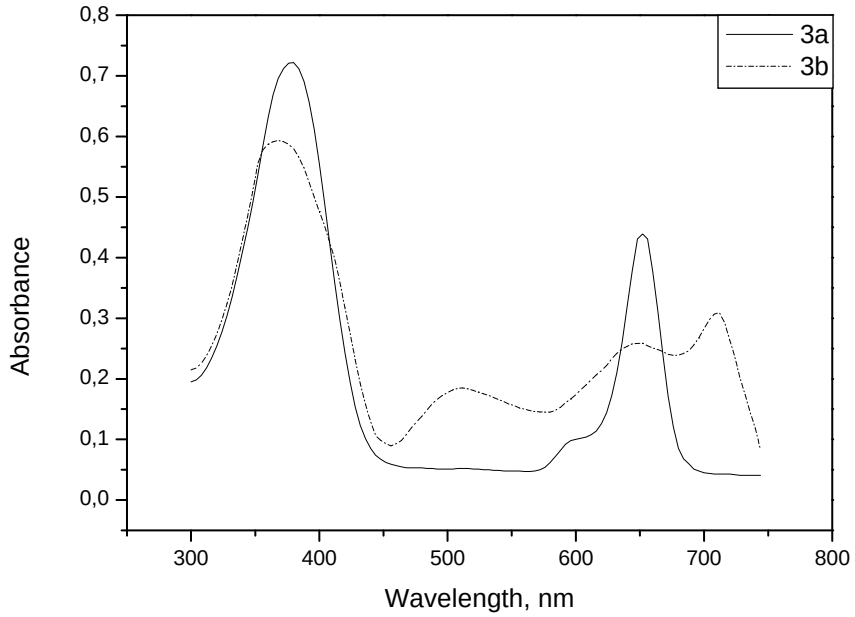


**Figure 5.14** UV-Vis spectra of **B3** and **B4** in chloroform.

# REFERENCES


1. Leznoff C.C., and Lever A. B. P., “Phthalocyanines Properties and Applications” VCH Weinheim, 1 (1989).
2. Leznoff C.C., and Lever A.B.P., “Phthalocyanines Properties and Applications”, VCH Weinheim, 2 (1993).
3. Leznoff C.C., and Lever A.B.P., “Phthalocyanines Properties and Applications”, VCH Weinheim, 3 (1993).
4. Leznoff C.C., and Lever A.B.P., “Phthalocyanines Properties and Applications”, VCH Weinheim, 4 (1996).
5. Mbatha B.G., Solubilisation of Porphyrins used in Photodynamic Therapy of Cancer M.S. Thesis, University of Transkei (1999).
6. Leznoff C.C., and Lever A.B.P., Eds. Phthalocyanines: Properties and Applications, VCH Publishers New York, 1-4 (1990-1996).
7. Weiss C., Kobayashi H., and Gouterman M.J., Mol. Spectrosc. 16 (1965) 415.
8. Stuzhin P.A., Bauer E.M., and Ercolani C., Inorg. Chem., 7 (1998) 1533.
9. Sibert J.W., Baumann T.F., Williams D.J., White A.J.P., Barrett A.G.M., and Hoffman B.M., J. Am .Chem. Soc, 118 (1996) 10487.
10. Cook M.J., and Jafari-Fini A., Tetrahedron, 56 (2000) 4085.
11. Linßen T.G., and Hanack M., Chem. Ber., 127 (1994) 2051.
12. Berezin B.D., Coordination Compounds of Porphyrines and Phthalocyanines, Translation by Vopian, V.G., John Wiley and Sons, New York (1981).
13. Berezin B.D., and Koifman O.I., Uspekhi Khimii, 42 (1973) 2007.
14. Structure and Bonding [Struktura i svyaz], Mir, Moskow (1969).
15. Kobayashi N., In: Smith K., Guilard R., and Kadish K.M., editors, Porphyrin handbook, New York: Academic Press, 2-3 (1999) 318.
16. Fitzgerald J., Taylor W., and Owen H., Synthesis, 9 (1991) 686.
17. Mbatha B.G., PhD. Thesis in University of Johannesburg (2006).
18. Forsyth T.P., Williams D.B.G., Montalban A.G., Stern C.L., Barret A.G.M., and Hoffman B.M., J.Org.Chem., 63 (1998) 331.

19. Baumann T.F., Nasir M.S., Sibert J.W., White A.J.P., Olmstead M.M., Williams D.J., Barret A.G.M., and Hoffman B.M., J. Am. Chem. Soc., 118 (1996) 10479.
20. Lange S.J., Nie H., Stern C.L., Barret A.G.M., and Hoffman B.M., Inorg. Chem., 37 (1998) 6435.
21. Beall L.S., Mani N.S., White A.J.P., Williams D.J., Barrett A.G.M., and Hoffman B.M., J. Org. Chem., 63 (1998) 5806.
22.a) Kadish K.M., Smith K.M., and Guilard R., Phthalocyanines, 15, 2003, 97.
b) Bottomley L.A., J. Electroanal. Chem., (1986) 331.
23. Goldberg D.P., Montalban A.G., White A.J.P., Williams D.J., Barrett A.G.M., and Hoffman B.M., Inorg. Chem., 37 (1998) 2873.
24. Faust R., and Weber C., J. Org. Chem., 64 (1999) 2571.
25. Kobayashi N., Ashida T., Osa T., and Konami H., Inorg.Chem., 33 (1994) 1735.
26. Milgrom L., and Robert S.M., Chemistry in Britain (1998)
27. Choi C., Tsang P., Huang J., Chan E.Y.M., Ko W., Fong W., and Ng D.K.P., Chem. Commun., Issue 19 (2004) 2236.
28. Antipas A., Dolphin D., Gouterman M., and Johnson E.C., J. Am. Chem. Soc., 100 (1978) 7705.
29. Nevin W.A., Liu W., Greenberg S., Hempstead M.R., Marcuccio S.M., Melník M., Leznoff C.C., and Lever A.B.P., Inorg. Chem., 26 (1987) 891.
30. Leznoff C.C., Marcuccio S.M., Greenberg S., and Lever A.B.P., Can. J. Chem., 63 (1985) 623.
31. Chen Y., Huang L., Ranade M.A., and Zhang X.P., J. Org. Chem., 68 (2003) 3714.
32. Ogunsipe A., Chen J., and Nyokong T., New J. Chem., 28 (2004) 1.
33. Uchida H., Reddy P., Nakamura S., and Toru T., J.Org. Chem., 68 (2003) 8736.
34. Mani N.S., Beall L.S., Miller T., Anderson O.P., Hope H., Parkin S.R., Williams D.J., Barrett A.G.M., and Hoffman B.M., J. Chem. Soc. Chem. Commun., (1994) 2095.
35. Khelevina O.G., and Rumyantseva S.V., Advances in Porphyrin Chemistry, Golubchikov O.A., Ed., St. Petersburg: NII Khimii SPbGU, 4 (2004) 128.
36. Stuzhin P.A., Khelevina O.G., and Berezin B.D., Phthalocyanines: Properties and Applications, Leznoff C.C., and Lever A.B.P.N., Eds., New York: VCH, 4 (1996) 19.
37. Stuzhin P.A., and Khelevina O.G., Koord. Khim., 24 (1998) 782.
38. Stuzhin P.A., J. Porphyrins Phthalocyanines, 3 (1999) 500.

39. Khelevine O.G., Romanenko Y.V., and Islyaikin M.K., Russian Journal of Coordination Chemistry, 33 (2007) 155.

40. Petrov O. A., Russian Journal of Coordination Chemistry, 27 (2001) 449.

41. (a) Bonnett R., New Scientist, (1989) 55; (b) Saleeby C.W., Sunlight and health 3rd ed. Nisbet and co (1923) (c) Leredde P., Photothèrapie et photobiologie Paris Naud. (1903) (d) Montgomery F.H., J. Cutan. Dis., 21 (1903) 529.

42. Pandy R.K., Shiau F.Y., Sumlin A.B., Dougherty T.J., and Smith K.M., Bioorg. Med. Chem. Lett., 4 (1994) 1263.

43. Pandy R.K., Jagerovic N., Ryan J.M., Dougherty T.J., and Smith K.M., Tetrahedron, 52 (1996) 5349.

44. Bonnett R., Chemical Soc. Rev., 24 (1995) 19.

45. Bonnet R., Djelal B., m-TPHC Photodyn., 6 (1993) 2.

46. Roberts W.G., Klein M.K., Loomis M., Weldy S., and Berns M.W., J. Natl. Cancer Inst., 83 (1991) 18.

47.Sakellariou E.G., Montalban A.G., Beall S.L., Henderson D., Meunier H.G., Phillips D., Suhling K., Barrett A.G.M., and Hoffman B.M., Tetrahedron, 59 (2003) 9083.

48.Sakellariou E.G., Montalban A.G., Meunier H.G., Ostler R.B., Rumbles G., Barrett A.M., and Hoffman B.M., J. Photochem. Photobiol. A: Chem., 136 (2000) 185.

49. Montalban A.G., Meunier H.G., Ostler R.B., Barrett A.G.M., Hoffman B.M., and Rumbles G., J. Phys. Chem. A., 103 (1999) 4352.

50. Sakellariou E.G., Montalban A.G., Meunier H.G., Rumbles G., Phillips D., Ostler R.B., Suhling K., Barrett A.G.M., and Hoffman B.M., Inorg. Chem., 41 (2000) 2182.

51. Bonnett R., Chemical Soc. Rev., 24 (1995) 19.

52. Montalban A.G., Lange S.J., Beall L. S., Mani N. S., Williams D. J., White A. J. P., Barrett A. G. M., and Hoffman B. M., J. Org. Chem., 62 (1997) 9284.

53. Nazlı A., Gonca E., and Gül A., J. Porphyrins Phthalocyanines, 10 (2006) 996.

54. Montalban A.G., Baum S.M., Barrett A.G.M., and Hoffman B.M., Dalton Trans., (2003) 2093.

55. Nie H., Stern C.L., Barrett A.G.M., and Hoffman B.M., Chem. Commun., (1999) 703.

56. Pullen A.E., Faulmann C., and Cassoux P., Eur. J.Inorg. Chem., (1999) 269.

57. van Nostrum C.F., and Nolte R.J.M., Chem. Commun., (1996) 2385.

58.Yenilmez H.Y., Özçeşmeci I., Okur A.I., and Gül A., Polyhedron, 23 (2001) 787.

59. Gonca E., Köseoğlu Y., Aktaş B., and Gül A., Polyhedron, 23 (2004) 1845.
60. Sessler J.L., Shevchuk S.V., Callaway W., and Lynch V., Chem. Commun., (2001) 968.
61. Sakellariou E.G., Montalban A.G., Beall S.L., Henderson D., Meunier H.G., Phillips D., Suhling K., Barrett A.G.M., and Hoffman B.M., Tetrahedron, 59 (2003) 9083.
62. Uslu R.Z., and Gül A., C. R. Acad. Sci. Paris, Serie IIc, Chimie : Chemistry, 3 (2000) 643.
63. Polat M., and Gül A., Dyes and Pigments, 45 (2000) 195.
64. Gonca E., and Gül A., Inorganic Chemistry Communications, 8 (2005) 343.
65. Gonca E., Journal of Chemical Research, 2008 (2008) 465.
66. Sesalan Ş.B., and Gül A., Monatshefte für Chemie, 131 (2000) 1191.
67. Sağlam Ö., and Gül A., Polyhedron, 20 (2001) 269.
68. Keskin B., Köseoğlu Y., Avcıata U., and Gül A., Polyhedron, 27 (2008) 1155.
69. Öztürk R., and Gül A., Tetrahedron Letters, 45 (2004) 947.
70. Gonca E., Transition Metal Chemistry, 33 (2008) 547.
71. Akkuş H., and Gül A., Transition Metal Chemistry, 26 (2001) 689.
72. Kemikli N., and Öztürk R., Inorganic Chemistry Communications, 11 (2008) 338.
73. Gonca E., Baklacı Ü.G., and Dinçer H.A., Polyhedron, 27 (2008) 2431.
74. Gonca E., Baklacı Ü.G., and Dinçer H.A., Journal of Porphyrins and Phthalocyanines, 12 (2008) 116.
75. Eastham J.F., Nations R.G., and Collins C.J., J. Org. Chem., 23 (1958) 1764.
76. Hohenlohe-Oehringer K., Monatsh., 89 (1958) 469.
77. Birkeland S.P., Daub G.H., Hayes F.N., and Ott D.G., J. Org. Chem., 26 (1961) 2662.

**APPENDIX A**

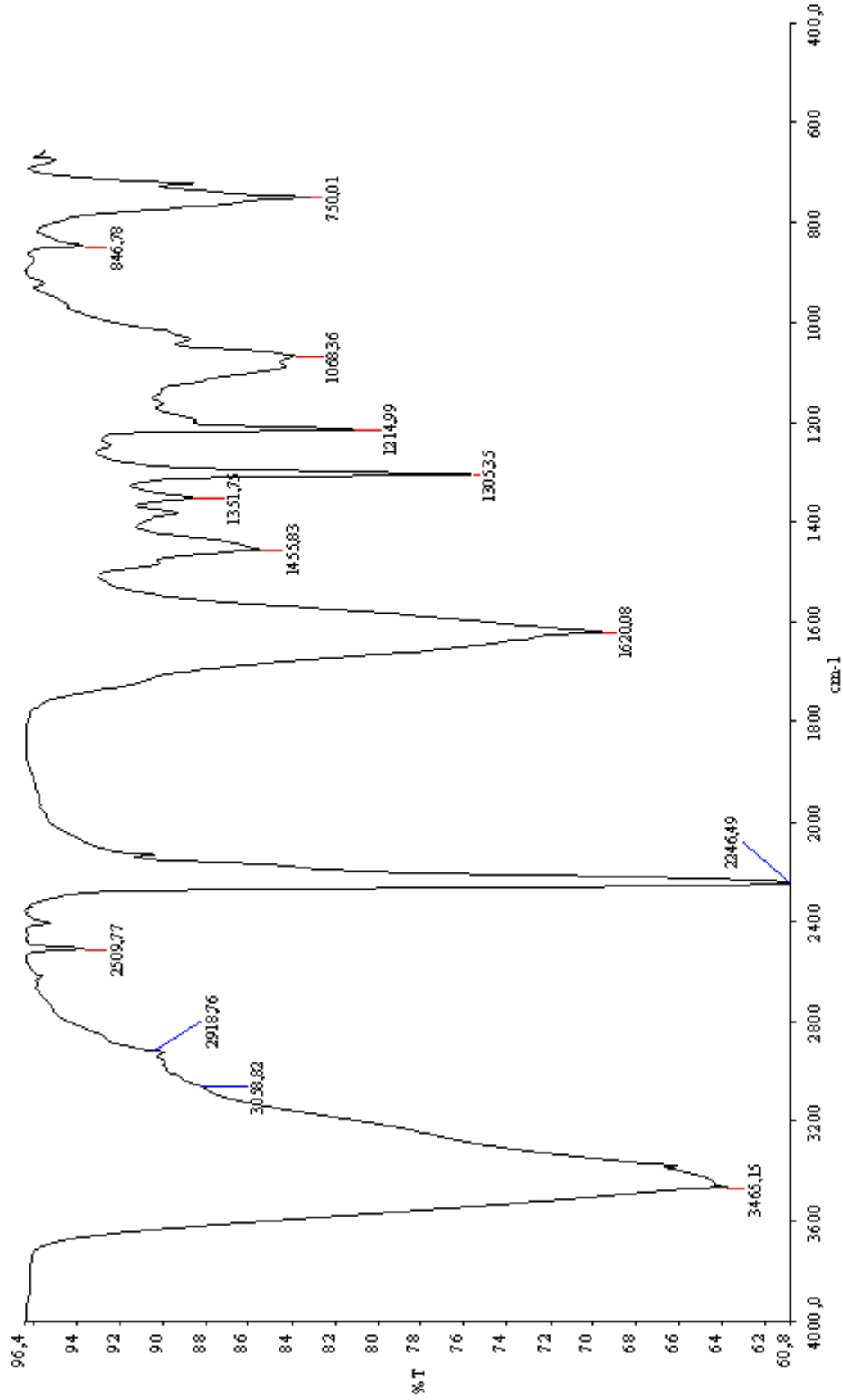


FT-IR Spectrum of **O2**

**APPENDIX B**

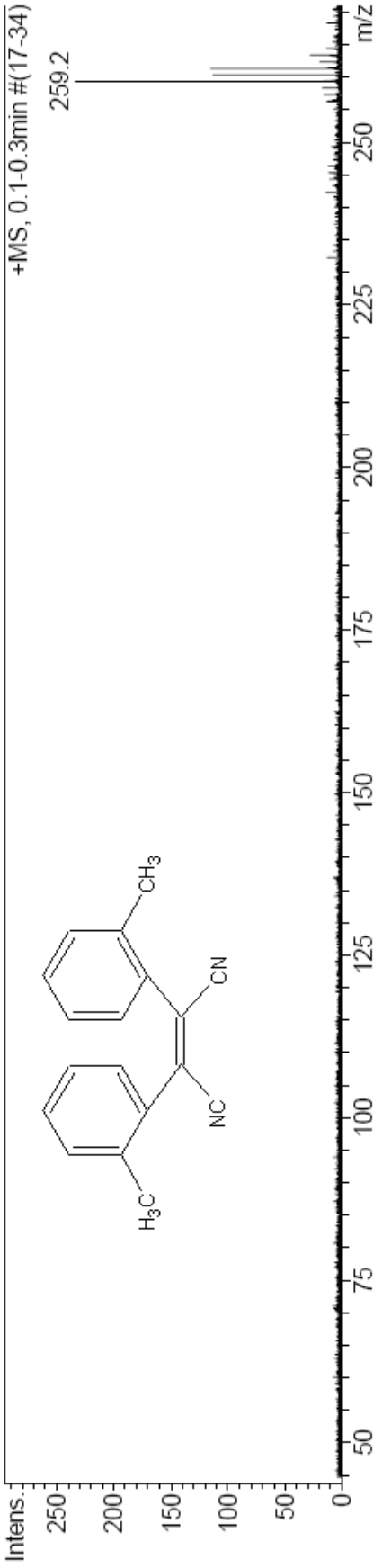


Mass Spectrum of **O2**

**APPENDIX C**

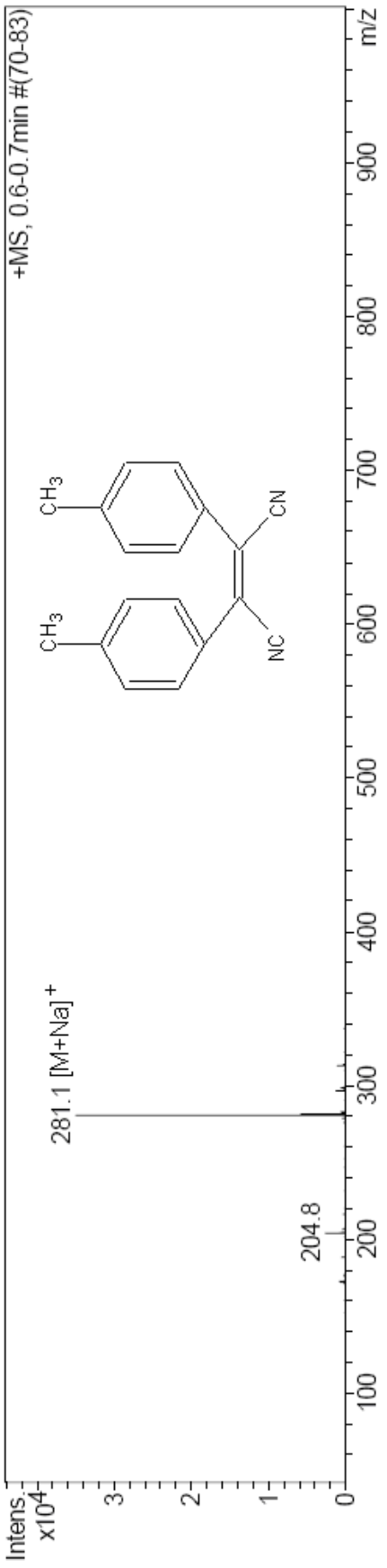


Mass Spectrum of **P2**

**APPENDIX D**

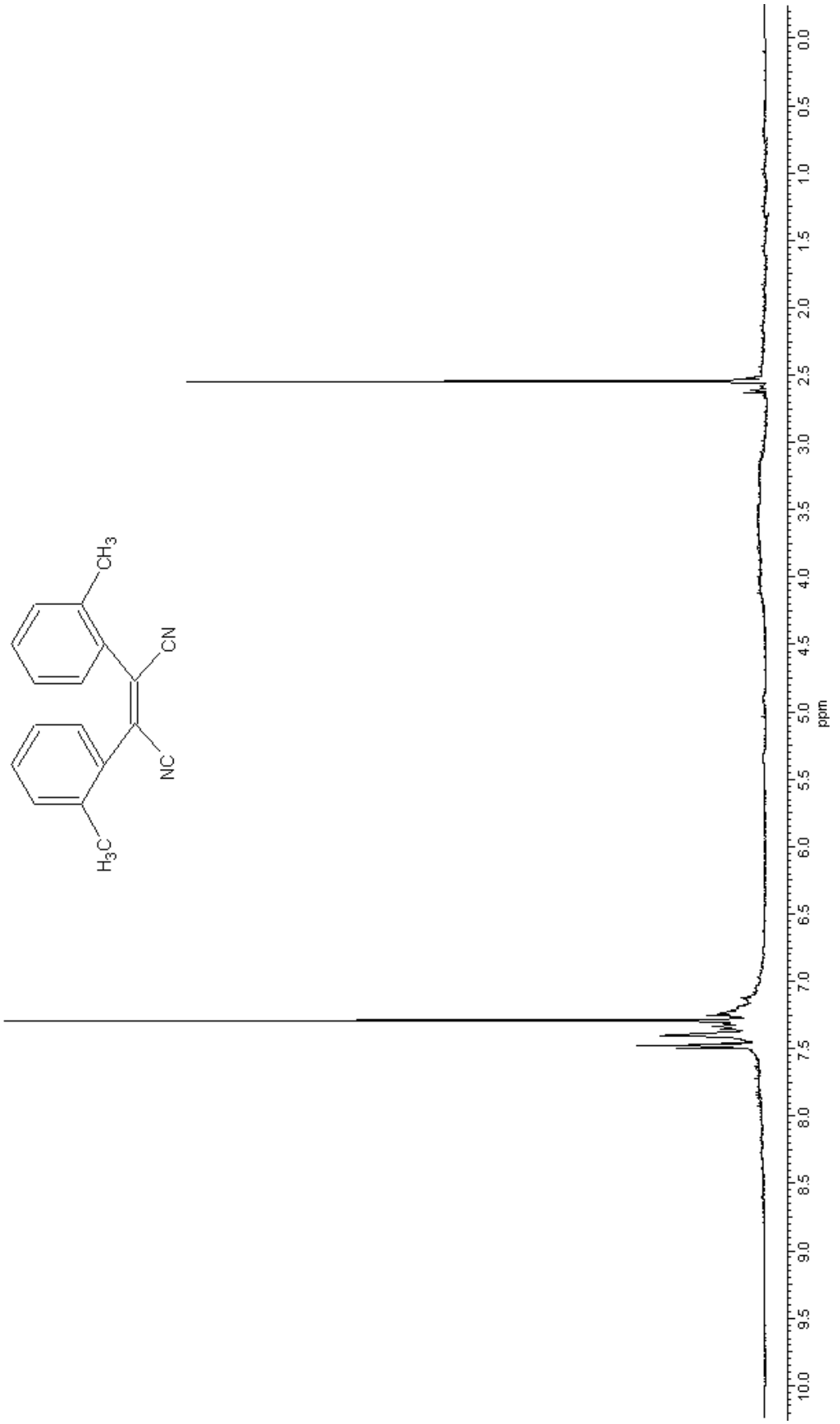


$^{1}$H NMR Spectrum of **O2**

**APPENDIX E**

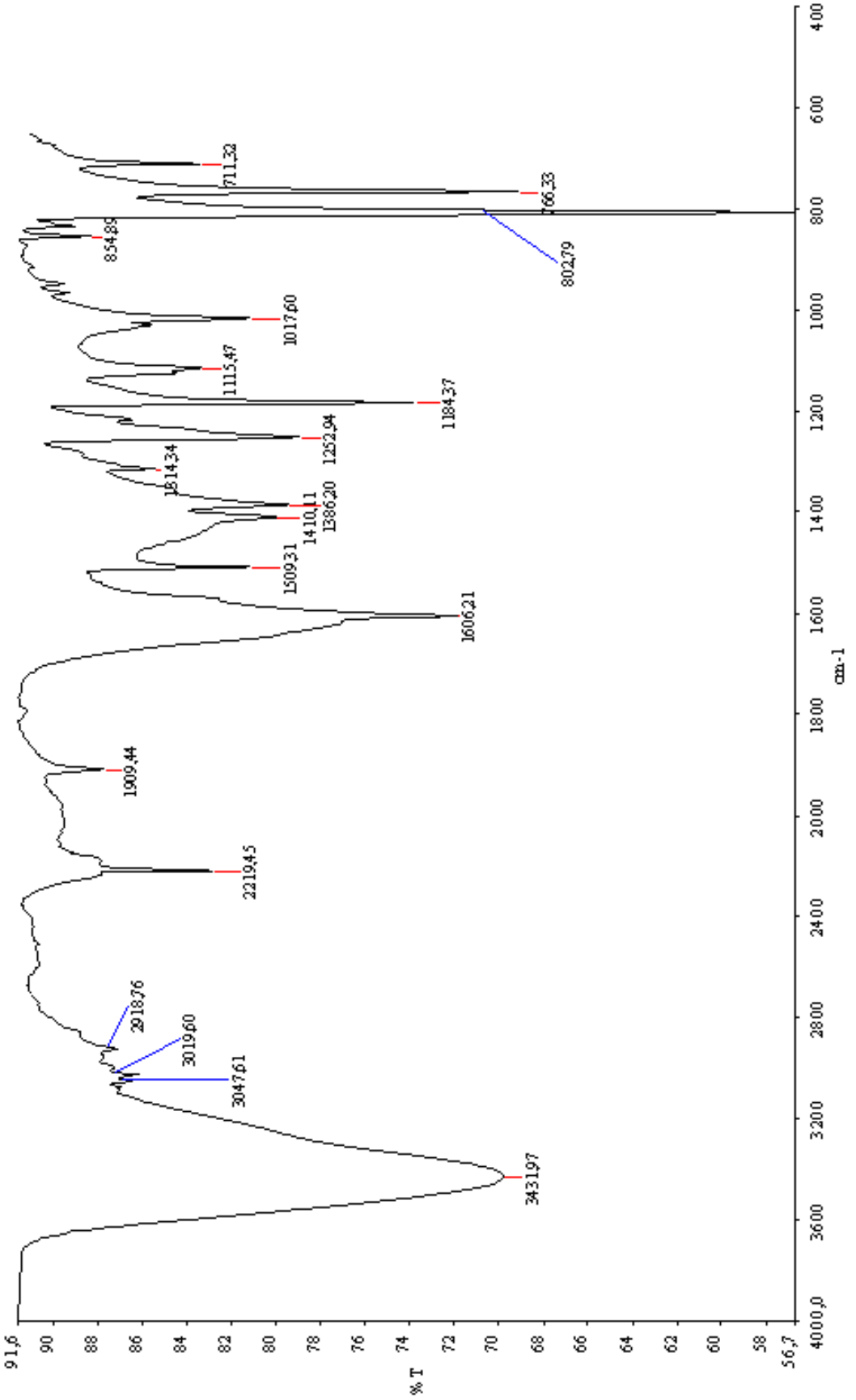


FT-IR Spectrum of **P2**

**APPENDIX F**

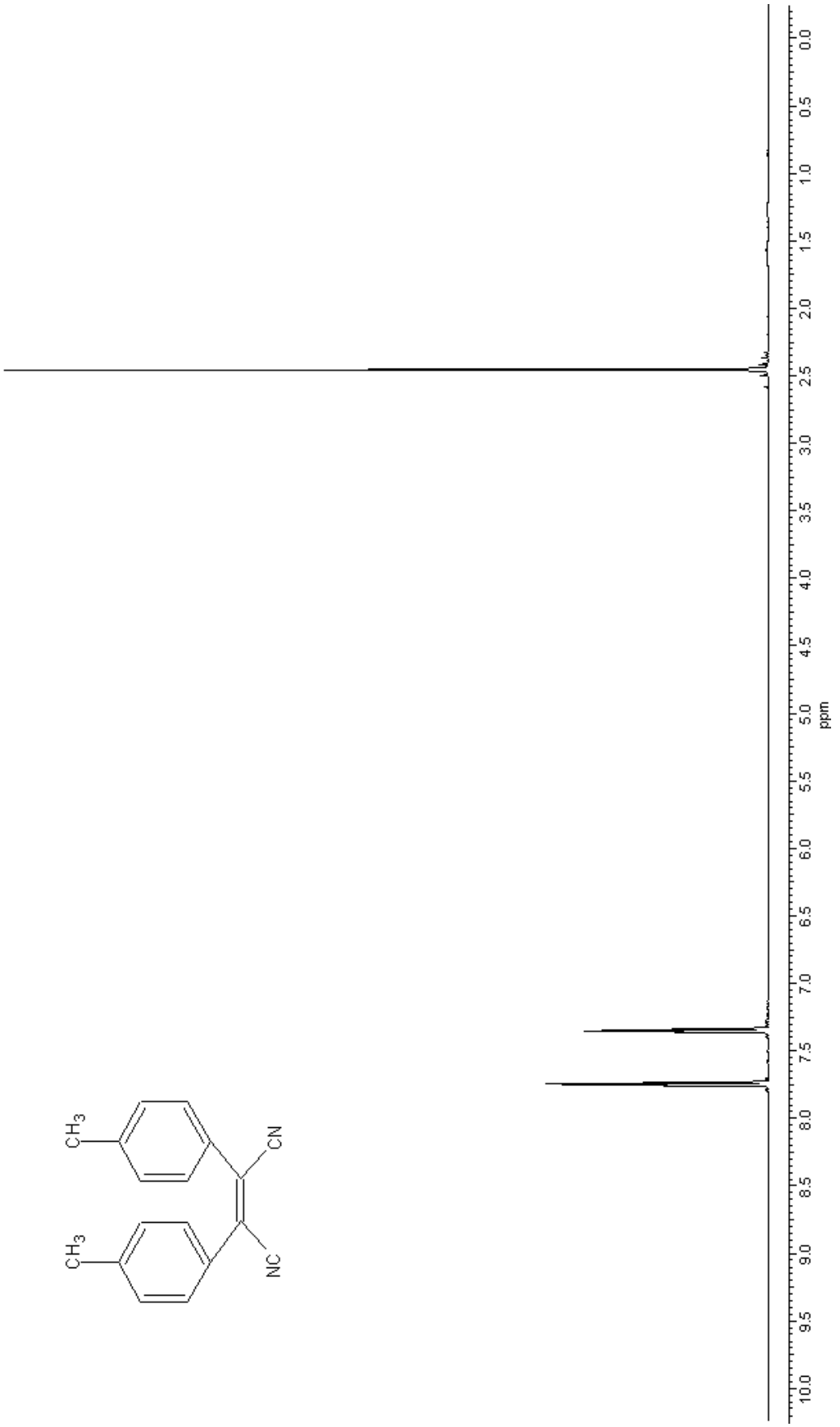


$^{1}$H NMR Spectrum of **P2**

# APPENDIX G

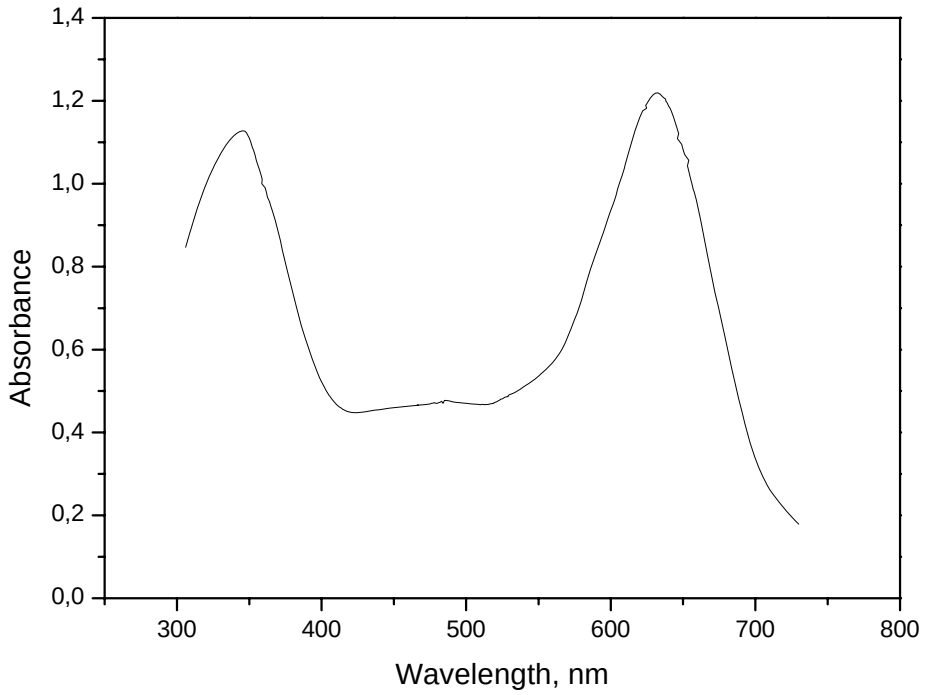


UV-Vis Spectrum of **O3** in Chloroform

**APPENDIX H**

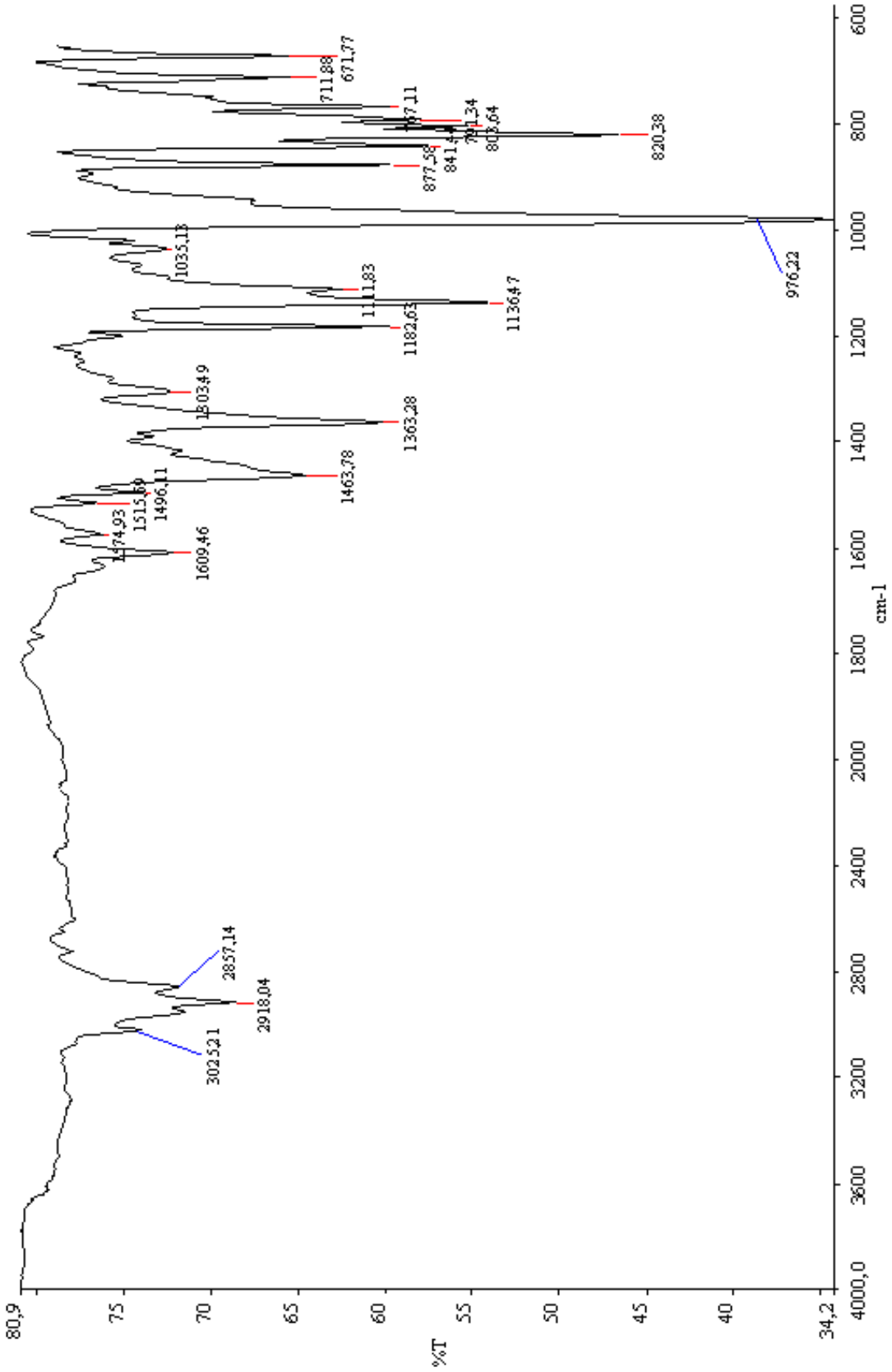


FT-IR Spectrum of **P3**

# APPENDIX I

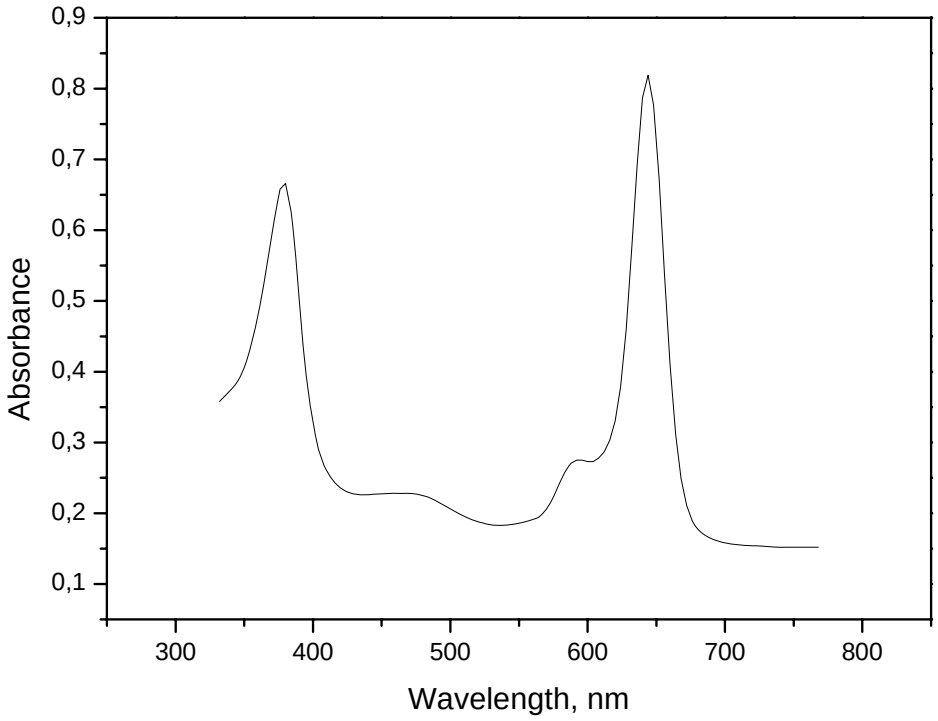


UV-Vis Spectrum of **P3** in Chloroform

**APPENDIX J**

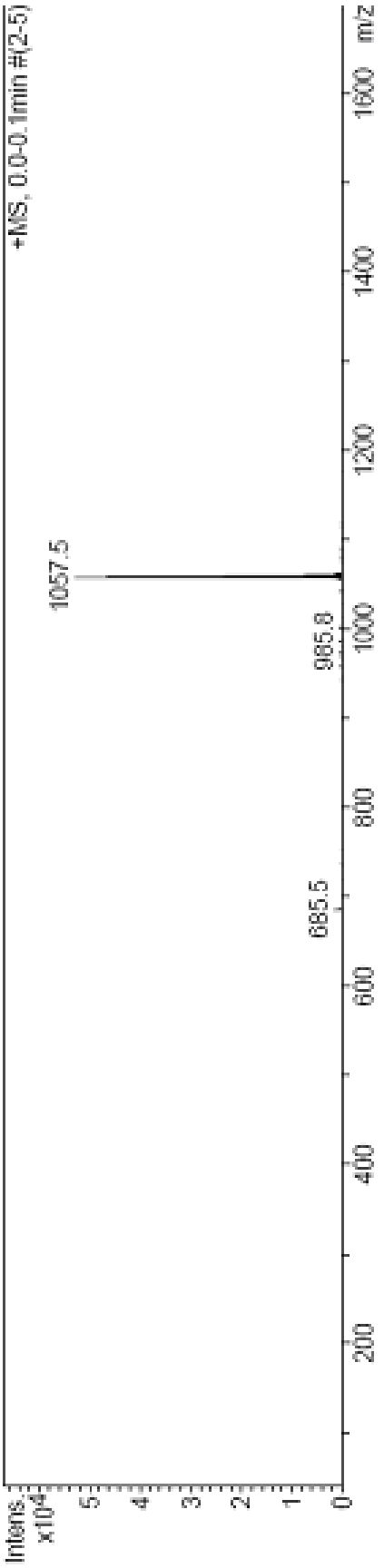


Mass Spectrum of **P3**

**APPENDIX K**

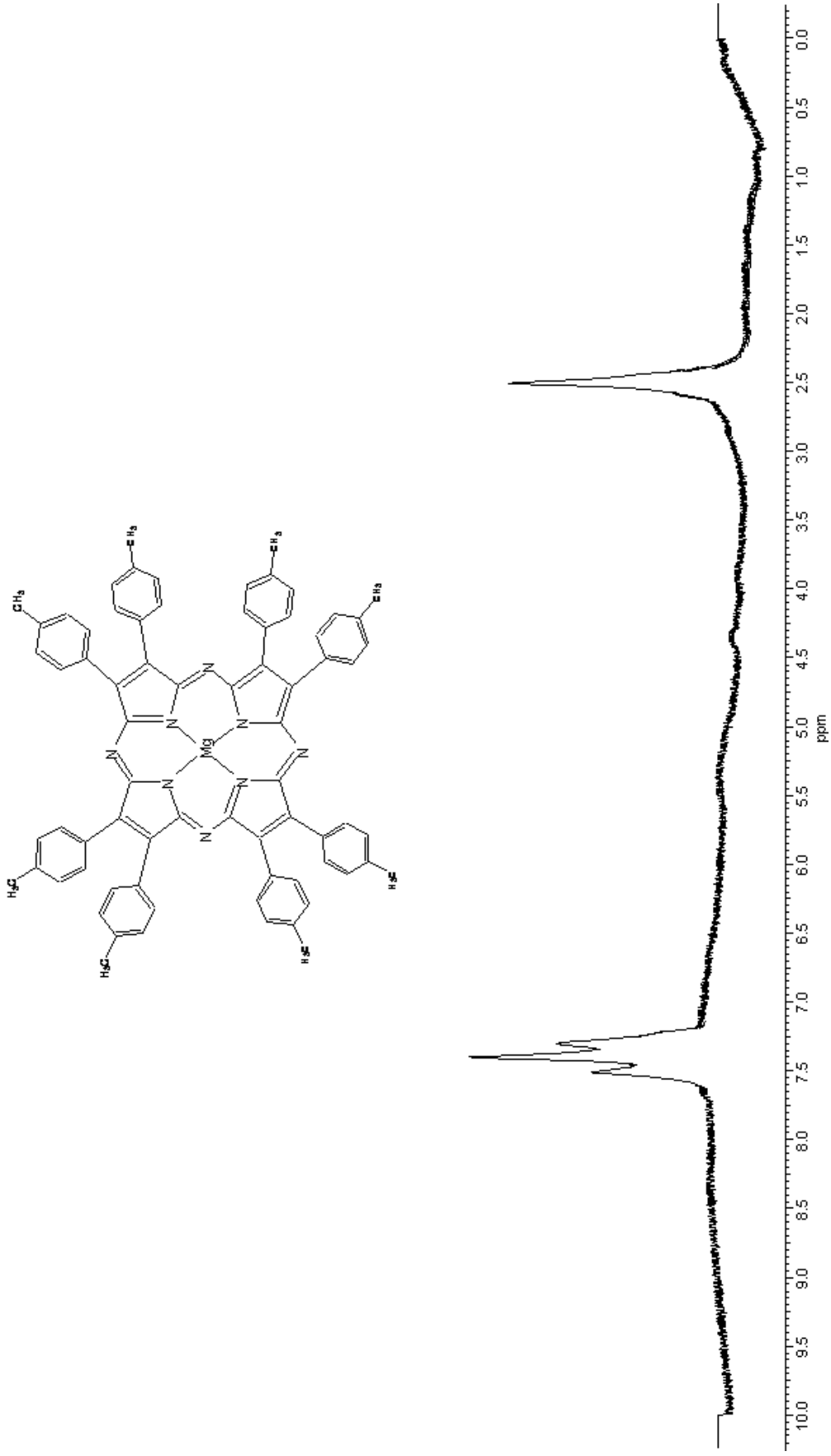


$^{1}$H NMR Spectrum of **P3**

# APPENDIX L

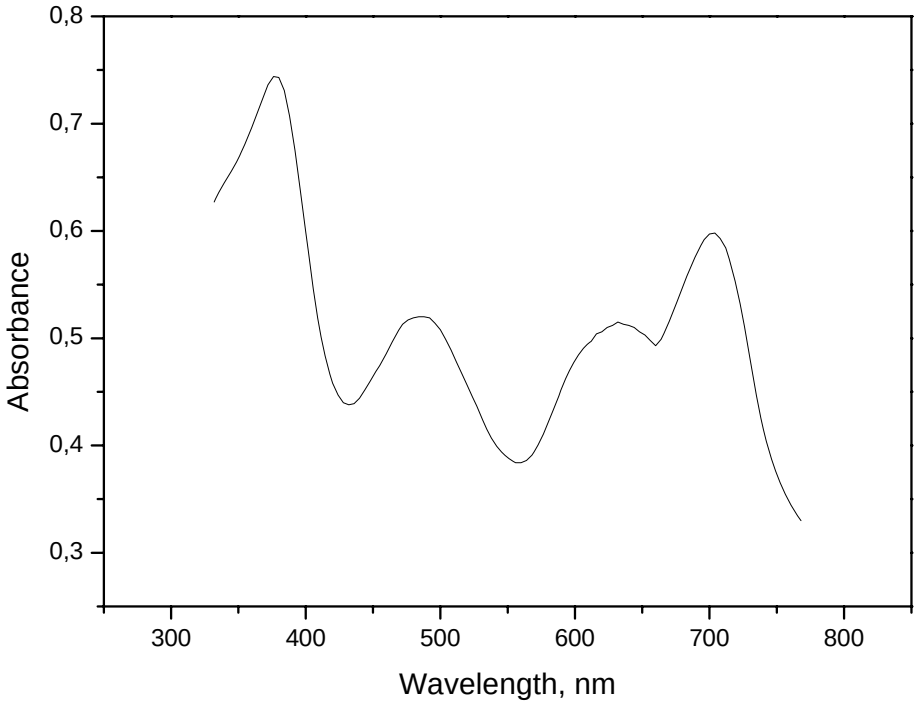


UV-Vis Spectrum of **P4** in Chloroform

**APPENDIX M**

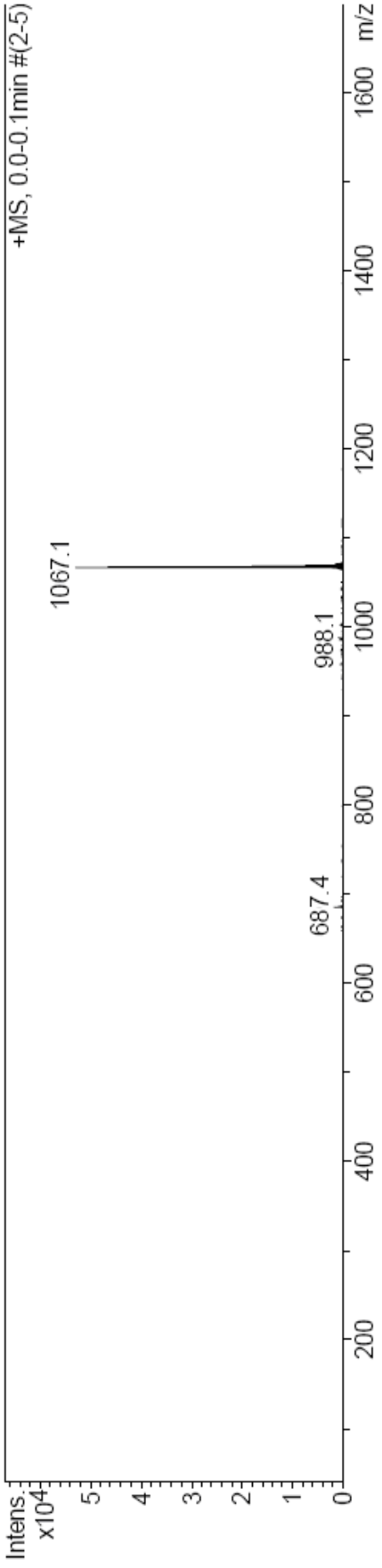


Mass Spectrum of **P4**

**APPENDIX N**

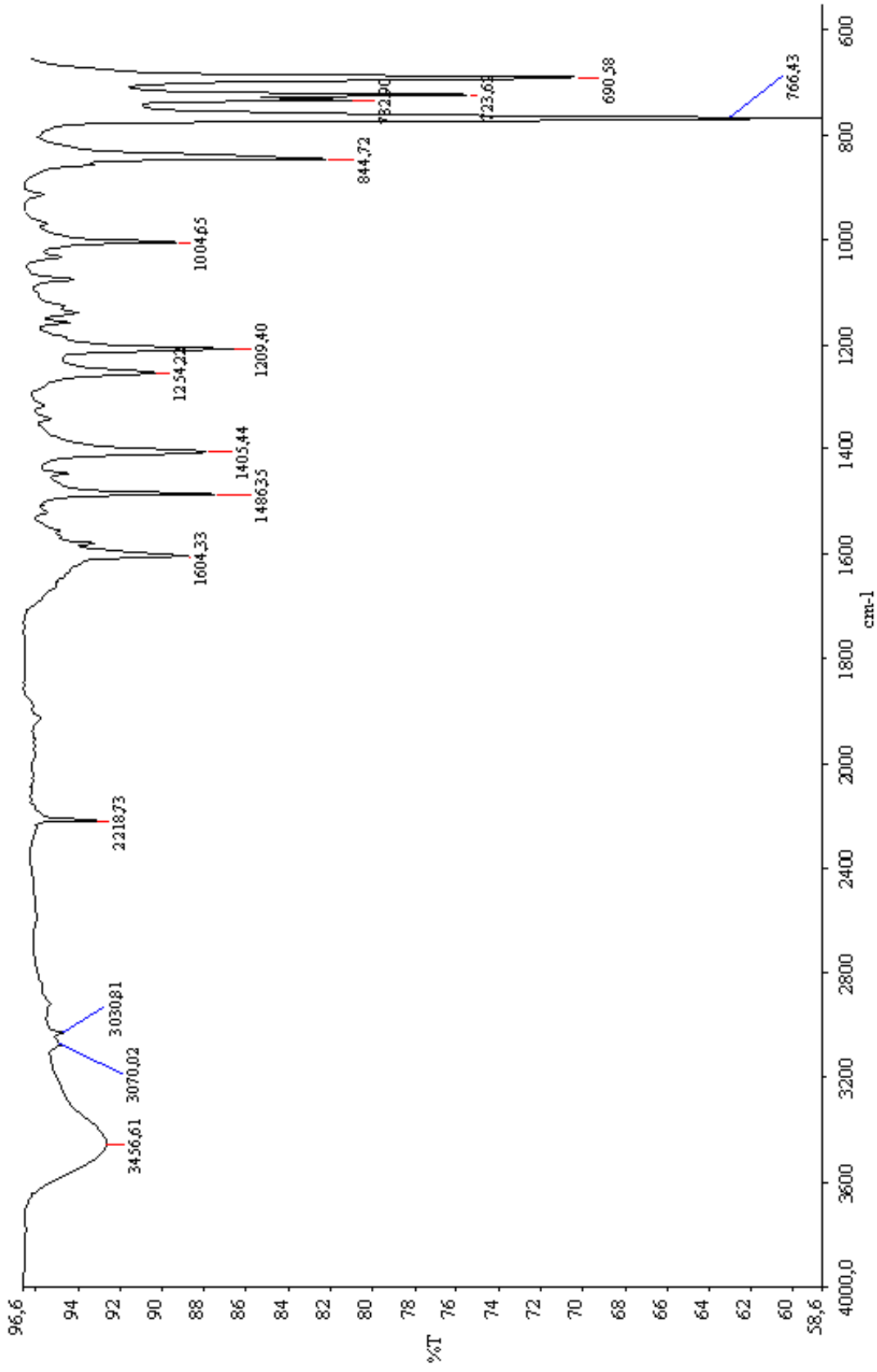


FT-IR Spectrum of **B2**

**APPENDIX O**

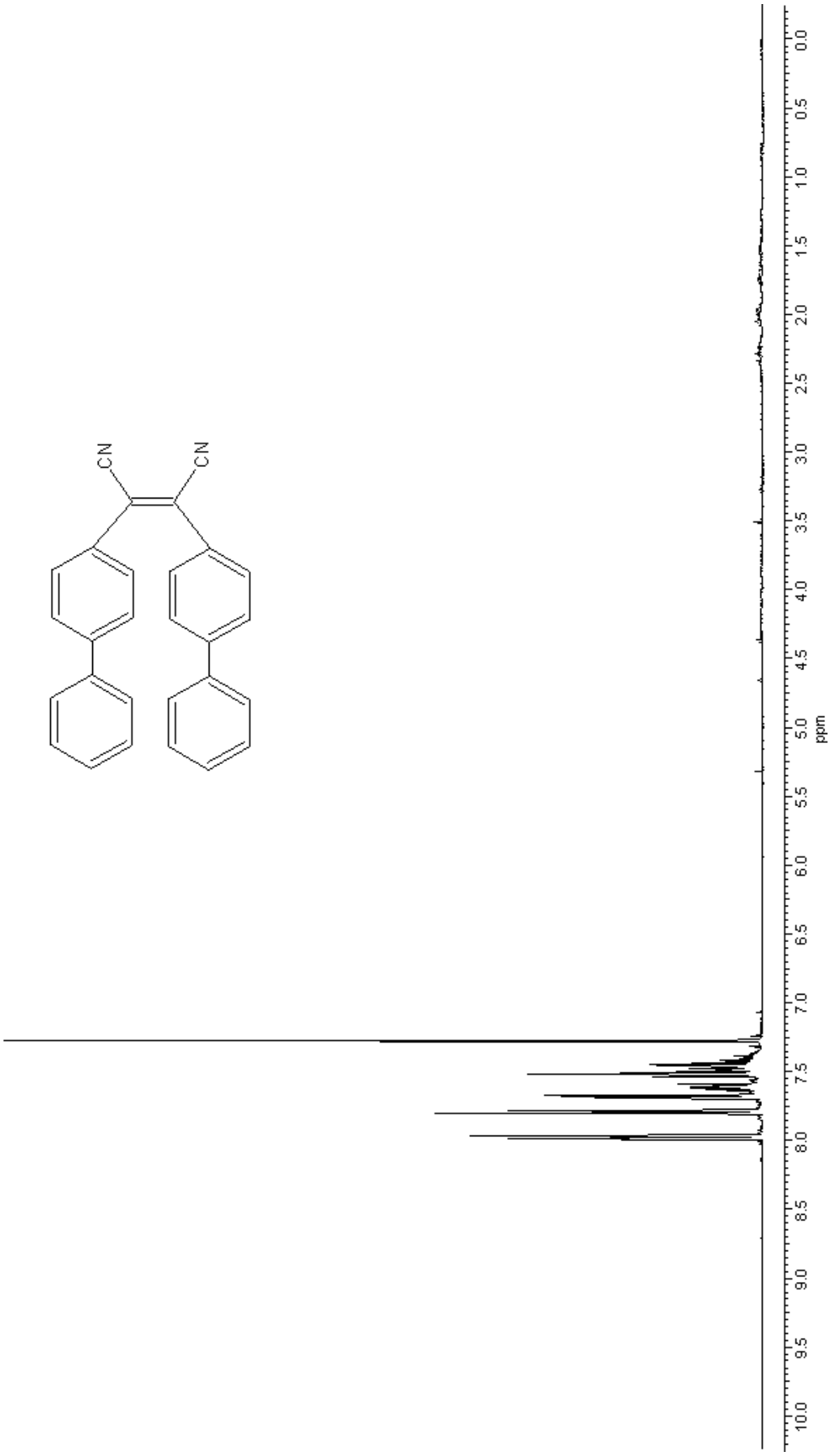


$^{1}$H NMR Spectrum of **B2**

**APPENDIX P**

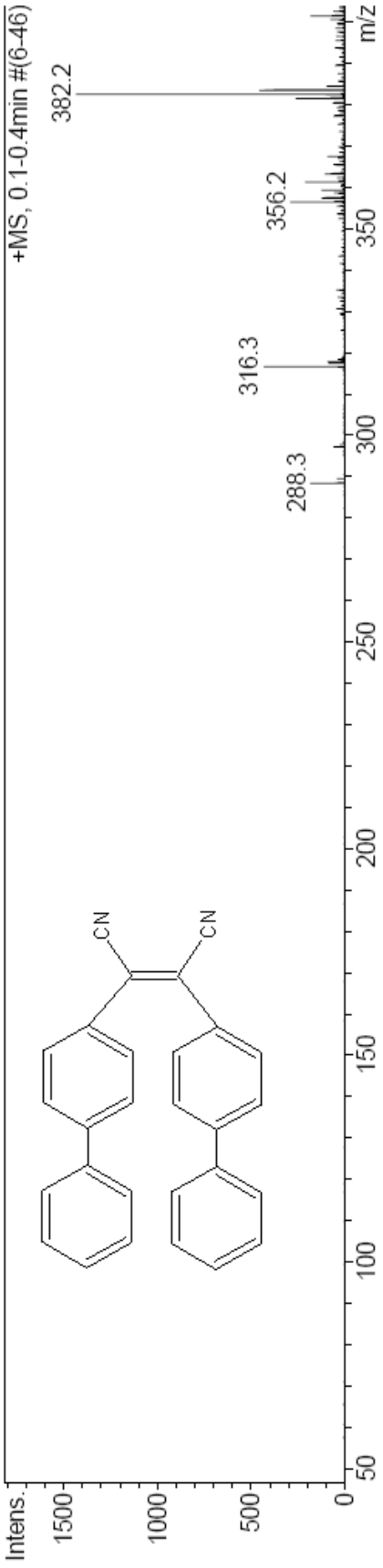


Mass Spectrum of **B2**

**APPENDIX Q**

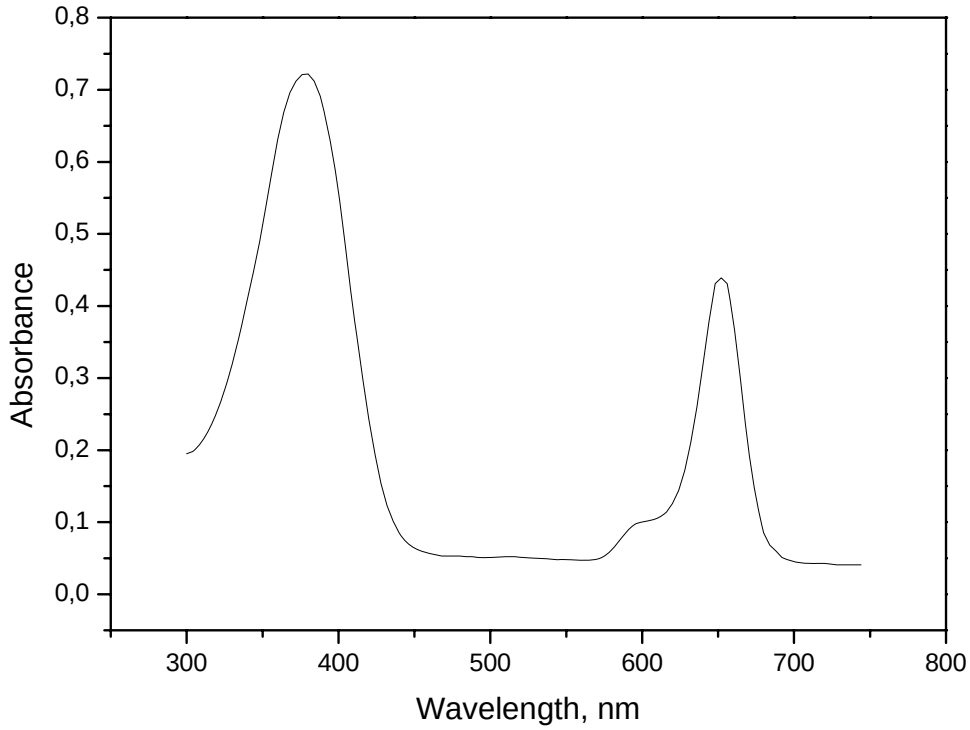


UV-Vis Spectrum of **B3** in Chloroform

**APPENDIX R**

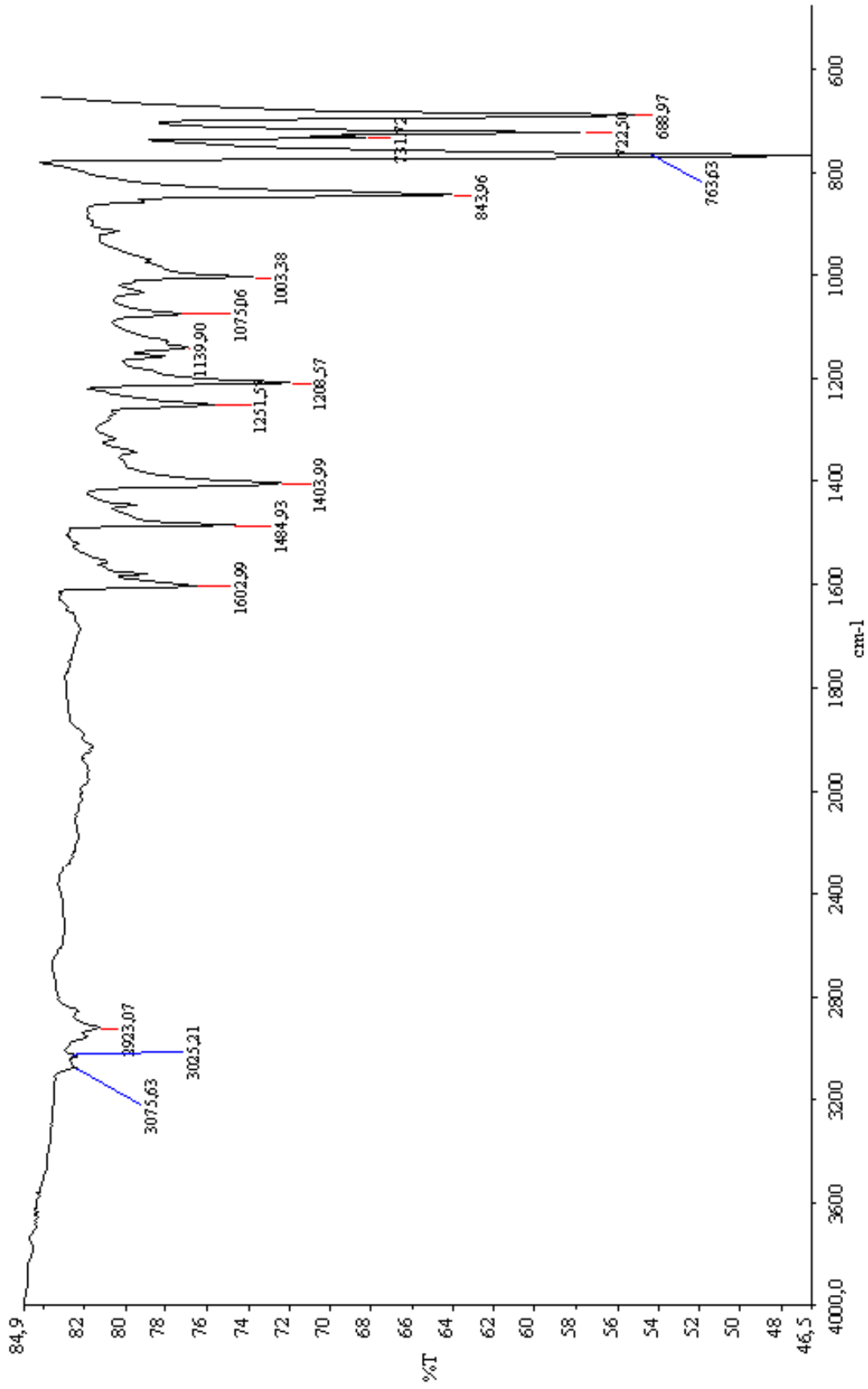


FT-IR Spectrum of **B3**

**APPENDIX S**

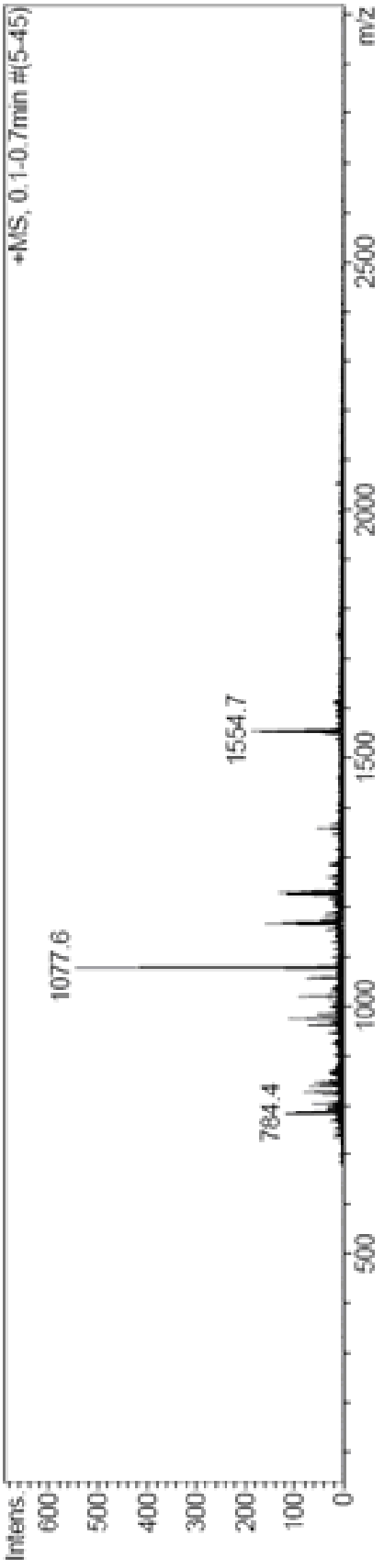


Mass Spectrum of **B3**

## APPENDIX T

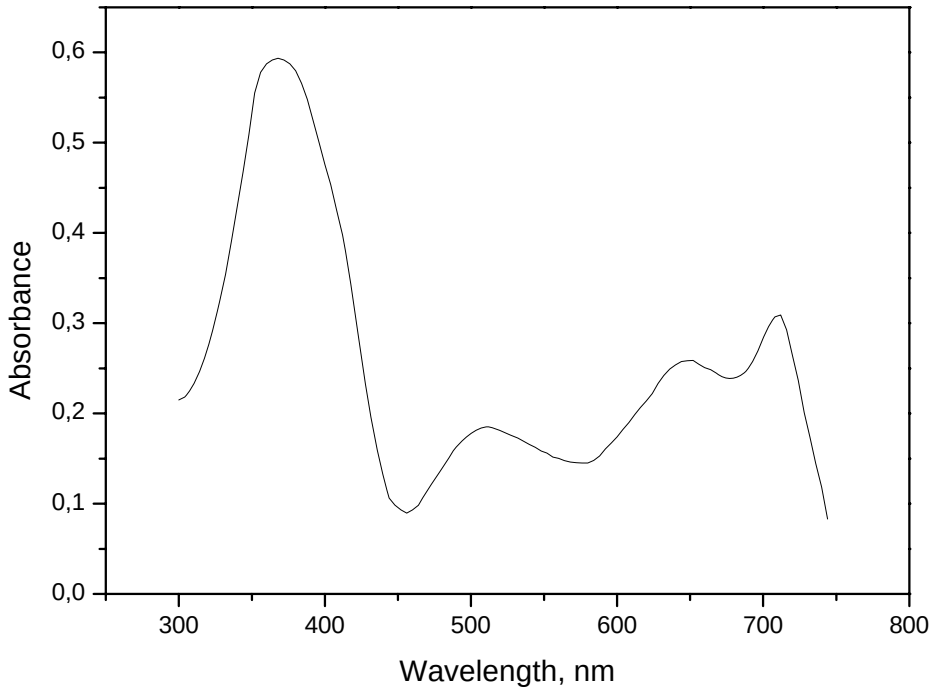


UV-Vis Spectrum of **B4** in Chloroform

**APPENDIX U**

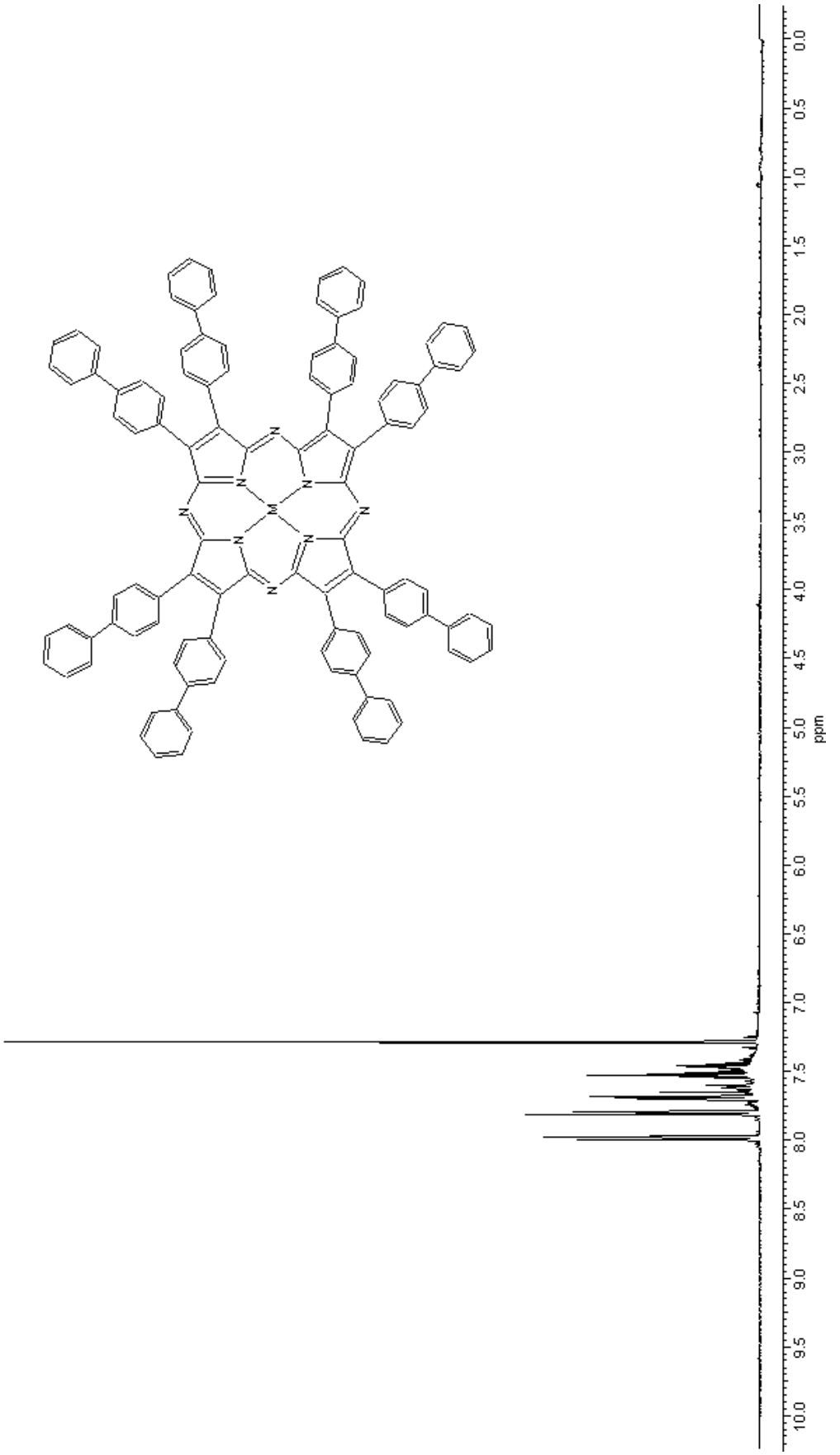


$^{1}$H NMR Spectrum of **B3**

**APPENDIX V**

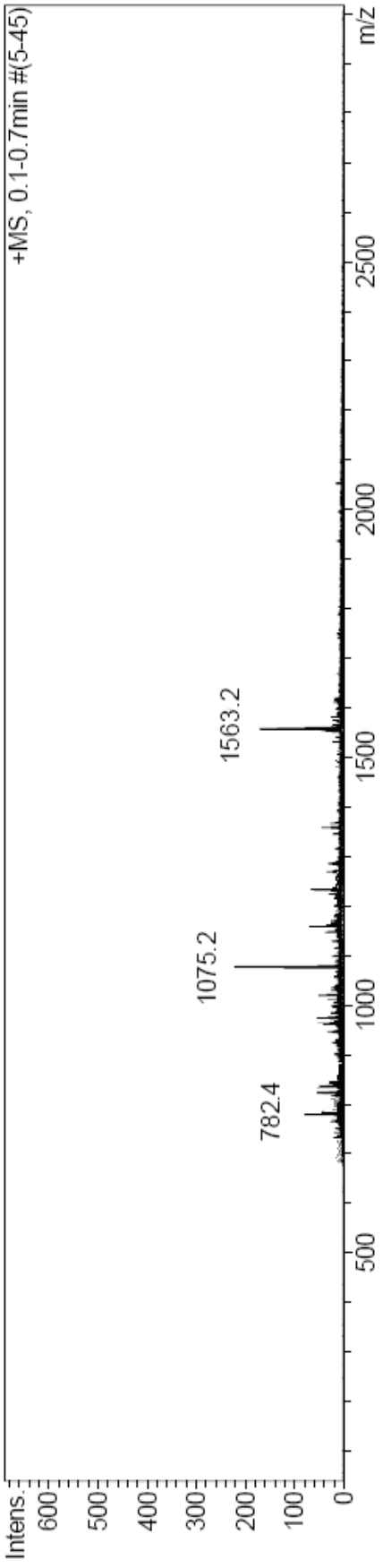


Mass Spectrum of **B4**